ASSESSMENT AND DEVELOPMENT OF SYNTHETIC DESIGN STORMS FOR USE IN URBAN ENVIRONMENTS: GAUTENG PILOT STUDY

Report to the
Water Research Commission

by

Mouton J.v.S.[1], Loots I.[1], Smithers J.C.[2]
[1] University of Pretoria,
[2] University of KwaZulu-Natal

WRC Report No. 3021/1/22
ISBN 978-0-6392-0428-4

May 2022

WATER
RESEARCH
COMMISSION

Obtainable from
Water Research Commission
Private Bag X03
Gezina
PRETORIA, 0031

orders@wrc.org.za or download from www.wrc.org.za

EXECUTIVE SUMMARY

This section provides a summary of the project background, aims, methodology and results. Conclusions drawn from the results, as well as recommendations for the next phase of this project, are also summarised.

BACKGROUND

Engineers have for centuries concerned themselves with redirecting and managing stormwater runoff to address the persistent increase in demands associated with civilisation. As a result, flood estimation methods were developed which have evolved into sophisticated computer-aided stormwater simulation modelling. The hydrological and hydraulic behaviour of an urban stormwater drainage network is frequently simulated using software such as the Stormwater Management Model (SWMM), developed by the United States Environmental Protection Agency (EPA). Simulations can either run on a continuous basis using observed rainfall data or based on a single-event model simulation, using a hypothetical rainstorm event (synthetic design storm) as input. Many urban stormwater and infrastructure designs are based on single-event based modelling using synthetic design storms. However, because of the abundance of methods to generate synthetic design storms, engineers frequently base their method choice on familiarity with a method and preference rather than sound evidence of the appropriateness of the selected method. The need for typical synthetic design storms applicable to single-event based modelling of small urban catchments in South Africa was identified.

AIMS

The aim of this study was to test the performance of the existing synthetic design storm generation methods, and to identify the method most suited for single-event based modelling of small urban catchments in Gauteng, using the 5-min interval rainfall records obtained from the South African Weather Services (SAWS). The specific objectives to meet the aim were to:

(a) Identify and assess the performance of currently available methods to generate synthetic design storms used as input for single-event based modelling in the selected pilot study area.

(b) Propose an improved procedure to generate a synthetic design storm that are applicable to single-event based modelling of small catchment areas in the study area.

(c) Disseminate the information to managers, designers and technicians involved in urban stormwater planning and design.

METHODOLOGY

In this project, existing methods for estimating temporal distributions of design rainfall were analysed and tested against recently measured sub-hourly rainfall data, using the Gauteng province in South Africa as a pilot study, to find the synthetic design storm most applicable to single-event based modelling of small urbanised catchment areas, with the case study area of Gauteng as the geographical focus.

This study commenced with a literature review and the identification of methods that are frequently used in Gauteng to generate synthetic design storm events required for single event-based modelling. The methods are broadly characterised into three distinct categories, which is an adaptation of the four categories defined by Veneziano and Villani (1999). The first category is based on Intensity Duration Frequency (IDF) curves, which includes: (i) methods that use a single point on the IDF curve, and (ii) methods that use the entire IDF curve. The second category utilises cumulative mass curves of observed rainfall events. The third category entails the use of stochastic methods which are not covered by this study.

Observed rainfall data recorded at 35 automatic rainfall stations situated in the Gauteng province were collated and assessed in terms of completeness. The completeness of the data sets was determined considering the periods of missing data and the period of available data. The data sets of nine stations were of poor quality and were subsequently omitted from the study. Five stations have good data sets with each having a data period of 26 years and less than 5% of missing data during the rainy months. A further 17 stations were identified with average quality data sets. Independent rainfall events were identified from the observed rainfall data. Various Maximum Dry Period (MDP) criteria were used, namely 0, 15, 30, 60 and 120 minutes. After the separation of the data into idealised single events, a minimum rainfall threshold and an intensity threshold was applied to each event to eliminate insignificant events. The remaining events were classified as significant events which were used in the assessments.

The correlation between the total storm duration and total rainfall depth related to different MDPs was consistent with Ramlall's (2020) finding, who found an increase in correlation by decreasing the MDP from 6-hour to 1-hour. However, this study is based on a MDP associated with the reaction time of a typical small urban catchment. It was argued that any rainfall after a 15-min MDP would not impact the peak discharge from the previous event, but it is rather seen as the start of the next event. Appropriate storm parameters were determined. These storm parameters were subsequently applied to the Chicago Design Storm (CDS) and Triangular (TRI) methods, respectively, to generate synthetic design storms for the assessment. The significant events were further used to determine standardised mass curves (Huff curves) which were also used as synthetic design storms, but it was shown that the design rainfall of shorter time steps are underestimated. This will

result in an underestimation of the peak discharge and therefore, this method was deemed inappropriate for single-event based modelling of small urban catchments with rapid response times.

The design rainfall ratios of the Soil Conservation Service method adapted for South Africa (SCS-SA) curves were compared with the ratios determined from the Design Rainfall Estimation for South Africa (DRESA) software's design rainfall. The sub-daily rainfall ratios in relation to the 24-hour rainfall were determined from the design values estimated using the observed data and compared with the ratios of the SCS-SA curves. The maximum within this range was determined for each station and assigned to that station. The inverse distance weighting (IDW) interpolation technique was adopted with a power coefficient of 2.5 for interpolation. The concept of an intermediate curve type was developed which could be used in combination with the interpolated map of Gauteng. The design rainfall ratios of the SCS curves were compared with the SCS-SA curves.

Distribution Curves (DC) were developed for the five best stations in Gauteng from the 1:5 year (DC5), 1:10 year (DC10) and 1:20 year (DC20) at-site design rainfall. The adopted procedure to develop a 24-hour DC was applied, as well as the procedure to extract events of < 24-hour durations. Both procedures were adopted from the National Engineering Handbook (NRCS, 2019), and the adaptations were documented.

The synthetic design storm evaluation was conducted by comparing the synthetic design storms with the observed rainfall events. Two aspects were evaluated, namely the shape of the mass curves, as well as the average intensities embedded in each synthetic design storm. The Goodness-Of-Fit (GOF) was determined using the Mean Absolute Relative Error (MARE) technique. An evaluation of the simulated runoff was undertaken following the synthetic design storm evaluation. This was achieved by simulating a hypothetical catchment with an area of 11.6 ha.

RESULTS AND DISCUSSION

The performance of various synthetic design storm methods, including: (a) the CDS method; (b) the SCS-SA Type 2 and 3 curves; (c) the DC5, DC10 and DC20 curves developed from the at-site design rainfall; (d) the REC method; and (e) the TRI method was assessed. This was achieved by comparing the synthetic design storms with the observed rainfall events which has proved that synthetic design storms do not exist in nature. A comparison of simulated and observed runoff was undertaken following the synthetic design storm evaluation. Various observations were made from these results. For example, the suggested values for the initial deficit associated with the Green-Ampt infiltration parameters did not result in good simulations. The CDS method was also shown to provide consistent results compared to continuous simulation. However, a sensitivity analysis must be conducted to

determine the effect of the advancement coefficient and total storm duration on the peak discharge.

The design rainfall ratios of the SCS-SA curves were compared with the ratios determined from the Design Rainfall Estimation for South Africa (DRESA) software's design rainfall. It was observed that the Gauteng stations are generally closer to the Type 2 curve rather than Type 3. Further comparisons were undertaken by estimating design rainfall using a Probability Distribution (PD) analysis on the observed rainfall data of Gauteng's stations. The General Extreme Value distribution was adopted for this analysis. The sub-daily rainfall ratios in relation to the 24-hour rainfall were determined from the design values estimated using the observed data and compared with the ratios of the SCS-SA curves. On average the ratios of Gauteng's stations compared well with the Type 2 curve, although a wide variation in ratios was observed. Due to the rapid response time of small urban catchments, emphasis was placed on the 5 to 30-min ratios. The maximum within this range was determined for each station and assigned to that station. The inverse distance weighting (IDW) interpolation technique was adopted with a power coefficient of 2.5 for interpolation. The concept of an intermediate curve type was developed which could be used in combination with the interpolated map of Gauteng. Further verifications and sensitivity analyses are, however, recommended. The design rainfall ratios of the SCS curves were compared with the SCS-SA curves and concluded that the SCS curves should be applied with caution in practice. The SCS Type II curve should be applied in areas with a maximum intermediate curve Type of 2.31 for a 30-min reaction time. Other maximum values apply to different durations, for example, the intermediate curve type for the 5-min duration is 1.63. The minimum and maximum for the SCS Type III for the 5-min to 30-min durations was 0.79 and 1.63 respectively. Therefore, the Type III is not recommended for single-event based modelling of small urban catchments in Gauteng.

In the synthetic design storm evaluation, the Rectangular (REC) method was found to be the worst representation of observed events. The performance of the methods concerned with the IDF curve were initially also poor but improved after the location of the peak intensity was manipulated. The variation of the Recurrent Interval (RI) relative to the average intensities of the standard time steps, also contributes to the poor performance. This analysis has therefore provided sound evidence that synthetic design storms do not exist in nature.

Various observations were made from the SWMM runoff comparison of which the most important was that the suggested values for the initial deficit associated with the Green-Ampt infiltration parameters did not result in good simulations, the result of the DC5, DC10 and DC20 curves provided an independent verification of the reaction time of the catchment, and the CDS method was also shown to provide consistent results compared to continuous simulation. However, a sensitivity analysis must be conducted to determine the effect of the advancement coefficient and total storm duration on the peak discharge.

CONCLUSIONS

It is, in general, concluded that synthetic design storms, applied to a single event-based model, provides the engineer with the ability to assess the complex hydrological and hydraulic characteristics of an urban stormwater network. Despite its unrealistic assumptions, shortcomings, and the criticism the synthetic design storm concept has received, applying it to a single event-based model has resulted in good peak discharge and runoff volume estimates. Three methods, to generate synthetic design storms, were identified that could be applied to a single event-based model. They are the REC, SCS-SA and CDS methods.

The REC method also provides a means of evaluating the response time of an urban catchment, but the initial deficit defined as the difference between the porosity and field capacity, associated with the Green-Ampt infiltration method, did not result in good simulations. The design rainfall ratio comparisons from both the at-site and DRESA design rainfall, provided the bases to conclude the inappropriateness of the SCS-SA Type 3 curve for Gauteng. However, it was also concluded that an interpolation between the standard type curves is needed for better single event-based simulation results. The methodology that was used to determine the CDS regression coefficients from the DRESA design rainfall was sufficient and resulted in good results when applied to a single event-based simulation.

It can be concluded that all three project aims were achieved, namely:

(a) The performance of currently available methods to estimate synthetic design storms was assessed and used as input for single-event modelling in the selected pilot study area.

(b) An improved procedure to generate a synthetic design storm for the study area was proposed. An improved procedure to generate a synthetic design storm applicable to small catchment areas in the study area is proposed through the development of intermediate SCS-SA curve types. The intermediate curves could be used in combination with the interpolated map of Gauteng with lower values to the north of the province and higher values to the south.

(c) The results of this project were disseminated to managers, designers and technicians involved in urban stormwater planning and design through a WRC workshop presented in conjunction with the annual National Flood Studies Programme’s workshop, as well as at the 2022 UP Flood Hydrology course.

The objective of the study was therefore successfully achieved by the identification of the three methods that are suitable for single event-based modelling. These methods are the REC hyetograph, the CDS with location specific regression coefficients and the SCS-SA curves with intermediate types that was developed for better modelling of different regions in Gauteng.

RECOMMENDATIONS

Based on the results of this pilot study, various recommendations are made for future phases of this project. They can be summarised as follows:

(a) The impact the advancement coefficient and total storm duration have on the peak discharge must be investigated by conducting a sensitivity analysis. The parameters that could be considered for the analysis includes the size of catchment, slope, roughness, soil types, and the initial deficit.

(b) The current DRESA software, be further developed to provide the user with an opportunity to determine a synthetic design storm for a specific location.

(c) The impact that missing data has on the design rainfall estimation and by implication the design rainfall ratios, in the context of this study, should be investigated.

(d) The discrepancy between the dates of the daily and 5-min data, and the annual maximum daily rainfalls from the daily and the 5-min data should be investigated.

(e) The inconsistency between the design rainfall estimated using data from Unisa and Proefplaas, compared to their neighbouring stations, should be investigated.

(f) The appropriateness of the GEV PD for short duration rainfall should be re-confirmed.

(g) An appropriate power coefficient for the IDW interpolation technique should be investigated.

(h) The suggested values for the initial deficit associated with the Green-Ampt infiltration parameters should be investigated.

(i) The relevance of the CDS, SCS-SA and REC methods for generating synthetic design storms applicable to single-event based modelling of small urban catchments must be expanded on a national scale, with the possibility of following a regional approach and ensemble modelling investigated.

ACKNOWLEDGEMENTS

The project team wishes to thank the following people for their contributions to the project.

Name	Role	Affiliation
Mr W Nomquphu (Chair)	Reference Group member	Water Research Commission
Mr S Dunsmore	Reference Group member	Fourth Element Consulting
Mr C Brooker	Reference Group member	CBA Specialist Engineers
Mr R Males	Reference Group member	DRA
Ms N Smal	Reference Group member	Ekurhuleni Metropolitan Municipality
Prof JG Ndiritu	Reference Group member	University of Witwatersrand
Prof J Gericke	Reference Group member	Central University of Technology
Prof JA du Plessis	Reference Group member	Stellenbosch University
Mr P Shepard	Reference Group member	SRK
Mr Musa Mkhwanazi	Provision of rainfall data	South African Weather Services
Mr Gerhard Munro	Assistance with code development	Oracle Certified Java SE Programmer

CONTENTS

LIST OF FIGURES

Page

LIST OF TABLES

Page

ACRONYMS AND ABBREVIATIONS

Acronym	Description
AMS	Annual maximum series
CDS	Chicago design storm
DC	Distribution Curve
DC5	1:5 year Distribution Curve
DC10	1:10 year Distribution Curve
DC20	1:20 year Distribution Curve
DDF	Depth Duration Frequency
DRESA	Design Rainfall Estimation in South Africa
EPA	Environmental Protection Agency
GEV	General Extreme Value
GOF	Goodness-of-Fit
i	Storm intensity (mm/hour)
i_a	Intensity after the peak intensity (mm/hour)
i_{av}	Average intensity (mm/hour)
i_b	Intensity before the peak intensity (mm/hour)
IC	Intermediate Curve
i_p	Peak intensity (mm/hour)
IDF	Intensity Duration Frequency
IDW	Inverse Distance Weighting
ILLUDAS	Illinois Urban Drainage Area Simulator
MAP	Mean annual precipitation (mm)
MARE	Mean Absolute Relative Error
MDP	Maximum Dry Period (min)
MIDUSS	A Windows-based software program that generates hydrographs for complex drainage networks from single event storms.
MRD	Minimum Rainfall Depth (mm)
MRI	Minimum Rainfall Intensity (mm/hour)

NOAA	National Oceanic and Atmospheric Administration
P	Total rainfall depth (mm)
P_a	Cumulative rainfall depth after the peak intensity (mm)
P_b	Cumulative rainfall depth before the peak intensity (mm)
PD	Probability Distribution
r	Storm advancement coefficient. The ratio of the storm duration of the peak intensity relative to the total storm duration
RE	Relative Error
REC	Rectangular hyetograph method
RI	Recurrence Interval (1:year)
R^2	Coefficient of determination
SA(T2)	SCS-SA Type 2
SA(T3)	SCS-SA Type 3
SAWS	South African Weather Services
SCS	Soil Conservation Services
SCS-SA	SCS curves adapted for Southern African conditions
SWMM	Stormwater Management Model
t_a	Storm duration after the peak intensity (min)
t_b	Storm duration before the peak intensity (min)
T_c	Critical storm duration (hour)
T_d	Total storm duration (min)
T_p	Time when peak intensity occurs (min)
TRI	Triangular hyetograph method

CHAPTER 1: BACKGROUND

1.1 INTRODUCTION

Engineers have for centuries concerned themselves with redirecting and managing stormwater runoff to address the persistent increase in demands associated with civilisation. As a result, flood estimation methods were developed which has evolved into sophisticated computer-aided stormwater simulation modelling. The hydrological and hydraulic behaviour of an urban stormwater drainage network is frequently simulated using software such as the Stormwater Management Model (SWMM), developed by the United States Environmental Protection Agency (EPA). Simulations can either run on a continuous basis using observed rainfall data, or based on a single-event model simulation, using a hypothetical rainstorm event (synthetic design storm) as input. Many urban stormwater and infrastructure designs are based on single-event based modelling using synthetic design storms. However, because of the abundance of methods to generate synthetic design storms, engineers frequently base their method choice on familiarity with a method and preference rather than sound evidence of the appropriateness of the selected method.

The focus of this pilot study in the Gauteng Province is to assess the performance of methods used to generate synthetic design storms for single-event based modelling, applicable to small urban catchments. Each of the considered methods presents some degree of insufficiency and has received criticism in previous studies from which the need to derive typical synthetic design storms for small urban catchments was identified. This document describes the methodology followed and results obtained from considering existing methods, and (1) comparing them against recently measured sub-hourly rainfall data and (2) applying them to a typical urban stormwater network.

1.2 PROJECT AIMS

The aim of this study was to test the performance of the existing synthetic design storm generation methods, and to identify the method most suited for conditions in small catchments in Gauteng, using the 5-min interval rainfall records obtained from the South African Weather Services (SAWS). The specific objectives to meet the aim are summarised in **Table 1.1**.

Table 1.1. Project objectives

No.	Objectives
1	To identify and assess the performance of currently available methods to generate synthetic design storms used as input for single-event modelling in the selected pilot study area.
2	To propose an improved procedure to generate synthetic design storms applicable to small catchment areas in the study area.
3	To disseminate the information to managers, designers and technicians involved in urban stormwater planning and design.

The complete list of tasks required to meet the project objectives include:

(a) Literature review – a literature review was conducted on the existing methods in terms of their development, application, and limitations.

(b) Data collection – the rainfall data for all the stations with sub-daily data in the Gauteng province were collected from the South African Weather Service (SAWS).

(c) Data verification – the data from each station was evaluated in terms of the length of the record, and the missing periods were identified.

(d) Storm event identification – the data selected for the evaluation was analysed to identify individual storm events in accordance with the single event-based.

(e) Storm analysis – the general storm parameters required to accurately apply certain methods were determined from the individual storm events.

(f) Synthetic design storm evaluation – the Goodness-of-Fit (GOF) was calculated in terms of the storm shape and peak intensities between the actual and the synthetic design storms.

(g) SWMM Modelling – a hypothetical stormwater network was created; catchment characteristics defined, and continuous simulation modelling conducted. A statistical analysis was conducted on the peak discharge and runoff volume and compared to results from single event modelling using different synthetic design storms.

(h) Report writing – the report detailing all analysis and results as well as knowledge dissemination activities was completed.

1.3 SCOPE AND LIMITATIONS

The observed rainfall data collection was limited to automatic recording rainfall stations with 5-min interval measurements operated by the SAWS within the boundaries of Gauteng. The existing methods considered in the literature review include the following methods:

(a) Rectangular hyetograph (Mulvaney, 1851);

(b) Chicago design storm (Keifer and Chu, 1957);

(c) The Huff curves (Huff, 1967);

(d) Unites States Department of Agriculture's Soil Conservation Services (SCS) synthetic storm distribution curves (SCS, 1973);

(e) The expanded SCS version adapted for Southern African conditions (SCS-SA) synthetic storm distribution curves (Schulze, 1984);

(f) Triangular hyetograph (Yen and Chow, 1980);

(g) Daily rainfall disaggregation model for South Africa (Knoesen, 2005); and

(h) HRU 1/72 time distribution for intermediate durations.

CHAPTER 2: LITERATURE REVIEW

2.1 BACKGROUND

A natural hydrological event, in its simplest form, starts with a hyetograph and ends with a hydrograph, each having many unique characteristics that are quantifiable, such as total volume, total duration, intensities and skewness (Adams and Howard, 1986). The link, being the catchment with its various characteristics and antecedent moisture conditions, determines the relationship between the hyetograph and hydrograph. For example, two different hyetographs with two identical catchments and antecedent conditions can result in differently shaped hydrographs, but with the same peak discharge. Conversely, two identical hyetographs with two different catchments and antecedent conditions can result in two different hydrographs with different peak discharges (Adams and Howard, 1986). Despite the uncertainties about this transitional stage that rainfall needs to pass through before runoff is generated, it is nevertheless assumed that the frequency of the hyetograph is identical to the frequency of the hydrograph. This unrealistic assumption is well documented by Adams and Howard (1986) who, as a result, states it should be used only in the strictest of circumstances due to the large potential for error associated with the synthetic design storm concept.

Despite the criticism synthetic design storms have received, these, together with Intensity-Duration-Frequency (IDF) curves, are used extensively internationally in many urban stormwater designs and studies (Balbastre et al. 2019). This is because of the complex hydrological and hydraulic behaviour pertaining to an urban stormwater network which calls for the use of sophisticated computer-aided rainfall-runoff simulation modelling. The inherent advantages of synthetic design storms are highlighted by Balbastre et al. (2019) which is summarised as follows:

(a) It guarantees a uniform level regarding quality and operation standards.
(b) It reduces and simplifies calculations, compared with continuous simulation modelling.
(c) It provides a way of overcoming the problem of scarcity of short-duration rainfall data.
(d) It can be regionalised which enhance its practicality.

To contextualise the advantages, the use of synthetic design storms for single event modelling is done with the intention that it will provide flow results that have the same frequency of exceedance then the statistical analysis of observed flow data. This is because observed flow data is hardly ever available and in the best of circumstances, will only be available at selective locations. In the case of a new stormwater network, observed flow data does not exist, and observed short duration rainfall data will provide the next best information

in the form of a continuous simulation. With the scarcity of short-duration rainfall data, the complexity of stochastic generated historic rainfall data, and the excessive time consumption of continuous simulation modelling, synthetic design storms have an important role to play in the design and assessment of urban stormwater networks.

It is important to simulate a storm event with not only the critical duration but also the hyetograph shape that will most likely be representative of the natural rainfall event, since storm shape may have a significant impact on the peak discharge and total flood volume. It becomes more noticeable at catchments with a high percentage of areas that saturate quickly. This is due to the rapid decline of the infiltration capacity during the early part of a rainstorm, which then tends towards an approximately constant value after a few hours for the remainder of the event (Horton, 1933). If the peak intensity of a synthetic design storm is applied earlier during the storm event, the infiltration capacity might be higher, which will result in a lower peak flow result. Conversely, a storm event peaking later during the event is likely to result in higher flow results. Although the existing synthetic design storms were developed using the best data, technology, and engineering judgement available at the time, they do present some degree of insufficiency. However, as identified previously, synthetic design storms have an important role to play in the design and assessment of urban stormwater networks, and, therefore, a review of each of the synthetic design storms is provided in this chapter. Emphasis is placed on their development and the criteria and assumptions on which it was based, which will provide the basis for the methodology that will be followed in this study to assess the applicability of the methods.

2.2 RECTANGULAR HYETOGRAPH

The rectangular hyetograph method is commonly associated with the Rational Method, which is the most employed formula in engineering hydrology (Gomez and Sanchez, 2014), and it is used worldwide for flood protection design (Cordery and Pilgrim, 1993). This method assumes that the peak discharge occurs when the duration of the rainfall event is equal to the time of concentration of the catchment; that the rainfall intensity does not vary; and is distributed uniformly over the catchment (Smithers, 2012). The first principle of the Rational Method, the runoff coefficient, was concluded through the gradual development of flood estimation methods by researchers in the British Isles before the year 1850. Thomas Mulvaney presented the second principle, the time of concentration, and the method of estimating the peak discharge in 1851, which became known as the Rational Method (Gomez and Sanchez, 2014). With the development of the St. Venant equations for modelling surface flow towards the end of the 19th century (Boussinesq and Flamant, 1871) and the soil infiltration models, like the Green-Ampt model during the early 20th century (Green and Ampt, 1911), methods like the Unit Hydrograph were developed. This method in its simple form also assumes a uniform rainfall intensity distribution with a duration equal to or greater than the longest time of concentration.

2.3 THE CHICAGO DESIGN STORM (CDS)

The CDS method was designed for the City of Chicago by Keifer and Chu (1957) because of the rapid increase in urbanization that followed the end of World War II. As depicted in Figure 2.1 the method encompasses three important characteristics, namely:

(a) average intensity within the maximum storm duration,
(b) antecedent rainfall before the maximum duration, and
(c) location of peak intensity (Keifer and Chu, 1957).

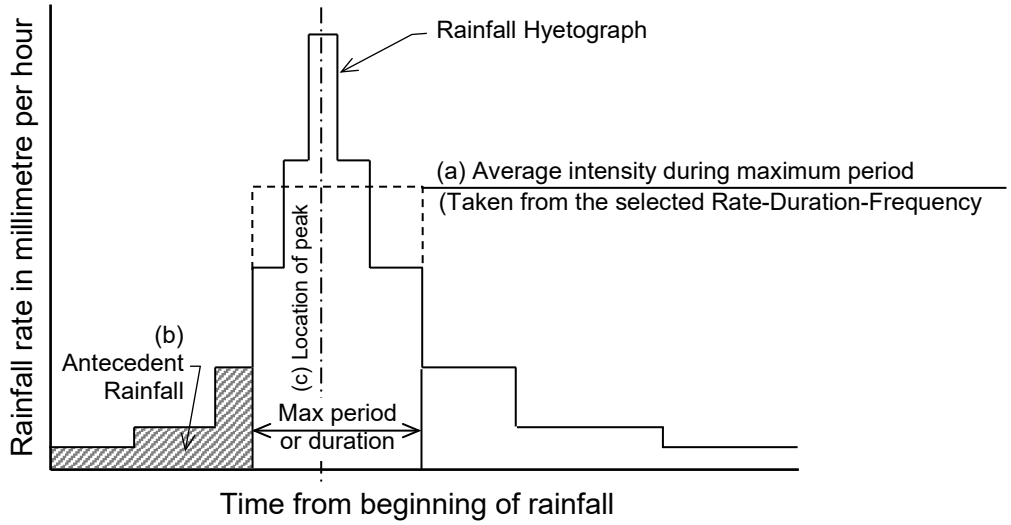

Figure 2.1: A rainfall hyetograph showing the three most important characteristics affecting the peak rate of runoff (Keifer and Chu, 1957)

The average rainfall intensities with associated probability or frequency of exceedance, are determined for particular storm durations using statistical analysis of historical rainfall data. These intensities concerning duration, expressed in terms of frequency of exceedance, are commonly known as Intensity-Duration-Frequency (IDF) curves. The IDF curves have a sigmoidal shape which can be related to a mathematical function in the form of Equation 2.1 and Equation 2.2 as follows:

$$i_{av} = \frac{a}{t^b + c} \qquad [\ 2.1\ ]$$

and:

$$i_{av} = \frac{a}{(b + t)^c} \qquad [\ 2.2\ ]$$

where:

i_{av} = average rainfall intensity for a particular storm duration (mm/hour),
a = site and recurrence interval specific constant,
b,c = site specific constants, and
t = storm duration (min).

Keifer and Chu (1957) addressed the first characteristic of the average intensity within the maximum storm duration, with the intensity distribution function which was derived from the IDF curve, whereas the second and third characteristics of the CDS were represented by the storm advancement coefficient (r). The IDF curve, presented by Equation 2.1 was used to develop the intensity distribution (Keifer and Chu, 1957). However, the development was somewhat transformed using a formula, presented by Equation 2.2 also known as the Sherman formula (Sherman, 1931). Preceded by various substitutions and differentiation, the intensity distribution of an advanced storm, which is a storm with the peak intensity located at the beginning of the event, was expressed in terms of Equation 2.3 as follows:

$$i = \frac{a[(1-c)t + b]}{(b+t)^{c+1}} \qquad [2.3]$$

The time before the peak intensity (t_b) and the time after the peak intensity (t_a) were expressed in terms of storm advancement coefficient in the form of Equations 2.4 and 2.5 as follows:

$$\frac{t_b}{t_d} = r$$
$$\therefore t_d = \frac{t_b}{r} \qquad [2.4]$$

and:

$$\frac{t_a}{t_d} = 1 - r$$
$$\therefore t_d = \frac{t_a}{1-r} \qquad [2.5]$$

Substituting the storm duration in Equation 2.3 with Equations 2.4 and 2.5, yielded the intensity distributions before and after the peak intensity in the form of Equation 2.6 and 2.7 as follows:

$$i_b = \frac{a\left[(1-c)\frac{t_b}{r} + b\right]}{\left(\frac{t_b}{r} + b\right)^{c+1}} \qquad [2.6]$$

and:

$$i_a = \frac{a\left[(1-c)\frac{t_a}{1-r} + b\right]}{\left(\frac{t_a}{1-r} + b\right)^{c+1}} \qquad [2.7]$$

where:

t_a = specific time interval after the peak (min),
t_b = specific time interval before the peak (min),
i_a = specific intensity after the peak intensity (mm/hour),

i_b = specific intensity before the peak intensity (mm/hour),
a,b,c = as defined in Equations 2.1 and 2.2, and
r = storm advancement coefficient (Smith, 2004; Watson, 1981).

The synthetic hyetograph for a completely advanced storm expressed by Equation 2.3 was illustrated graphically by Keifer and Chu (1957) which is reproduced here as Figure 2.2. However, Watson (1981) went further and illustrated the intensity distributions before and after the peak intensity, which were derived from the IDF curve and expressed in terms of Equations 2.6 and 2.7. The synthetic hyetograph illustrated by Watson (1981) with the peak intensity positioned closer to the middle of the storm duration, is depicted in Figure 2.3. The purpose of both these illustrations was to demonstrate that for a storm duration, the rainfall volume obtained from the IDF curve, is equal to the cumulative rainfall volume obtained from the hyetograph of the synthetic design storm.

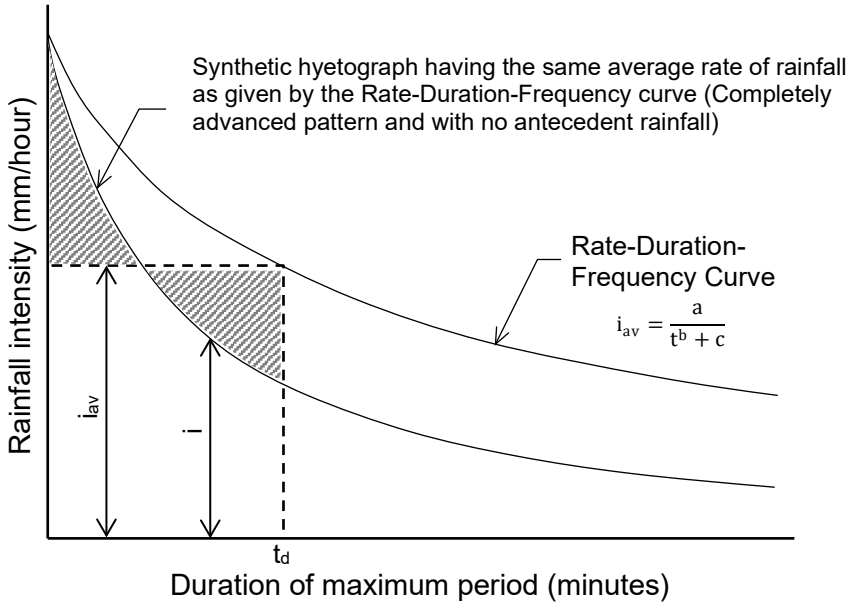

Figure 2.2: Development of a synthetic storm pattern from the Intensity-Duration-Frequency curve (Keifer and Chu, 1957)

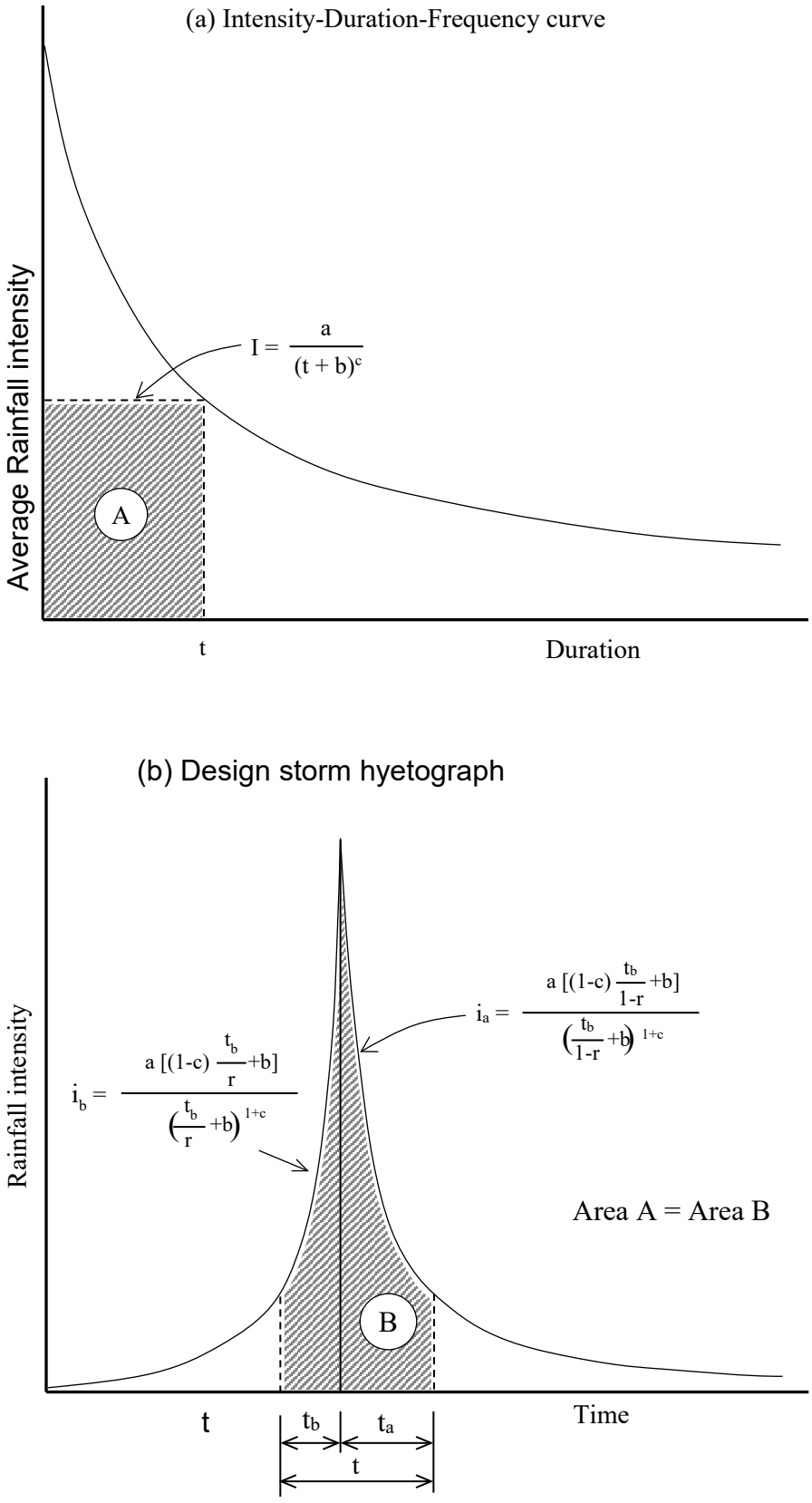

Figure 2.3: Chicago Design Storm (Watson, 1981)

By integrating Equation 2.6 and 2.7 from the beginning of the hyetograph to a time interval before and after the peak intensity, Silveira (2016) formulated two cumulative rainfall equations in the form of Equation 2.8 and Equation 2.9 as follows:

$$P_b = r \cdot P - \frac{a\left(T_p - T\right)}{\left(b + \frac{T_p - T}{r}\right)^c} \quad [2.8]$$

and:

$$P_a = r \cdot P + \frac{a\left(T - T_p\right)}{\left(b + \frac{T - T_p}{1 - r}\right)^c} \quad [2.9]$$

where:

P	= total rainfall depth (mm),
P_a	= cumulative rainfall depth after the peak intensity (mm),
P_b	= cumulative rainfall depth before the peak intensity (mm),
r	= storm advancement coefficient,
T	= time interval from the start of the event (min),
T_p	= time when peak intensity occurs (min), and
a,b,c	= as defined in Equations 2.1 and 2.2.

To address the second and third characteristic, Keifer and Chu (1957) calculated the storm advancement coefficient for different durations and weighted in proportion to the antecedent rainfall volume. The average antecedent rainfall volume was calculated for the 15, 30, 60 and 120-min storm durations. Keifer and Chu (1957) considered the rainfall volume before the peak intensity, for which the antecedent rainfall volume was expressed in terms of the storm advancement coefficient (r). The storm advancement coefficient for the specific storm duration, using the average antecedent rainfall volume, was then calculated. The storm advancement coefficient was then weighted proportionally to the average antecedent rainfall volume for specific storm durations and then averaged for all durations. Following this approach and assuming a total storm duration of 180-min for the City of Chicago, Keifer and Chu (1957) determined the advancement coefficient for the 15, 30, 60 and 120-min storm durations for which the weighted average was 0.386.

Watson (1981) determined the storm advancement coefficient for Norwood, Johannesburg from 28 significant storms also following this approach. For total storm durations of two and three hours, the storm advancement coefficient was 0.28 and 0.22, respectively. A graphical comparison was conducted between the CDS and two real storms, and an Illinois Urban Drainage Area Simulator (ILLUDAS) stormwater model was used to determine the peak discharges. Based on this limited extent of testing, it was concluded that the CDS is an adequate technique for predicting peak discharge.

The second approach which was adopted for calculating the storm advancement coefficient was to ignore the second characteristic, which is the antecedent rainfall before the maximum duration. Since the rainfall data was recorded in 5-min intervals, it was assumed that the peak intensity is located exactly in the middle of the peak 5-min interval (Keifer and Chu, 1957). Keifer and Chu (1957) then determined the weighted average storm advancement coefficient for all durations considering only the location of the peak intensity and weighted proportionally to the time of duration. The weighted average was 0.375. Weesakul et al. (2017) conducted a similar investigation on rainfall data recorded at the meteorological station at the Asian Institute of Technology in Bangkok, Thailand, on data covering 21 years. The storm advancement coefficient was between 0.20 and 0.49.

2.4 HUFF CURVES

According to Bonta (1997), cited by Bonta and Shahalam (2003), the curves presented by Huff (1967) were developed by separating independent storms and then non-dimensionalising each mass curve in terms of the total rainfall volume and total storm duration. The dimensionless mass curves were then superimposed graphically showing the breakpoints at 0.02 intervals along the horizontal axis with the fraction of the total rainfall depth along the vertical axis, followed by the construction of curves with probability values from 10% to 90% (Bonta and Shahalam, 2003). This methodology of developing the Huff curves was, however, according to Bonta (2004), never documented which led to the formulated methodology presented by Bonta (1997). In terms of identifying independent rainstorms, Huff (1967) used a criterion of 6-hours as the minimum dry period to separate consecutive rainstorms (Huff, 1990), whereas Bonta (1997) determined a minimum dry period following the method of identification of independent rainstorms developed by Restrepo and Eagleson (1982). The minimum threshold criterion for individual rainstorms was 25 mm (Huff, 1990).

Typical dimensionless mass curves, also known as isopleths, which are lines connecting intersecting points with equal probabilities of dimensionless storm depths, developed by Bonta and Shahalam (2003) are depicted in Figure 2.4. Huff (1967) investigated the time distributions from 261 storm events recorded in East-Central Illinois from 49 recording rain gauges over 12 years from 1955 to 1966. The rain gauges were distributed over 1,036 km². He divided the rainfall distributions between four quarters based on whether the heaviest rainfall within each storm event occurred in the first, second, third or fourth quarter of the total storm duration. The curves, with probability values from 10% to 90%, developed by Huff are depicted in Figure 2.5. Huff (1990) further suggested that the first and second quartile distributions be used for storm durations of less than 12-hours, the third quartile for storm durations between 12 and 24-hours, and the fourth quartile for storm durations of more than 24-hours. It is suggested that the 50% percentile is likely applicable for most purposes.

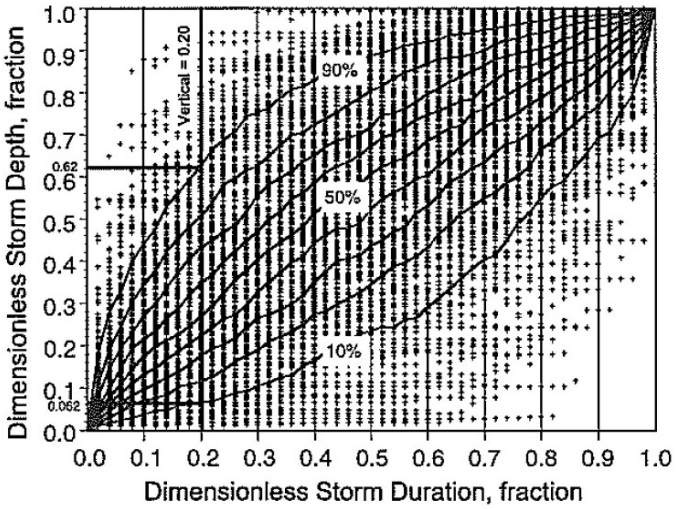

Figure 2.4: Dimensionless storm mass curve intersections with isopleths connecting equal probabilities of dimensionless storm depths (i.e. Huff curves) for a sample size of 322 May and June storms at Invercargill (base/smooth curves) (Bonta and Shahalam, 2003)

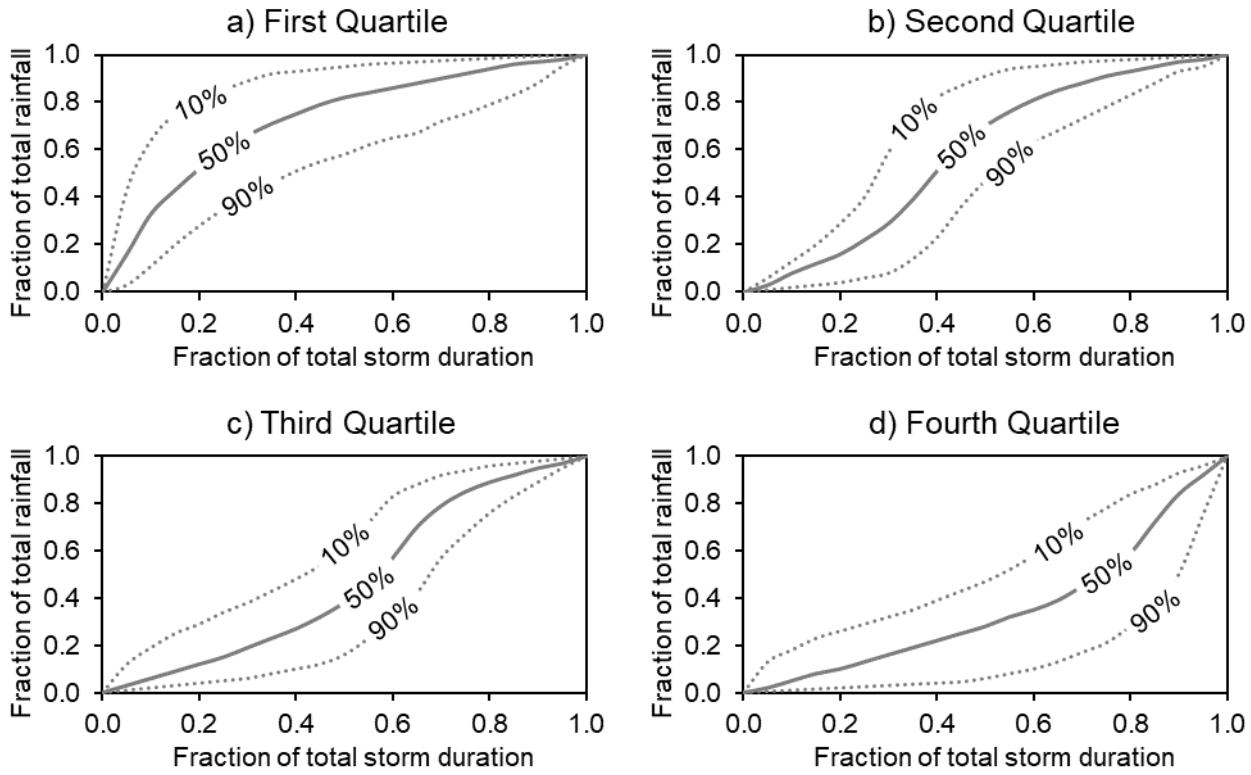

Figure 2.5: Huff curves (Huff, 1990)

2.5 SCS CURVES

Since the initial publication of the standard SCS temporal distribution curves, several derivatives of the curves were developed (e.g. SCS, 1973; Schulze and Arnold, 1979; El-Sayed, 2017; NRCS, 2019). The adaptations included in this review are the South African version, called the SCS-SA, the NOAA Atlas 14 curves that replaces the standard SCS curves (NRCS, 2019). The development of each of these curves are discussed in detail in this section.

2.5.1 Standard SCS temporal distribution curves

Standard SCS temporal distribution curves, Types I and II, were first published in 1973 by the Soil Conservation Service (SCS), which later became the Natural Resources Conservation Services (NRCS). These two curves were developed from the generalised rainfall depth-duration relationships obtained from the US Weather Bureau technical papers (TP-42) published in 1961 (US Weather Bureau, 1961), of which Type II covers most of the USA. Types IA and III were later developed in the same way and were subsequently published by the NRCS in 1986 (NRCS, 1986). The approximate geographic boundaries for the four SCS rainfall distributions are depicted in Figure 2.6. However, according to the National Engineering Handbook, little documentation is available that describes the development of Type II and other legacy rainfall distributions (NRCS, 2019). From the available information, the depth ratios relative to the 24-hour rainfall depth were plotted against the duration for several locations in each of the four regions and then a curve was selected with the best fit (SCS, 1973).

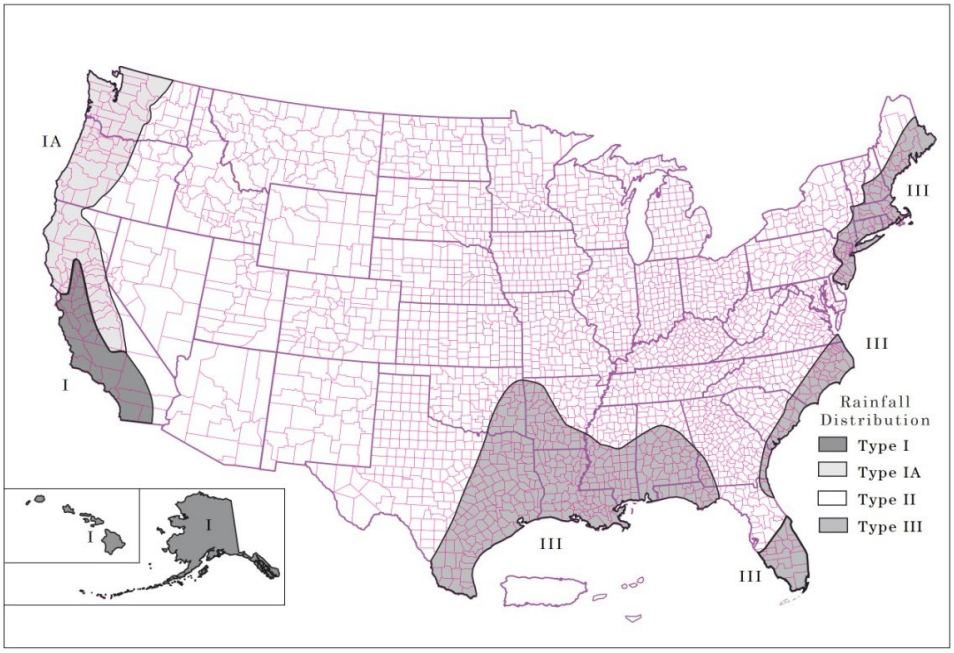

Figure 2.6: Approximate geographic boundaries for SCS rainfall distributions (NRCS, 1986)

The curves were then developed for each of the four regions by positioning the greatest 30-min rainfall depth at the 10-hour and 8-hour points for the Types I and IA respectively, and the 12-hour point for both the Types II and III curves. It is important to note that the positioning of the greatest 30-min rainfall depths at the 8-, 10- and 12-hour points were not based on any meteorological factors but rather on design considerations (SCS, 1973). The second-largest 30-min depth was positioned 30-min later, and the third-largest 30-min depth was positioned at the preceding 30-min. The alternation of 30-min depths, which decrease in magnitude, was repeated until the smallest 30-min depths were located at the beginning and end of the 24-hour (SCS, 1973). The four SCS curves are depicted in Figure 2.7.

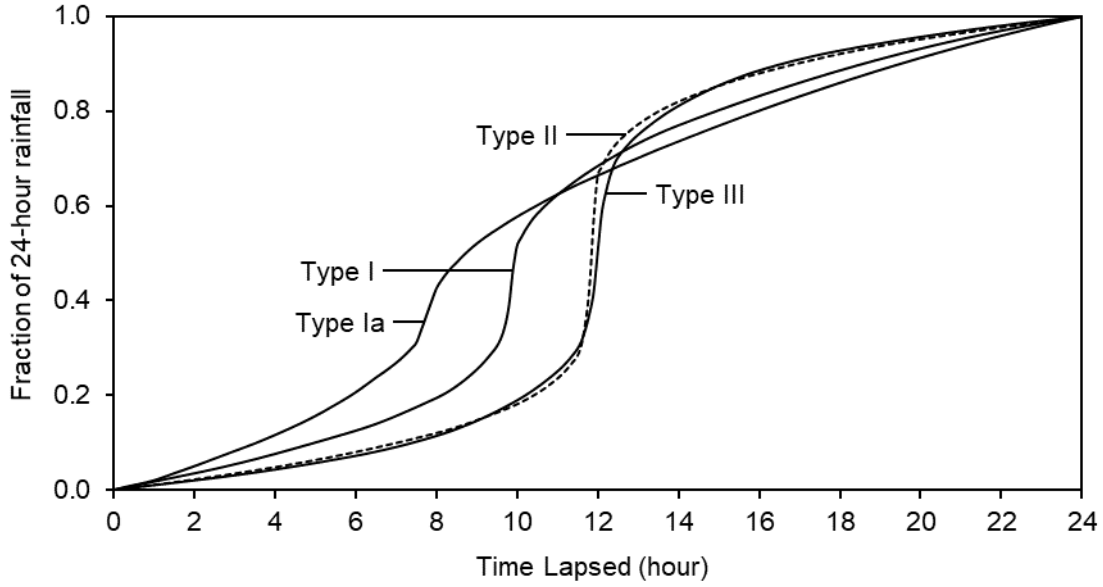

Figure 2.7: SCS Types I, IA, II and III curves (NRCS, 1986)

However, according to NRCS (2019), it was concluded that the use of the SCS curves be discontinued and replaced by the National Oceanic and Atmospheric Administration (NOAA) Atlas 14 curves. Locations in the USA that are already covered by the NOAA Atlas 14 data are depicted in Figure 2.8.

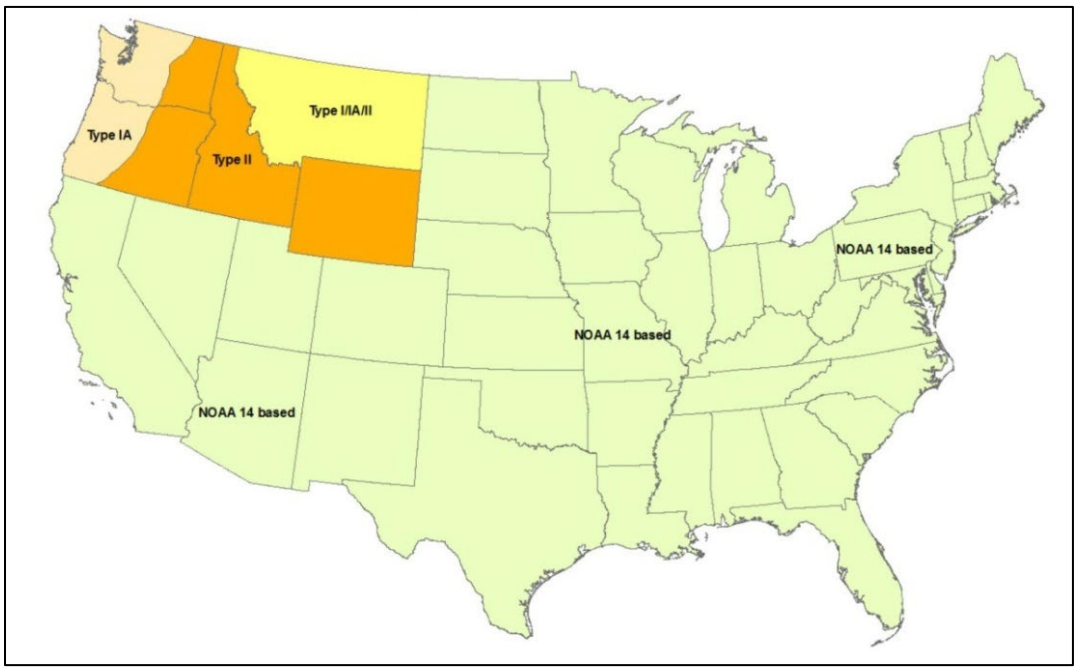

Figure 2.8: Map of States with updated synthetic rainfall distributions as of January 2016 (NRCS, 2019).

2.5.2 SCS-SA curves

The standard SCS Types I and II curves were originally adopted for use in South Africa (Schulze and Arnold, 1979), but the need for revised synthesised storm distributions for South Africa was identified after an analysis of digitised data for Natal (Schulze, 1984). The development of the SCS-SA synthetic rainfall distributions was based on the selection of four D-hour to one-day rainfall ratio range classes for various durations from 5-min to 24-hours, which became known as the SCS-SA synthetic rainfall distributions Type 1 to 4 (Weddepohl, 1988). The D-hour to one-day rainfall ratios for 40 autographic rainfall stations in South Africa were determined and the appropriate ratio range class was assigned to each station (Schmidt and Schulze, 1987). Based on this analysis a map was drawn that represents the regionalisation of the four ratio range classes, depicted in Figure 2.9. The D-hour to one-day rainfall ratios for the four distributions were represented by Equation 2.10 as follows:

$$R = \frac{a \cdot D}{(b + D)^c} \qquad [2.10]$$

where:

R = ratio of D-hour to one-day design rainfall depth,
D = storm duration (hour), and
a,b,c = regression constants summarised in Table 2.1 (Schmidt and Schulze, 1987).

The rainfall distributions were then derived by positioning the middle of the peak 5-min ratio at the 12-hour point, and distributing the ratios of increasing durations, equally on either side of the peak intensity. The cumulative rainfall distributions depicted in Figure 2.10, therefore represent the increase in intensity between consecutive durations from the start of the 24-hour duration up to the 12-hour point, followed by the decrease in intensity up to the end of the 24-hour duration. For example, the difference between the ratios of the 30-min before and 30-min after the peak intensity is equal to the ratio of the 1-hour ratio determined with Equation 2.15. More recently Smithers and Schulze (2002) demarcated the City of Tshwane Metropolitan Municipality (CTMM) into four distinct regions with similar distributions of short and long duration extreme rainfall. Males et al. (2004) then developed an integrated catchment management plan for the City of Tshwane Metropolitan Municipality (CTMM) by compiling a VisualSWMM model. It was found that the four regions conform to the SCS-SA Type 2 rainfall distributions by considering the ratio range classes defined by Weddepohl (1988).

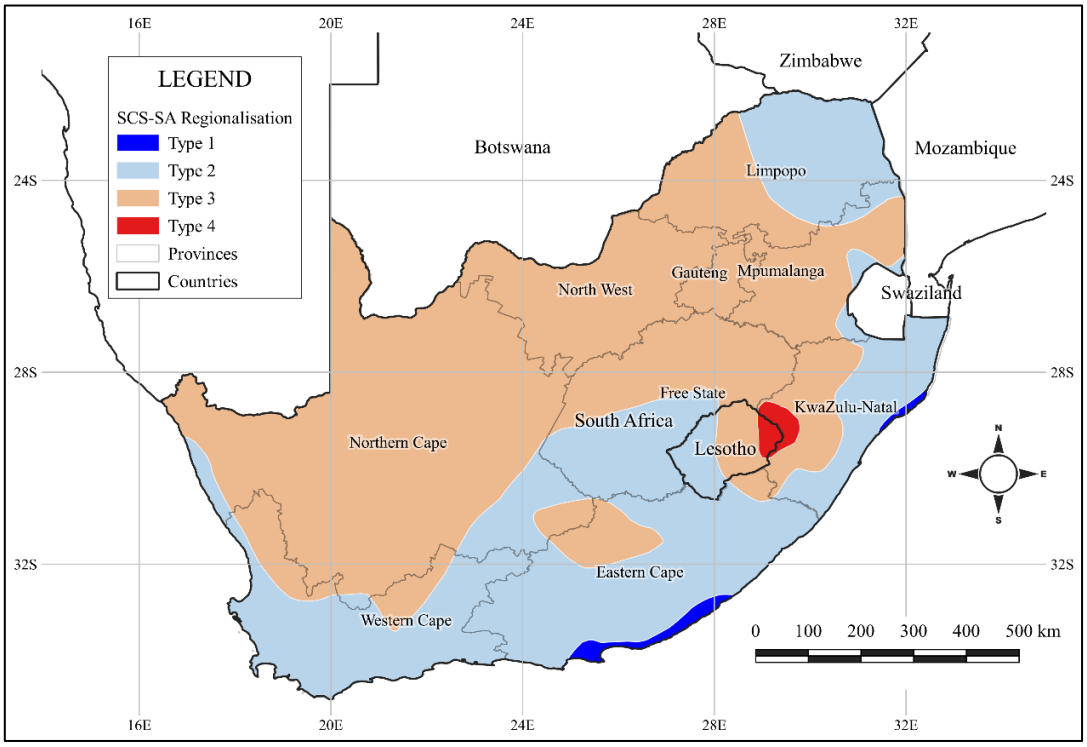

Figure 2.9: Regionalisation of synthetic rainfall distributions in southern Africa (Weddepohl, 1988)

Table 2.1: Regression constants for the four southern African synthetic rainfall distributions (Schmidt and Schulze, 1987)

Distribution Type	a	b	c
1	0.29935	0.059	0.62
2	0.45321	0.100	0.75
3	0.73402	0.230	0.90
4	1.01330	0.320	1.00

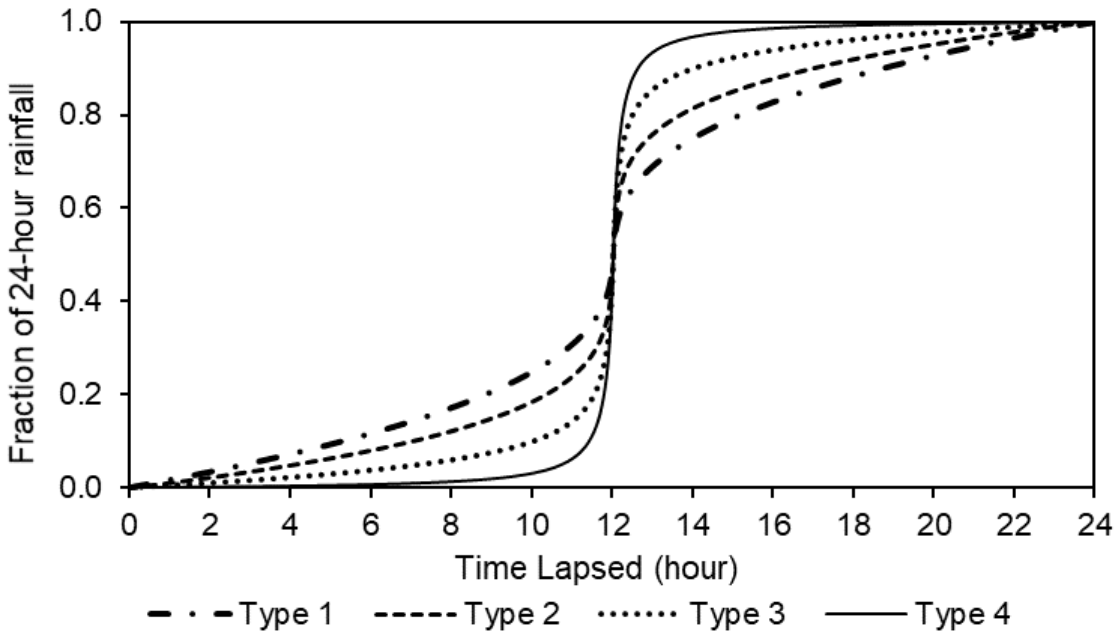

Figure 2.10: Time distributions of accumulated rainfall depth divided by total rainfall depths (Schmidt and Schulze, 1987)

2.5.3 NOAA Atlas 14 curves

The NOAA Atlas 14 consists of a series of volumes that contains the estimates of the design rainfall for standard duration time steps and associated frequencies, together with 90% confidence intervals for the USA, similar to the design rainfall estimates developed by Smithers and Schulze (2000). Curves were also developed for four storm duration classes (6, 12, 24, and 96-hours), separated depending on which quartile the greatest percentage of the total rainfall occurred. According to Bonnin et al. (2011) and Perica et al. (2018), the NOAA Atlas 14 curves were developed in the same way as the ones developed by Huff (1967), except that a storm event was defined in terms of a fixed duration. In other words, events always started with rainfall, but the end of the storm event was located after 6, 12, 24, and 96-hours respectively, irrespective of an event ending sooner (Bonnin et al. 2011). Therefore, many storm events ended sooner than the duration class which lead to events that were more front-loaded, compared to events selected based on the single event approach like Huff (1967). Typical 6-hour NOAA Atlas 14 storm distributions for the Interior Highlands region of the USA are depicted in Figure 2.11. Another approach of utilising the NOAA Atlas 14 design rainfall, is by developing a 24-hour rainfall distribution from the 5-min through to 24-hour design rainfall values. The procedure involves the calculation of ratios of short durations to the 24-hour rainfall, that is distributed equally either side of 12-hours. Equations were developed to interpolate the design rainfall for durations in between the standard time steps (NRCS, 2019).

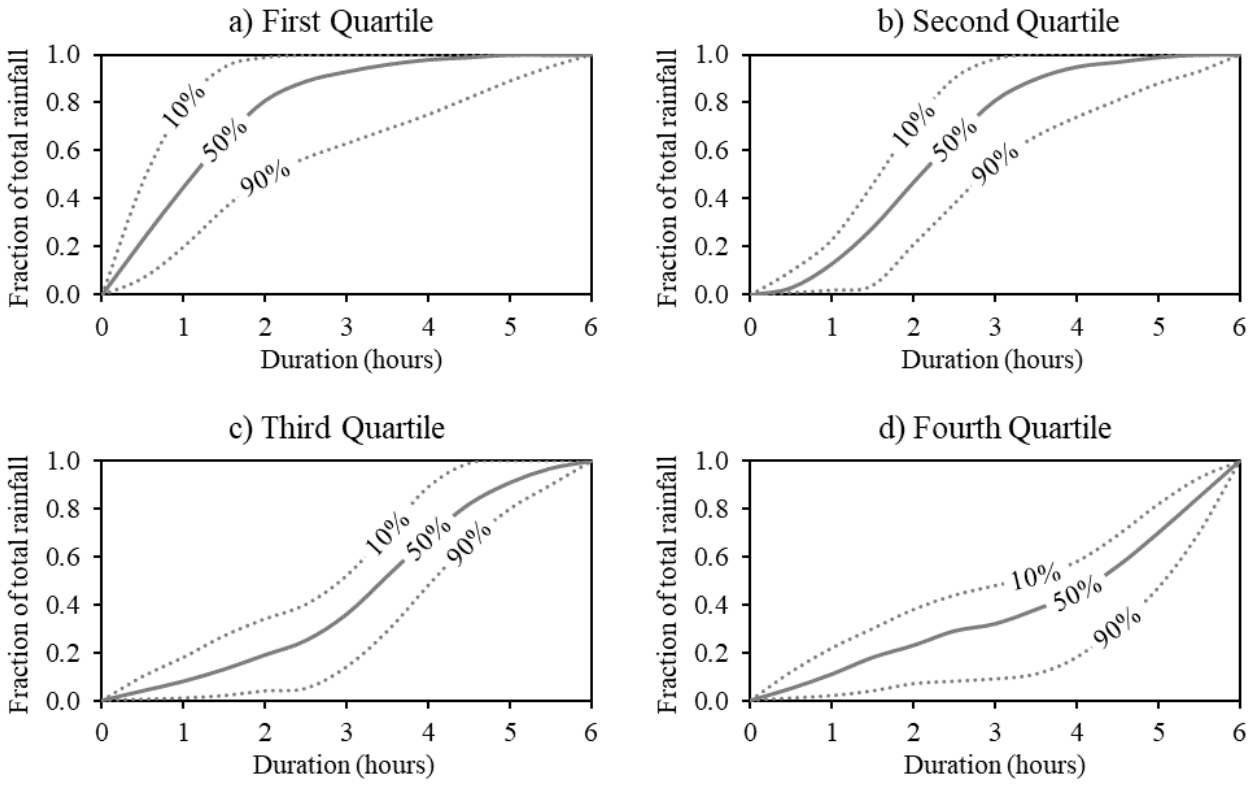

Figure 2.11: Typical 6-Hour curves for the Interior Highlands region (Perica et al., 2018)

2.6 TRIANGULAR HYETOGRAPH

The triangular hyetograph method was formulated by Yen and Chow (1980). The first-moment arm was calculated for the recorded hyetograph concerning the beginning of the rainstorm. It was then related to a triangular representation of the hyetograph with an equal total rainfall volume and total storm duration. Each triangular hyetograph was then non-dimensionalised in terms of the maximum intensity as well as the time to the maximum intensity, relative to the total storm duration. Yen and Chow (1980) considered the typically recorded hyetograph depicted in Figure 2.12, and defined the first-moment arm concerning the beginning of the rainstorm in terms of Equation 2.11 as follows:

$$\bar{t} = \frac{\Delta t\left[\sum_{j=1}^{n}(j-0.5)d_j\right]}{\sum_{j=1}^{n} d_j} \qquad [2.11]$$

where:

$\bar{t}$ = first-moment arm of the hyetograph (min),
d_j = depth for the j-th time interval (mm),
Δt = equal time interval (min), and
n = number of time intervals for the rainstorm (Yen and Chow, 1980).

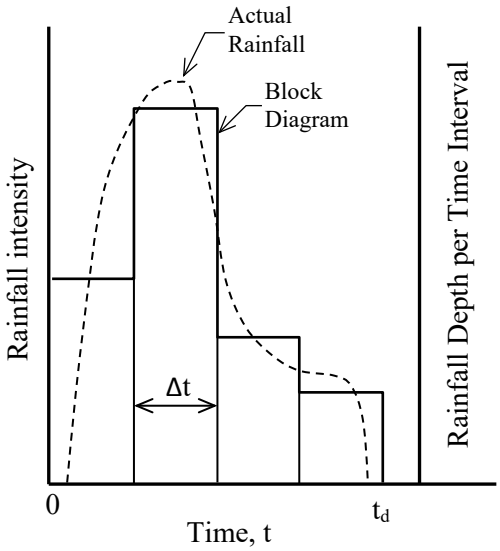

Figure 2.12: Example Hyetograph (Yen and Chow, 1980)

Yen and Chow (1980) then considered the triangular hyetograph depicted in Figure 2.13, which is defined in terms of the total storm duration (T_d) and the maximum rainfall intensity (h). The first-moment arm of the triangular hyetograph concerning the beginning of the rainstorm was expressed in terms of Equation 2.12 as follows:

$$\bar{t} = \frac{T_d + a}{3} \qquad [2.12]$$

Solving for the time to the peak intensity (a) of the triangular hyetograph yielded Equation 2.13 as follows:

$$a = 3\bar{t} - T_d \qquad [2.13]$$

Equation 2.13 was then solved using the first-moment arm and the total storm duration of the recorded hyetograph. The maximum intensity of the triangular hyetograph was expressed in terms of Equation 2.14 as follows:

$$h = \frac{2D}{T_d} \qquad [2.14]$$

where:

a = the time to peak intensity (min),
D = total rainfall volume (mm),
h = maximum rainfall intensity (mm/min), and
T_d = total storm duration (min) (Yen and Chow, 1980).

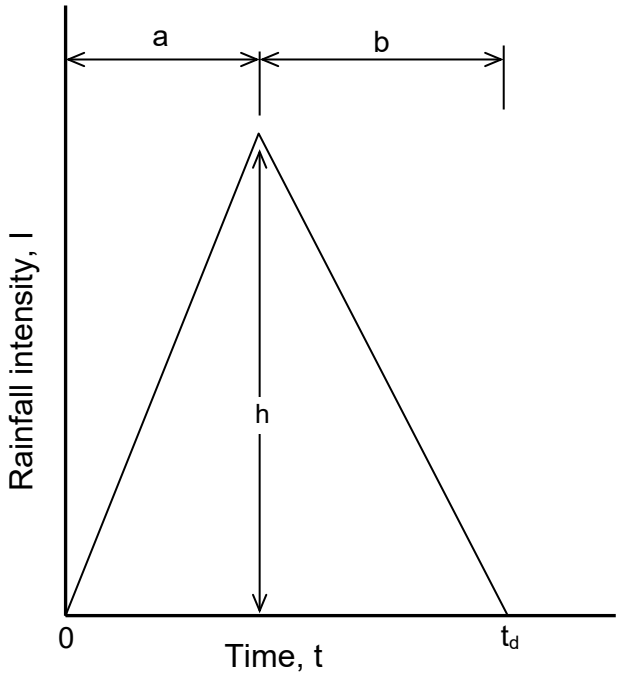

Figure 2.13: Triangular representation of the hyetograph (Yen and Chow, 1980)

To generalise the geometric parameters of each hyetograph for all storm events, Yen and Chow (1980) non-dimensionalised the time to the peak intensity (a) and the maximum rainfall intensity (h) using Equation 2.15 and Equation 2.16 respectively:

$$a^o = \frac{a}{T_d} \qquad [2.15]$$

$$h^o = \frac{h}{\left(\frac{D}{T_d}\right)} = 2 \qquad [2.16]$$

where:

a^o = dimensionless time to the peak intensity, and
h^o = dimensionless maximum rainfall intensity.

Asquith et al. (2007) developed a method to estimate the rainstorm parameters using the dimensionless cumulative hyetograph ordinates and the fraction of storm duration. For fractions smaller and equal to the time to peak intensity, the quantile function Q(F) was expressed in terms of Equation 2.17, and for fractions larger than the time to peak intensity was expressed in terms of Equation 2.18 as follow:

$$Q_1(0 \leq F \leq a^o) = \frac{1}{2}\frac{h}{a}F^2 \qquad [2.17]$$

$$Q_2(a^o < F \leq 1) = \frac{1}{2}h^o a^o + h^o(F - a^o) - \frac{1}{2}\frac{h}{b}(F - a^o)^2 \quad [2.18]$$

By integration of the quantile functions and substitution of the dimensionless peak intensity, the mean of the dimensionless cumulative hyetograph ordinates was expressed in terms of Equation 2.19 as follows:

$$\mu = \frac{2 - a^o}{3} \quad [2.19]$$

where:

- a^o = dimensionless time to peak intensity,
- F = fraction of storm duration,
- h^o = dimensionless peak intensity,
- Q_1 = dimensionless cumulative hyetograph ordinate for fractions of storm durations smaller and equal than a^o,
- Q_2 = dimensionless cumulative hyetograph ordinate for fractions of storm durations larger than a^o, and
- μ = the mean of the dimensionless cumulative hyetograph ordinates (Asquith et al. 2007).

Yen and Chow (1980) conducted a statistical analysis after the determination of the dimensionless parameters. The effect of different total storm durations, total rainfall volumes and different seasons, on the parameters were investigated by applying the triangular hyetograph method to rainstorms which were defined as periods of nonzero rainfall. Altogether 7 484 rainstorms were analysed for three weather stations located in the USA: Boston, Urbana and Elizabeth City. The recorded hyetographs consisted of hourly recorded data. The mean values of the time to peak intensity considering different total storm durations, total rainfall volumes and seasons are depicted in Figure 2.14.

Yen and Chow (1980) also determined that the triangular hyetograph method produces acceptably accurate design hyetographs and applied the method to the experimental data of Izzard (1946) as well as Yu and McNown (1964), which consists of measured runoff hydrographs from artificial catchments. Ellouze et al. (2009) conducted a similar investigation by analysing hourly recorded rainfall data, recorded between 1974 and 1997, at 10 rainfall stations located within a 7.74 km² catchment in central Tunisia. Altogether, 2,799 rainstorms were analysed. According to Ellouze et al. (2009), the observed hyetographs conformed adequately with the synthetic hyetographs. Asquith et al. (2007) used a database of 1 659 storms for 91 small catchments with streamflow gauging stations in Texas. Using the model developed by Asquith et al. (2007), the storm parameters were estimated for two storm duration ranges, 0 to 24 hours, and 24 to 72 hours. For each duration range, storms were classified into a sequence of integer depth intervals. The weighted averages of the mean of the dimensionless hyetographs were 0.59 and 0.55 respectively.

The weighted averages were based on the number of storms in each depth interval. Applying Equation 2.16, the time to peak intensity was 0.23 and 0.35 respectively. The dimensionless cumulative hyetograph depicted in Figure 2.15, was calculated using the quantile functions before and after the peak intensity expressed in terms of Equations 2.17 and 2.18.

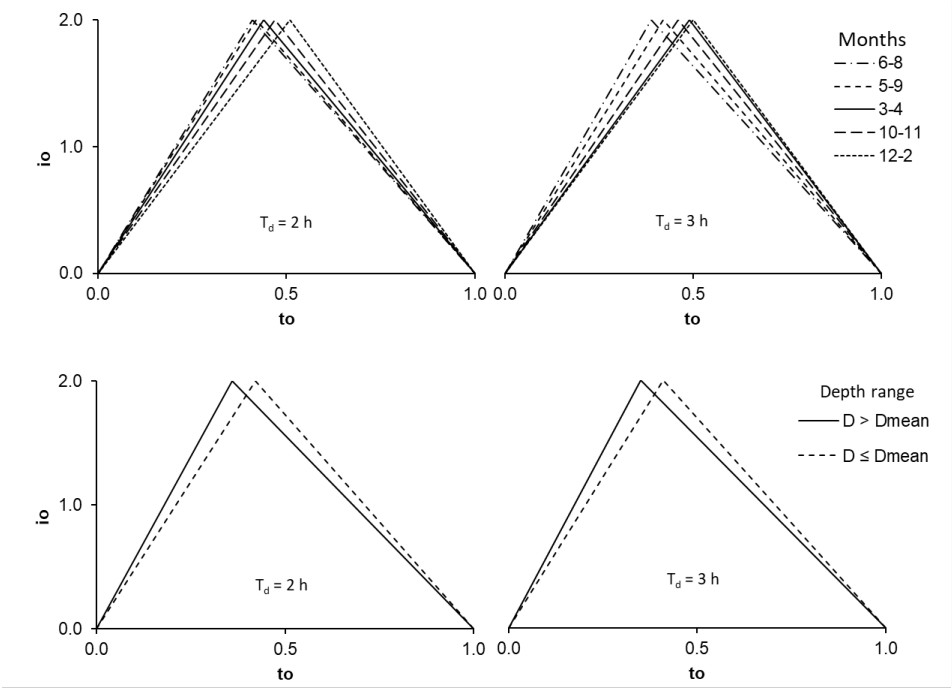

Figure 2.14: Mean values of aº for nondimensional triangular hyetographs for Boston, Massachusetts (Yen and Chow, 1980)

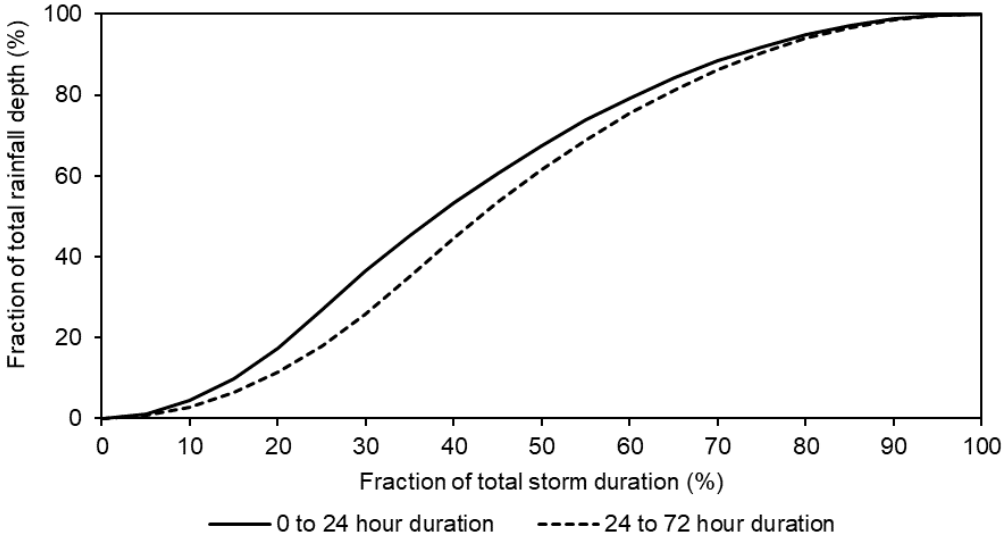

Figure 2.15: Dimensionless cumulative rainfall hyetographs for runoff producing storms having 0 to 24-hour and 24 to 72-hour durations computed by the triangular hyetograph model for Texas (Asquith et al., 2007)

2.7 DAILY RAINFALL DISAGGREGATION MODEL FOR SOUTH AFRICA

Based on the work done by Boughton (2000), Knoesen (2005) developed and assessed a model to disaggregate daily rainfall into hourly rainfall for South Africa. A total of 157 stations, all of which had more than 10 years of hourly data were used to develop this model and to regionalise the distribution of the maximum hourly fraction. According to Boughton (2000), as cited by Knoesen (2005), the model treats each day as an independent event. Therefore, only data of independent events of which all 24 hours from 00:00 to 00:00 with at least 1 mm rainfall recorded were used.

The model is primarily based on the hourly fractions of the daily rainfall; the frequency of the maximum hourly fraction; the clustering of the other 23 hourly fractions; and the arrangement of the clusters into random daily temporal patterns. The average maximum fraction for each independent event was collated into 20 ranges. The average highest 2-hour, 3-hour, 6-hour and 12-hour factions for each range of maximum hourly fraction were calculated. The second-highest hourly fraction added to the highest fraction was then found that best approximates the 2-hour fraction, and the third-highest to approximates the 3-hour fraction and so on, which then formed the clustered sequence (Knoesen, 2005). With the regionalisation of the model, the maximum hourly fraction of all the stations were collated into four revised ranges, and the average distribution of each range was calculated. Using inverse distance weighting, a regionalised map was developed based on the mean value of the maximum hourly fraction. The map, depicted in Figure 2.16, is then used to find the appropriate range for the site of interest.

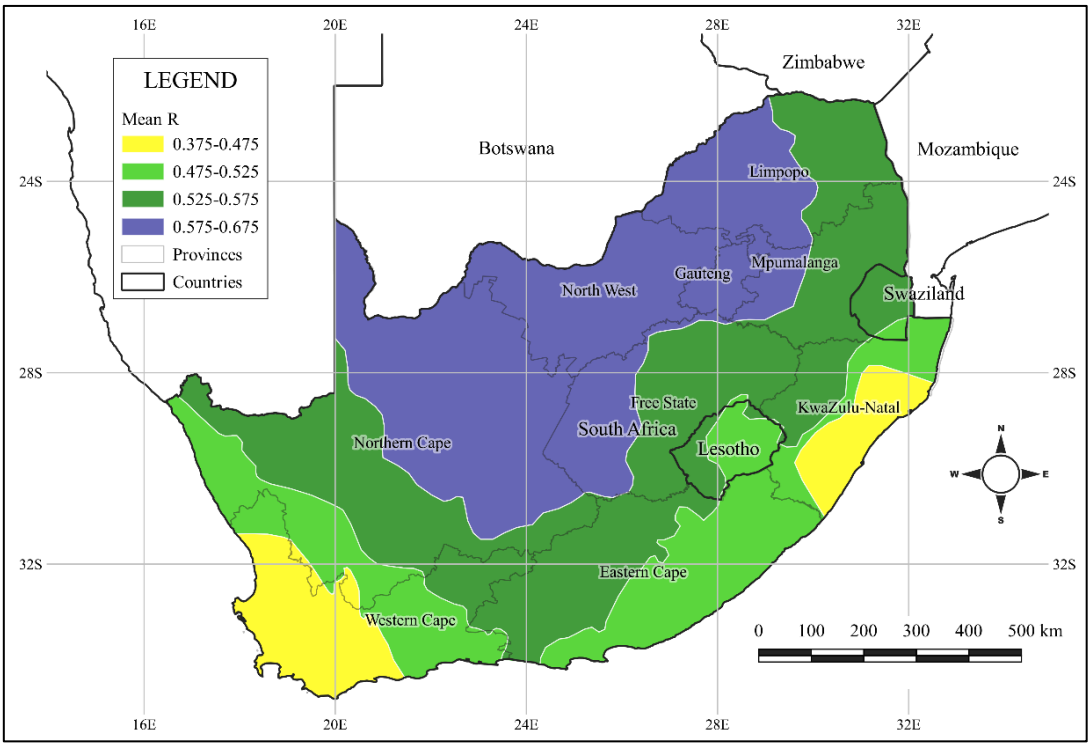

Figure 2.16: Regionalised map of the mean maximum hourly fraction (Knoesen, 2005)

The advantage of this model is that it can be applied to a site where only daily recorded rainfall is available since short duration rainfall data are scarce compared to daily rainfall data. However, the disadvantage of this model is that the distribution of the highest fraction, considering the 20 ranges, and the 24 sequencings of the clustered fractions selected by Boughton (2000), results in 480 different temporal patterns (Knoesen, 2005), whereas the focus of this study is on single event modelling. Furthermore, this model disaggregates daily rainfall into hourly rainfall, whereas sub-hourly disaggregation would be more appropriate for this study. Based on this, this model was not considered.

2.8 SUMMARY AND CRITICAL EVALUATION OF METHODS

As identified in the literature review, the existing synthetic design storms have a strong scientific basis. It guides the classification of existing synthetic design storms into three categories, which is an adaptation of the four categories defined by Veneziano and Villani (1999), as follows (Figure 2.17):

(a) Methods that are derived from the Intensity Duration Frequency (IDF) curves:

   i. Methods based on a simple geometrical shape using a single point on the IDF curve. This category includes the rectangular and triangular methods;

   ii. Methods that use the entire IDF curve, which includes the CDS method and to some degree the SCS and SCS-SA curves;

(b) Standardised mass curves generated directly from rainfall records, which includes the Huff and NOAA Atlas 14 curves; and

(c) The simulation from a stochastic rainfall model, which includes the daily rainfall disaggregation model for South Africa.

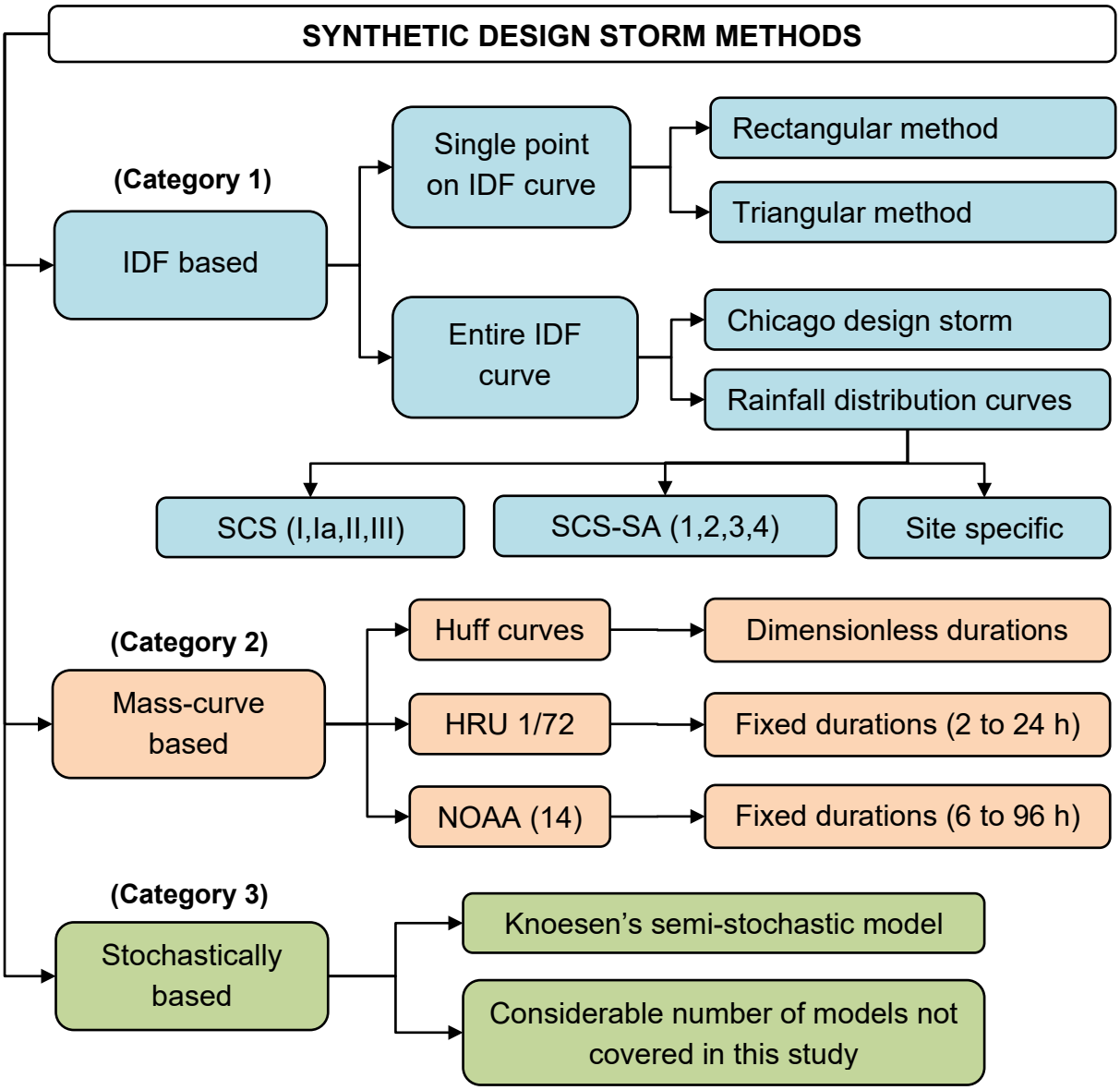

Figure 2.17: Categorization of synthetic design storm methods covered in the literature review

Although the existing synthetic design storms were developed using the best data, technology, and engineering judgement available at the time, they do present some degree of insufficiency. For example, the total precipitation volume is systematically underestimated by the rectangular hyetograph (Arnell, 1982), and it was also realised that it gives a wrong picture of a hyetograph (Niemczynowicz, 1982). In terms of the triangular hyetograph method, Veneziano and Villani (1999) have noticed that, although it is quite simple and intuitive, it does not have a strong conceptual basis and may produce biased flow estimates. The CDS method, on the other hand, utilises point rainfall data that applies to a particular site and therefore the variability and unique character of the rainfall patterns will automatically be embedded in the CDS method.

However, the CDS overestimates the peak discharge comparing with results from a continuous simulation modelling analysis (Malik and James, 2007). Veneziano and Viallani (1999) state that it tends to overestimate the peak discharge because it produces an unrealistic single event.

Methods that utilise the entire IDF curve to generate a synthetic design storm hold much potential since the design rainfall has been regionalised by Smithers and Schulze (2000). Some of the variability and unique character of the rainfall pattern will therefore automatically be embedded in these methods. In terms of Huff curves, Adamson (1981) suggested that it may be considered representative of regions in Southern Africa with similar rainfall climate and topography to the Mid-West of the United States of America (USA). However, to determine the similarity, variables like latitude, longitude, altitude, distance from the sea, mean annual precipitation (MAP) need all to be considered. Sufficient data also exists which provide for an opportunity to develop similar type curves for the Gauteng province. The standard SCS Types I and II curves, on the other hand, were developed from data in the USA during the 1960 and 1970s. These curves are, however, in the process of being replaced by the NOAA Atlas 14 curves, which are regionalised curves for the USA, developed similarly to the Huff curves (NRCS, 2019), using the latest rainfall data. The standard SCS Types I and II curves were originally adopted for use in South Africa (Schulze and Arnold, 1979), but were further developed into four revised curves by Weddepohl (1988) as cited by Ramlall (2020). The four curves were regionalised, resulting in the SCS-SA Type 1, 2, 3 and 4 curves (Ramlall, 2020). Following the regionalisation map of the four SCS-SA curves, Type 3 applies to the Gauteng province, as well as the North-West, Northern Cape, and parts of the Eastern Cape, Mpumalanga, and Limpopo provinces. However, from practical experience, it appears that the Type 3 curve yields peak discharges that seem too high for specific sites in Gauteng when applied to a SWMM model (Males et al., 2004). This is partly due to too high ratios for the D-hour to one-day rainfall compared to the ratios calculated using the design rainfall of Smithers and Schulze (2000).

CHAPTER 3: DATA COLLECTION AND STORM EVENT IDENTIFICATION

The first aim of this study is to identify and assess the performance of currently available methods to estimate synthetic design storms used as input for single-event modelling in the selected pilot study area. In order to achieve this aim, short-duration rainfall data for the study area had to be collated and reviewed, and applicable observed storm events identified. This chapter describes the data collection, quality assessment and storm event identification processes applied in this study.

3.1 SAWS RAINFALL DATA SOURCE

Rainfall data, recorded in 5-min intervals, were obtained from the SAWS for 35 stations situated in Gauteng. The stations consist of four Weather Office Stations (WO), 13 Automatic Weather Stations (AWS) and 17 Automatic Rain Stations (ARS). The locations of the stations are depicted in Figure 3.1 and their general details summarised in Table 3.1.

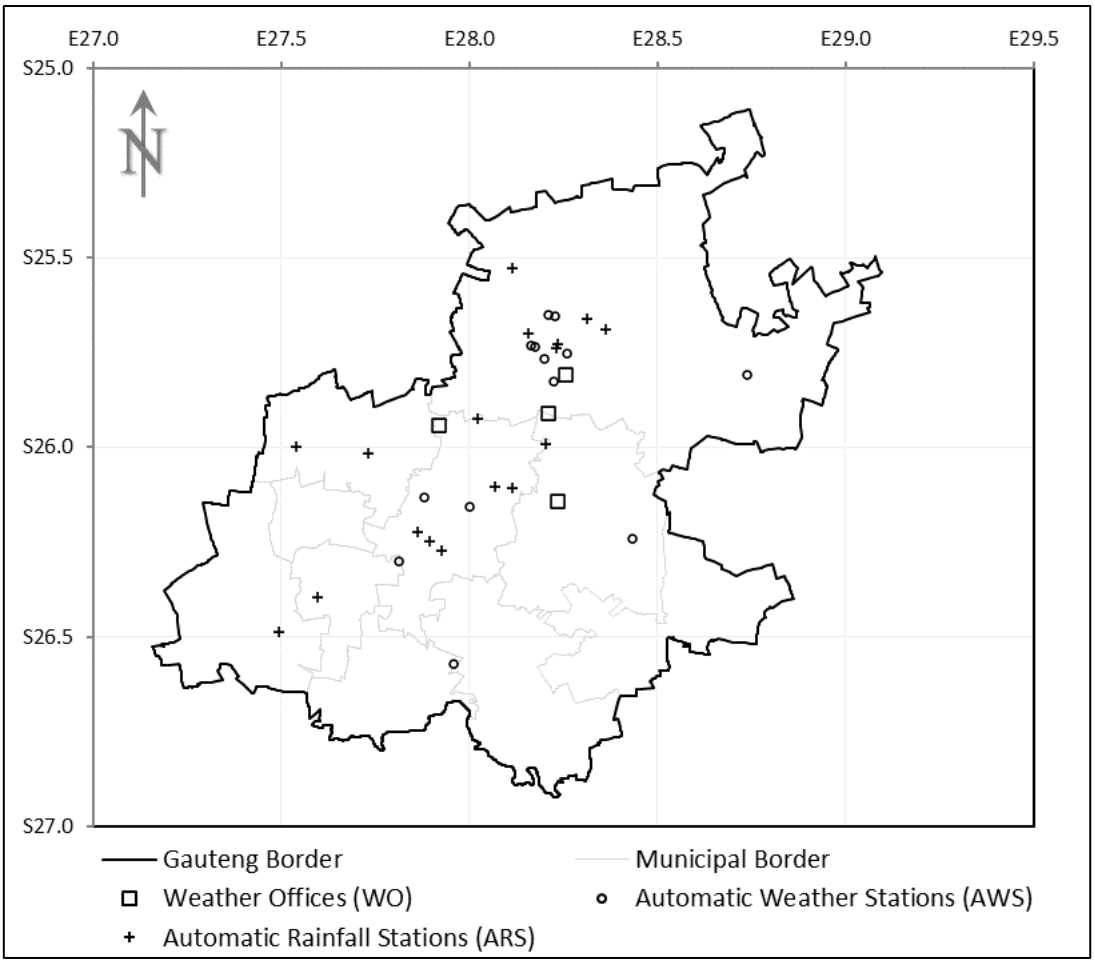

Figure 3.1: SAWS stations with short duration rainfall data in Gauteng

Rainfall is recorded at all the stations using a tipping bucket rain gauge, which consists of a funnel and a seesaw-like container that is divided in the middle into two individual compartments. The funnel channels the rainfall into the bucket, one compartment at a time, with a rainfall resolution of 0.2 mm. When the bucket tips an electronic pulse is sent to a data logger which records the total number the bucket has tipped in 5-min and translate it to a rainfall depth. The data logger records a zero value for each 5-min interval during periods of no rainfall. If the power supply is interrupted, the data logger will not record which will result in a gap in the dataset. The data recordings are described in detail in the next section.

Table 3.1: SAWS short duration rainfall stations in Gauteng

ID	Name	Number	Latitude	Longitude	Type	Data Period (Years)
1	Jhb OR Tambo	0476399_0	26.1430	28.2346	WO	26.2
2	Lanseria	0512746_7	25.9436	27.9188	WO	10.7
3	Irene	0513385A2	25.9105	28.2106	WO	26.2
4	Bolepi House	0513439A1	25.8094	28.2564	WO	17.6
5	Vereeniging	0438784_3	26.5699	27.9582	AWS	26.2
6	Zuurbekom	0475528B7	26.3008	27.8136	AWS	6.3
7	Kloofendal	0475637_1	26.1308	27.8799	AWS	3.9
8	Jhb Bot Gardens	0475879_0	26.1566	27.9991	AWS	26.1
9	Springs	0476764_2	26.2395	28.4351	AWS	3.9
10	Bronkhorstspruit	0514408AX	25.8087	28.7386	AWS	11.7
11	Waterkloof AFB	0513379_8	25.8277	28.2235	AWS	7.9
12	Pretoria Unisa	0513346_0	25.7663	28.2005	AWS	26.2
13	Pretoria Proefplaas	0513435A4	25.7520	28.2585	AWS	9.9
14	Pretoria Pur	0513284_8	25.7351	28.1760	AWS	2.5
15	Pretoria TUT	0513253B3	25.7301	28.1627	AWS	1.9
16	Wonderboom RWY11	0513339B8	25.6516	28.2115	AWS	0.4
17	Wonderboom RWY24	0513369C4	25.6525	28.2272	AWS	0.4
18	Fochville Police	0474899_9	26.4877	27.4941	ARS	9.3
19	Westonaria Kloof	0475174_4	26.3944	27.5979	ARS	9.3
20	Goudkoppies	0475736B8	26.2715	27.9265	ARS	11.0
21	Dube	0475674_5	26.2466	27.8947	ARS	9.2
22	Dobsonville	0475613_X	26.2232	27.8626	ARS	9.2
23	Magaliesburg Police	0512090_5	25.9980	27.5386	ARS	9.2
24	Sterkfontein	0475361_8	26.0174	27.7317	ARS	11.2
25	Jhb Sandton	0476096_0	26.1026	28.0690	ARS	10.8
26	Alexandra Depot	0476156_X	26.1088	28.1130	ARS	9.2
27	Ivory Park	0513359_3	25.9906	28.2019	ARS	9.2
28	Diepsloot	0513025_X	25.9239	28.0218	ARS	9.2
29	Pta presidency	0513404_6	25.7394	28.2325	ARS	10.9
30	Pta Rietondale	0513404A0	25.7292	28.2361	ARS	9.7
31	Pta Mountain View	0513222_0	25.6994	28.1567	ARS	9.0
32	Baviaanspoort	0513611_4	25.6908	28.3633	ARS	9.3
33	Kameeldrift	0513550_3	25.6603	28.3144	ARS	9.8
34	Shoshanguve	0550115_8	25.5289	28.1137	ARS	11.4
35	Wonderboom	0513369_0	25.6631	28.2166	AWS	10.6

3.2 DATA COLLATION

Each rain gauge is equipped with a solar panel and a General Packet Radio Service (GPRS) so that data can be remotely downloaded. Each AWS and ARS is assigned to a WO from where the data for the previous day's recordings are downloaded daily. The data then goes through several quality checks before it gets uploaded into the SAWS database. If any irregularities are noticed in the data during the quality checks which cannot be meteorologically explained, the rainfall recordings are then manually deleted. Therefore, an interval will be present in the data set, but the rainfall column will be left blank. Typical deleted rainfall and missing intervals in a data set are depicted in Table 3.2.

Table 3.2: Typical short duration rainfall data set

Number	Name	Lat	Long	year	month	day	hour	minute	Rain
.....	.....	.....	.....	.....	.....	.....	.....	.....	.....
0476399_0	JHB INT WO	-26,14	28,23	1994	12	31	1	35	0,0
0476399_0	JHB INT WO	-26,14	28,23	1994	12	31	1	40	0,0
0476399_0	JHB INT WO	-26,14	28,23	1994	12	31	1	45	0,0
0476399_0	JHB INT WO	-26,14	28,23	1994	12	31	1	50	0,0
0476399_0	JHB INT WO	-26,14	28,23	1994	12	31	1	55	0,0
0476399_0	JHB INT WO	-26,14	28,23	1994	12	31	2	0	0,0
0476399_0	JHB INT WO	-26,14	28,23	1995	1	1	2	5	0,0
0476399_0	JHB INT WO	-26,14	28,23	1995	1	1	2	10	0,0
0476399_0	JHB INT WO	-26,14	28,23	1995	1	1	2	15	0,0
0476399_0	JHB INT WO	-26,14	28,23	1995	1	1	2	20	0,0
0476399_0	JHB INT WO	-26,14	28,23	1995	1	1	2	25	0,0
.....	.....	.....	.....	.....	.....	.....	.....	.....	.....
0476399_0	JHB INT WO	-26,14	28,23	2000	10	20	17	15	0,2
0476399_0	JHB INT WO	-26,14	28,23	2000	10	20	17	20	0,0
0476399_0	JHB INT WO	-26,14	28,23	2000	10	20	17	25	0,0
0476399_0	JHB INT WO	-26,14	28,23	2000	10	20	17	30	0,0
0476399_0	JHB INT WO	-26,14	28,23	2000	10	20	17	35	
0476399_0	JHB INT WO	-26,14	28,23	2000	10	20	17	40	
0476399_0	JHB INT WO	-26,14	28,23	2000	10	20	17	45	
0476399_0	JHB INT WO	-26,14	28,23	2000	10	20	17	50	
0476399_0	JHB INT WO	-26,14	28,23	2000	10	20	17	55	
0476399_0	JHB INT WO	-26,14	28,23	2000	10	20	18	0	
0476399_0	JHB INT WO	-26,14	28,23	2000	10	20	18	5	
0476399_0	JHB INT WO	-26,14	28,23	2000	10	20	18	10	
0476399_0	JHB INT WO	-26,14	28,23	2000	10	20	18	15	
0476399_0	JHB INT WO	-26,14	28,23	2000	10	20	18	20	
0476399_0	JHB INT WO	-26,14	28,23	2000	10	20	18	25	
0476399_0	JHB INT WO	-26,14	28,23	2000	10	20	18	30	
0476399_0	JHB INT WO	-26,14	28,23	2000	10	20	18	35	0,0
0476399_0	JHB INT WO	-26,14	28,23	2000	10	20	18	40	0,0
.....	.....	.....	.....	.....	.....	.....	.....	.....	.....

Missing intervals

Deleted rainfall

3.3 DATA PROCESSING

The short duration rainfall data sets were processed using a Java application called the Rainfall Processor (Rain-Pro), which was developed using IntelliJ IDEA Community Edition 2019.1.3 and JDK 1.8 with JRE 1.8 (Munro, 2021, personal communication, 23 August). Subsequent analysis of the data was done using Microsoft (MS) Excel. The order in which the data was processed is summarised in the flow chart depicted in Figure 3.2.

The process began with the short duration rainfall data of a station (RAW DATA SET.txt) as input for the Rain-Pro software, and the output consists of three files. The first being the PROCESSED.txt file, which consisted of the rainfall data, except for all intervals with zero rainfall. This file was used as input to the ANNUAL MAXIMUM SERIES.xlsx, which provided the input for the STATISTICAL ANALYSIS.xlsx file. This file provided the design rainfall estimations as described in Section 4.2. The PROCESSED.txt file was also used as input to the MS Excel file, STORM FILTER.xlsx, which applied the maximum dry period and the minimum rainfall depth criteria, described in Sections 3.5.1 and 3.5.2, respectively. After applying the maximum dry period and minimum rainfall depth criteria, the STORM FILTER.xlsx file provided the start and end dates of all individual events, which was used to create the STRIP DATES.txt file. The second output file of the Rain-Pro software, the MISSING_INTERVAL.txt file, contained the missing data which was subsequently used as input to the MISSING ANALYSER.xlsx file as described in Section 3.4. The third output file of the Rain-Pro software, the STATS.txt file provided a summary of the data set. This summary consisted of the total number of lines processed, total number of lines with zero rainfall as well as lines with rainfall larger than zero, the start and end dates of the data set, the data period, and the total duration of missing data.

The Rain-Pro software was executed for a second time, which extracted the individual events from the RAW DATA SET.txt file according to the STRIP DATES.txt file. The output from the Rain-Pro software, after the second run, consisted of the storm event files, 0M_EVENTS.txt, 15M_EVENTS.txt, etc., which contained the individual events according to the maximum dry period and minimum rainfall depth criteria. These files were used as input to the RI FILTER.xlsx file, which applied the minimum rainfall intensity criterion described in Section 3.5.3. The RI FILTER.xlsx file provided the start and end dates of the significant events, which was used to update the STRIP DATES.txt file.

The Rain-Pro software was executed for a third time, and the storm event files were subsequently updated. These files contained the rainfall data of only the significant events which were used as input for the STORM PARAMETERS.xlsx file. This file determined the storm parameters described in Sections 4.1.2 and 4.1.3, respectively. The storm event files were also used as input for the SHAPE ASSESSMENT.xlsx and INTENSITY ASSESSMENT.xlsx files, which were used for the storm shape and average intensity assessments described in Sections 5.1 and 5.3.

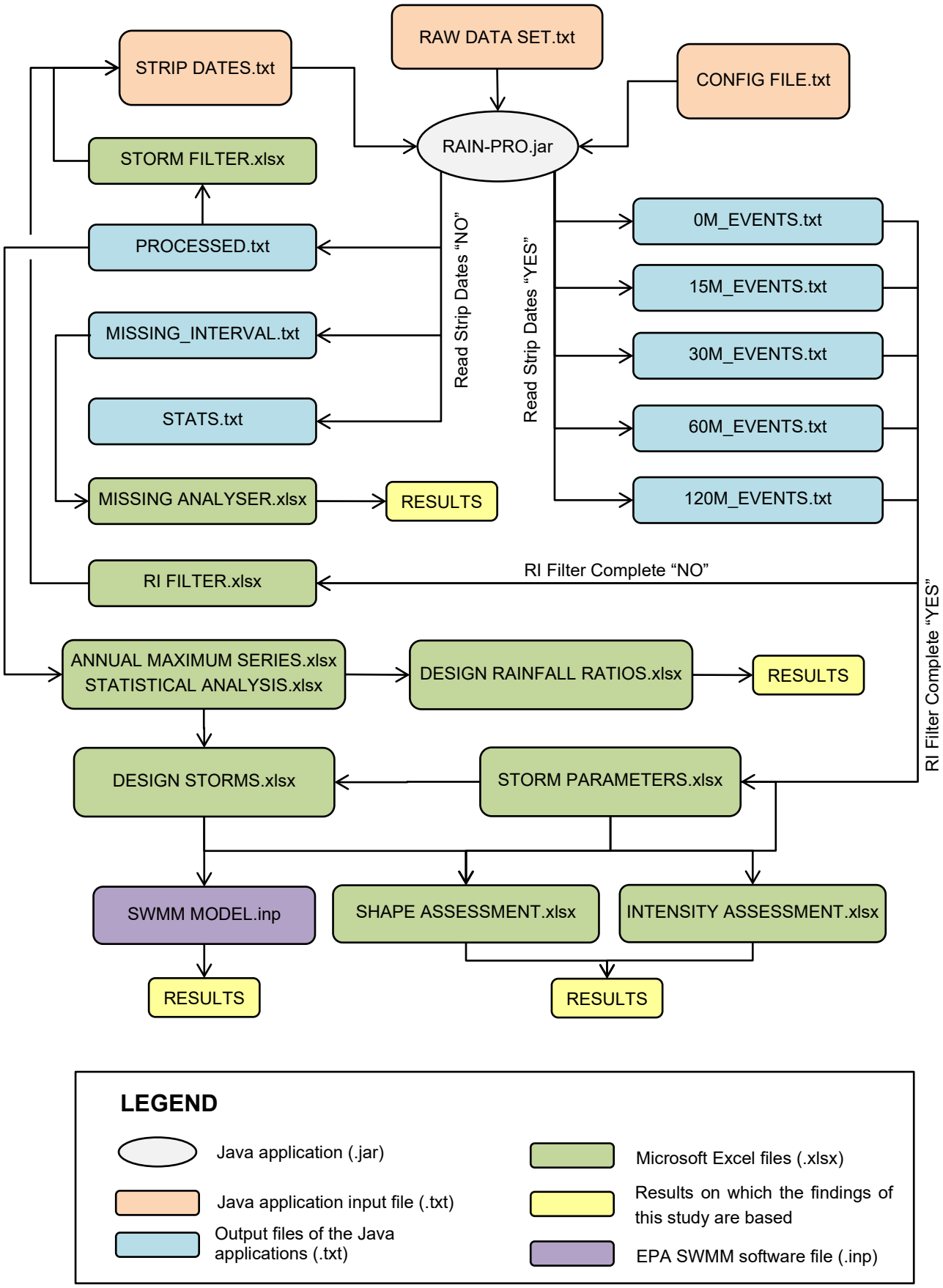

Figure 3.2: Data processing flow chart

3.4 MISSING DATA ANALYSIS

The missing data analysis was done by identifying missing periods of data, consisting of missing 5-min intervals, as well as intervals that had no rainfall value assigned, as depicted in Table 3.2. The information of all the missing periods of each station was written to a separate text file (MISSING_INTERVAL.txt) which was used for further processing in MS Excel. The time of the year when missing data occurs was taken into consideration. The average monthly rainfall, depicted in Figure 3.3, for the three stations situated at O.R. Tambo International Airport, Irene, and Johannesburg Botanical Gardens, were used to guide this process. Also indicated in Figure 3.3 are the minimum and maximum values of the three stations, which indicates the variances in the average rainfall. Based on this analysis, the months of May to September were considered to be 'dry' months and as a result, missing data occurring during these months were assumed to be zero rainfall. Only missing data occurring during the 'wet' months were used for the classification of the data quality.

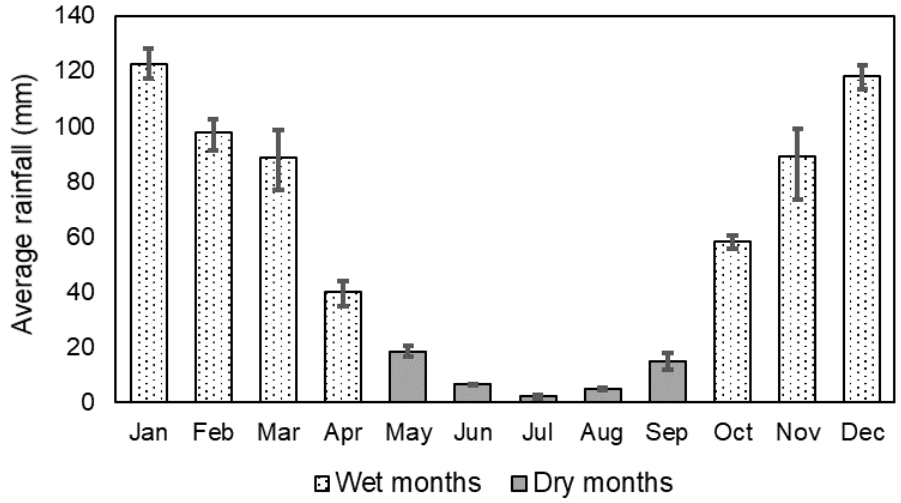

Figure 3.3: Average monthly rainfall for O.R. Tambo, Irene and Jhb Bot Gardens

The data quality of each station was characterised according to the criteria summarised in Table 3.3 and the results are summarised in Table 3.4. Stations with data periods of more than 20 years and periods of missing data during 'wet' months of less than 5% were classified as stations with good data sets. These stations were used to determine the storm parameters and design rainfall estimation described in Chapter 4. They were also used for the shape and intensity assessments, as well as the continuous simulation modelling described in Chapter 5. Data period of less than 20 years but more than 10 years, and missing data less than 20%, were classified as Average data sets. These stations were considered to be less reliable and were only used for the design rainfall estimation. Data period of less than 10 years, and missing data of more than 20%, were classified as poor sets. These stations were omitted from this study due to the data sets being incomplete. In total 35 stations were assessed, with five having good data sets, 17 average, and 13 poor, as depicted in Figure 3.4.

Table 3.3: Data quality classification criteria

Description		Data Period		
		years ≥ 20	20 > years ≥ 10	10 > years
Missing data during wet months	≤ 5%	Good	Average	Poor
	≤ 20%	Average	Poor	Poor
	> 20%	Poor	Poor	Poor

Table 3.4: Missing data analysis summary

ID	Name	Data Period (Years)	Missing Data (%)		Data Quality
			All year round	Wet months	
1	Jhb OR Tambo	26.2	1.9	1.0	Good
2	Lanseria	10.7	1.1	1.0	Average
3	Irene	26.2	1.2	0.7	Good
4	Bolepi House	17.6	16.3	10.6	Average
5	Vereeniging	26.2	6.9	5.2	Good
6	Zuurbekom	6.3	1.4	0.6	Poor
7	Kloofendal	3.9	17.9	17.0	Poor
8	Jhb Bot Tuine	26.1	4.1	2.8	Good
9	Springs	3.9	55.7	31.7	Poor
10	Bronkhorstspruit	11.7	3.5	3.0	Average
11	Waterkloof AFB	7.9	7.6	7.0	Poor
12	Pretoria Unisa	26.2	8.6	4.7	Good
13	Pta Proefplaas	9.9	1.4	1.1	Average
14	Pretoria Pur	2.5	18.3	3.3	Poor
15	Pretoria TUT	1.9	23.5	19.6	Poor
16	Wonderb. RWY11	0.4	17.0	16.3	Poor
17	Wonderb. RWY24	0.4	10.1	8.8	Poor
18	Fochville Police	9.3	2.2	2.0	Average
19	Westonaria Kloof	9.3	13.4	7.8	Average
20	Goudkoppies	11.0	6.5	4.2	Average
21	Dube	9.2	9.2	5.8	Average
22	Dobsonville	9.2	25.5	17.2	Average
23	Magalies Police	9.2	40.0	18.8	Average
24	Sterkfontein	11.2	11.8	6.8	Average
25	Jhb Sandton	10.8	8.2	7.1	Average
26	Alexandra Depot	9.2	7.3	6.1	Average
27	Ivory Park	9.2	20.4	12.4	Average
28	Diepsloot	9.2	3.9	2.6	Average
29	Pta presidency	10.9	35.1	23.2	Poor
30	Pta Rietondale	9.7	51.5	31.3	Poor
31	Pta Mount. View	9.0	42.1	23.0	Poor
32	Baviaanspoort	9.3	38.0	22.6	Poor
33	Kameeldrift	9.8	52.7	31.6	Poor
34	Shoshanguve	11.4	13.2	9.3	Average
35	Wonderboom	10.6	4.5	3.5	Average

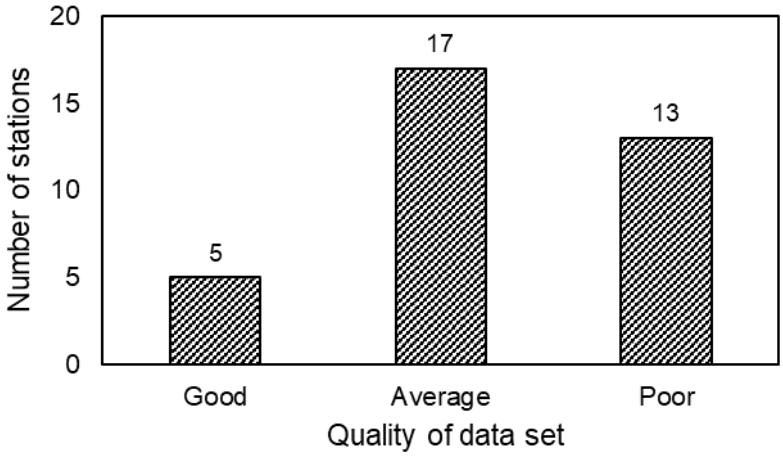

Figure 3.4: Total number of stations according to quality classification criteria

A further assessment of the data quality was conducted by comparing the daily rainfall data measured by a standard non-recording raingauge at 08:00 every day with the 5-min data accumulated for the same 24 h period. The daily rainfall at each WO is recorded daily at 08:00 am, using a standard non-recording rain gauge that is independent from the automatic rain gauge. To verify the accuracy of the 5-min data, the total rainfall was determined between 08:00 am of each day and the previous day. The total rainfall for each day was then compared with the recorded daily rainfall. For example, the difference at the OR Tambo station between the two totals, on a daily scale, is depicted in Figure 3.5. This was compiled by subtracting the total rainfall from the 5-min data between 08:00 and 08:00, from the daily rainfall. It was observed that the daily rainfall was frequently assigned to the incorrect day. For example, the total rainfall from the 5-min data on 29 April 1995, was 23.4 mm. The same value was recorded in the daily rainfall, but on the day before. The same applies to all intervals where two identical amounts are depicted but in opposite directions, for example, 26 January 2015.

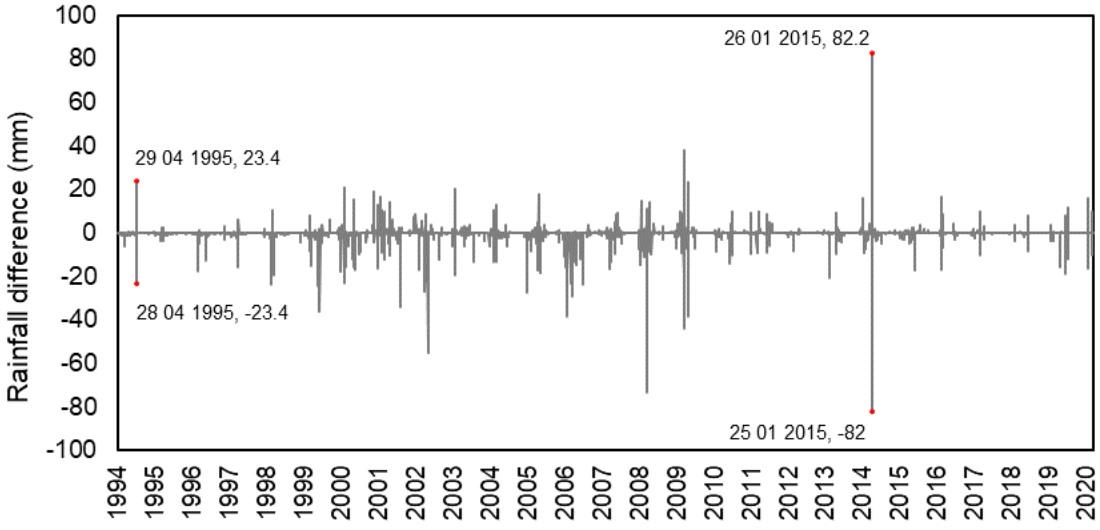

Figure 3.5: Rainfall difference between daily and 5-min data on a daily scale at O.R. Tambo station

Due to the discrepancy between the dates of the daily and 5-min rainfall, the verification could not be conducted daily. The verification was therefore conducted by comparing the annual maximum daily rainfalls from the daily and the 5-min data as depicted in Figure 3.6. The highest discrepancies are observed for the years 2001, 2006, 2009 and 2020. However, according to Figure 3.7, the missing data for O.R. Tambo occurred mostly between 1999 and 2003. This provided the basis to conclude that there were substantial discrepancies between the daily and the 5-min rainfall data and that more investigation is needed. It was, however, assumed for this study that the 5-min data is sufficiently accurate to conduct this study.

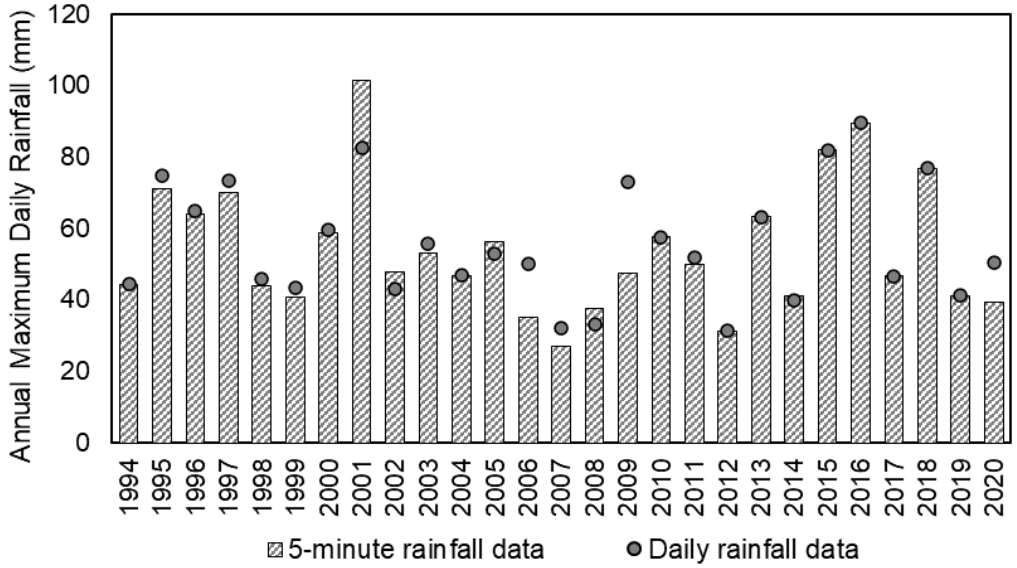

Figure 3.6: Annual maximum daily rainfall from the 5-min and daily rainfall data for the O.R. Tambo station

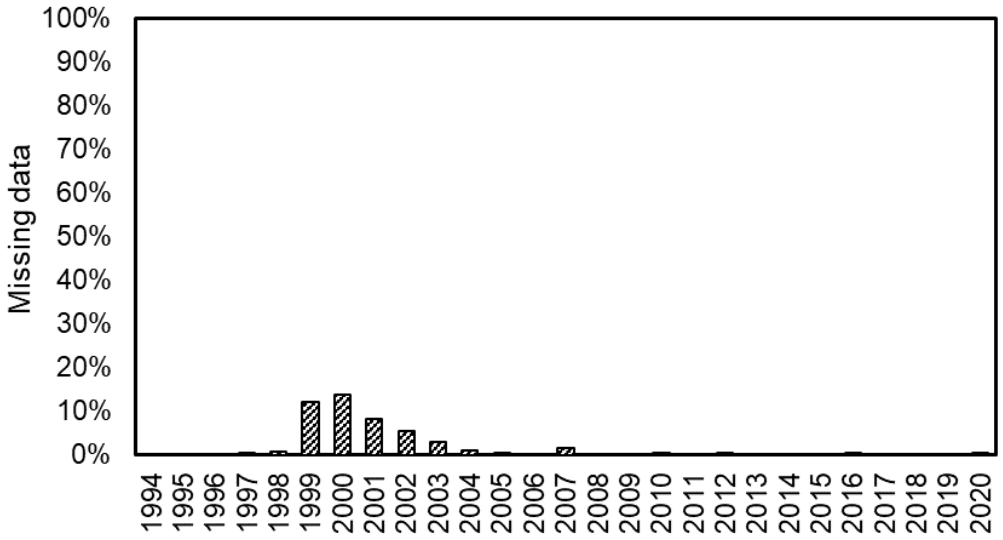

Figure 3.7: Annual missing data for the O.R. Tambo station

3.5 STORM EVENT IDENTIFICATION

A single event-based methodology was adopted for this study to identify independent storm events. Generally, this methodology consists of defining an allowable Maximum Dry Period (MDP) between rainfall spells, as depicted in Figure 3.8, as well as a Minimum Rainfall Depth (MRD) threshold. This methodology was adapted by the addition of a third threshold criterion that is related to the Minimum Rainfall Intensity (MRI) of the storm event. The three criteria and the results are described in this section.

3.5.1 Maximum Dry Period (MDP)

The MDP criterion refers to the threshold period of no rainfall that occurs between two rainfall spells. If the dry period exceeds the MDP threshold, then the two spells are considered as two separate events. Conversely, if the dry period is less than the MDP, then the two spells are considered as one event. This concept is depicted in Figure 3.8. Different methods to identify dry periods are documented in the literature. For example, Huff (1967) used a maximum of 6-hours to separate independent rainfall events. Ramlall (2020) initially used 6-hours as the MDP but found that events frequently included extensive periods of low to zero rainfall. Subsequently, the MDP was reduced to 1-hour which resulted in an improved coefficient of determination (R^2) between total rainfall depth and total storm duration.

The MDP can also be determined by considering the statistical independence of events using an empirical relation for estimating the minimum time between independent events (Restrepo and Eagleson, 1980). This process involves the computation of the mean and standard deviation of dry periods in a continuous rainfall data set. In an iterative process, the smallest dry periods are omitted until the mean and standard deviation is equal (Bonta, 2004). However, for this study, the MDP was systematically increased from 0 to 120-min to identify idealised independent events on which the assessments were conducted. In other words, each data set was assessed from start to finish using a zero MDP criterion. Then a second assessment was conducted on the same data set but with a 15-min MDP criterion, then the 30-min MDP, and so on. The total rainfall depth and total storm duration of a particular storm event could therefore differ depending on the MDP used to distinguish between idealised events.

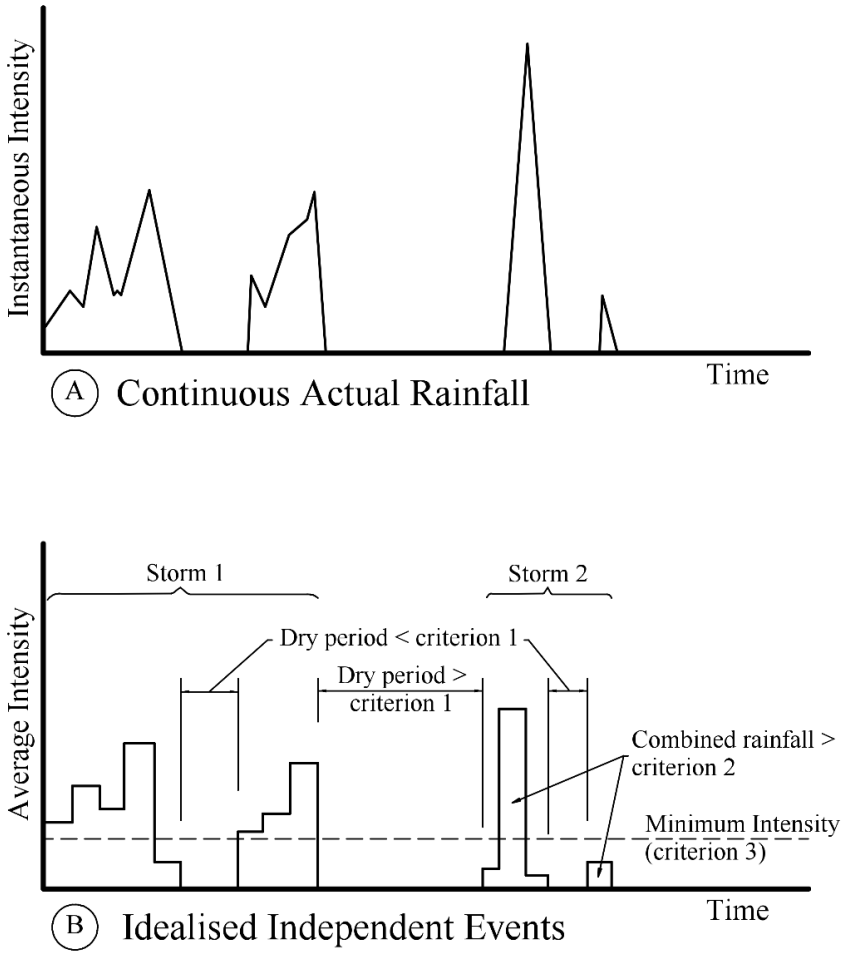

Figure 3.8: Idealised independent events (after Restrepo and Eagleson, 1982)

3.5.2 Minimum Rainfall Depth (MRD)

Following the separation of the continuous rainfall data into individual storm events, the total rainfall of each event was considered. A storm event was ignored if the total rainfall was less than 10 mm. The minimum rainfall of 10 mm was selected considering the design rainfall obtained from the computer software, Design Rainfall Estimation in South Africa (DRESA) (Smithers and Schulze, 2003), which implements the procedures to estimate design rainfall in South Africa per Smithers and Schulze (2000). For example, the five and 10-min design rainfall for the O.R. Tambo station with a recurrence interval of two years depicted in Figure 3.9 are 8.8 and 12.7 mm, respectively. This implies that if the total rainfall is less than 10 mm, the total duration of the event was between five and 10 min, which would have been recorded in only one or two five-min intervals. The location of the peak intensity of such an event will therefore be either at the beginning of, or the end, of the event whereas it is expected for the peak to be somewhere within the event.

The second argument is that if the total rainfall of 10 mm was achieved over a longer period, the intensities will be lower than the 5-min design rainfall with a two-year recurrence interval.

Therefore, limiting the minimum rainfall to 10 mm to select events ensured that insignificant storm events were eliminated early during the storm event identification process.

User selection has the following criteria:
Coordinates: Latitude: 26 degrees 9 minutes; Longitude: 28 degreess 14 minutes
Durations requested: 5 m, 10 m, 15 m, 30 m, 45 m, 1 h, 1.5 h, 2 h, 4 h, 6 h, 8 h, 10 h, 12 h, 16 h, 20 h, 24 h, 1 d, 2 d, 3 d
Return Periods requested: 2 yr, 5 yr, 10 yr, 20 yr, 50 yr, 100 yr, 200 yr
Block Size requested: 1 minutes

Gridded values of all points within the specified block

Latitude (°)	Latitude (')	Longitude (°)	Longitude (')	MAP (mm)	Altitude (m)	Duration (m/h/d)	Return Period (years) 2	2L	2U	5	5L	5U	10	10L	10U
26	10	28	13	722	1675	5 m	8.8	7.1	10.5	12.1	9.8	14.5	14.7	11.8	17.5
						10 m	12.7	10.0	15.3	17.5	13.9	21.1	21.1	16.7	25.5
						15 m	15.7	12.3	19.1	21.6	17.0	26.3	26.1	20.5	31.8
						30 m	20.1	16.0	24.1	27.7	22.1	33.3	33.5	26.8	40.3
						45 m	23.2	18.7	27.7	32.1	25.8	38.3	38.8	31.2	46.3
						1 h	25.7	20.9	30.6	35.5	28.9	42.3	43.0	34.9	51.1
						1.5 h	29.8	24.4	35.1	41.1	33.7	48.5	49.7	40.7	58.7
						2 h	33.0	27.2	38.8	45.5	37.6	53.5	55.1	45.5	64.7
						4 h	39.5	33.5	45.5	54.6	46.2	62.9	66.0	55.9	76.0
						6 h	43.9	37.8	50.0	60.7	52.2	69.1	73.3	63.1	83.6
						8 h	47.4	41.2	53.5	65.4	56.9	73.9	79.1	68.7	89.3
						10 h	50.2	44.0	56.4	69.3	60.8	77.8	83.8	73.4	94.1
						12 h	52.7	46.4	58.8	72.7	64.2	81.2	87.9	77.5	98.2
						16 h	56.8	50.6	62.9	78.4	69.9	86.8	94.7	84.5	105.0
						20 h	60.2	54.1	66.2	83.1	74.7	91.4	100.4	90.3	110.5
						24 h	63.1	57.1	69.1	87.1	78.9	95.4	105.3	95.3	115.3

Figure 3.9: Typical design rainfall estimation results for O.R. Tambo International Airport obtained from the DRESA software

3.5.3 Minimum Rainfall Intensity (MRI)

The minimum intensity was the final criterion that was applied before an event could be classified as a significant event. The recurrence interval of each storm event was estimated using the DRESA software. The ninety per cent upper (U) and lower (L) bounds for the design rainfall values were not considered for this study. The depth-frequency relationship for the design rainfall was then approximated using an exponential function. The 5-min design rainfall for the O.R. Tambo International Airport station, for example, is depicted in Figure 3.10 as well as the fitted exponential regression line. If the maximum recurrence interval of the event was less than two years, the storm event was ignored. This was done to eliminate storm events with insignificant intensities considering the 5-min to 24-hour design rainfall for each station.

A typical application of this criterion is depicted in Figure 3.11, which was applied to the storm event that occurred at the O.R. Tambo station on 13 March 2011. The total storm duration for this event was 12 hours. A moving window was used to extract the maximum rainfall for each of the standard time steps from 5 minutes to 12 hours. As depicted in Figure 3.11 the 5-min to 6-hour time steps were less than the specified threshold of two years, however, the 8, 10 and 12-hour time steps exceeded the threshold which therefore qualified this storm event.

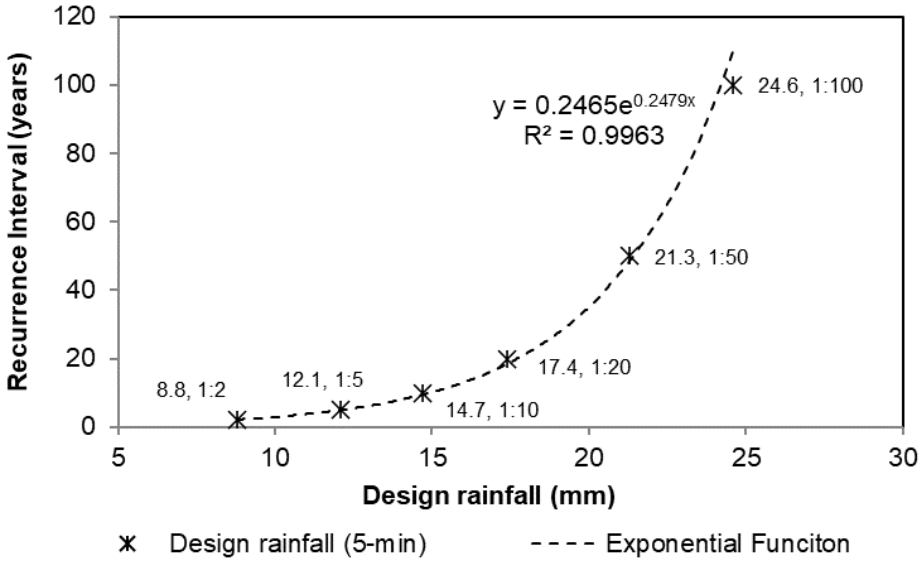

Figure 3.10: Typical depth-frequency relationship for O.R. Tambo International Airport

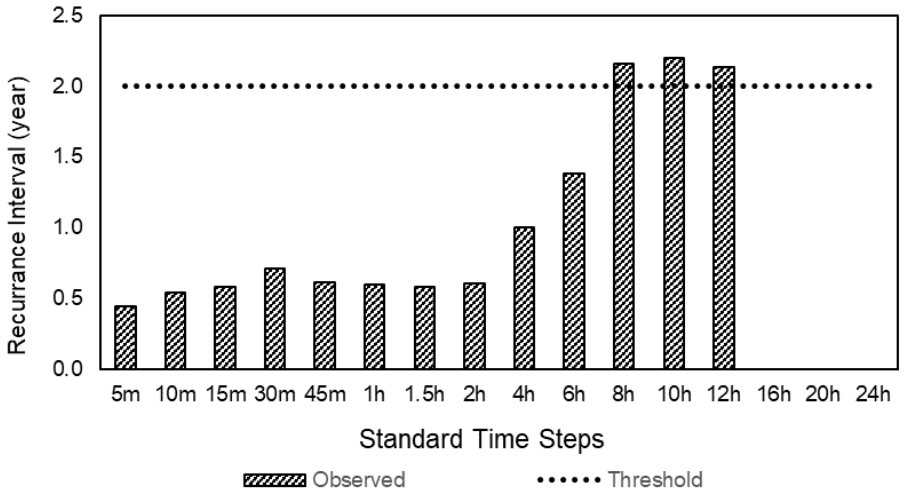

Figure 3.11: Typical maximum recurrence intervals per standard time step for the storm event that occurred on 13 March 2011 at the O.R. Tambo International Airport

3.5.4 Identification of single storm events

The Rain-Pro software was programmed to extract all data records with rainfall values more than zero rainfall from the raw data set. A new data file was then written to a separate text file (PROCESSED.txt). This process simplified the data file in terms of the number of line items, because the data loggers of the SAWS automatic rain gauges continuously records data in 5-min intervals. In any raw data file, more than 95% of the line items have zero rainfall. Because all these items have the same value, namely zero, these items are, therefore, not unique.

All further processing of the new data set could, therefore, assume that all intermediate intervals of time have zero rainfall. The processing of the PROCESSED.txt file was done in MS Excel. For a MDP of 0-min, which means that a storm event ended immediately when precipitation stopped, the total number of storm events identified from the 22 stations with good to average data sets, was 4 052 events. The number of events consistently increased as the dry period increased. This is because of the combined precipitation of short spells, forming a single event that exceeds the threshold of 10 mm, whereas individually the spells do not meet the criterion. As a result, the total number of events for a MDP of 120-min was 5 726. The total number of storm events for the selected stations are depicted in Figure 3.12.

It is also important to note that a large portion of the total number of events consisted of events for which the recurrence interval was less than two years, which are insignificant storm events. Over 80% of the events had a recurrence interval of less than two years. The storm events with recurrence intervals exceeding two years were considered significant, and the analyses were conducted on these events. The frequency of events for the 22 stations with good to average data sets, considering different MDPs, is depicted in Figure 3.13. It can be seen that 80 to 85% of all events are insignificant.

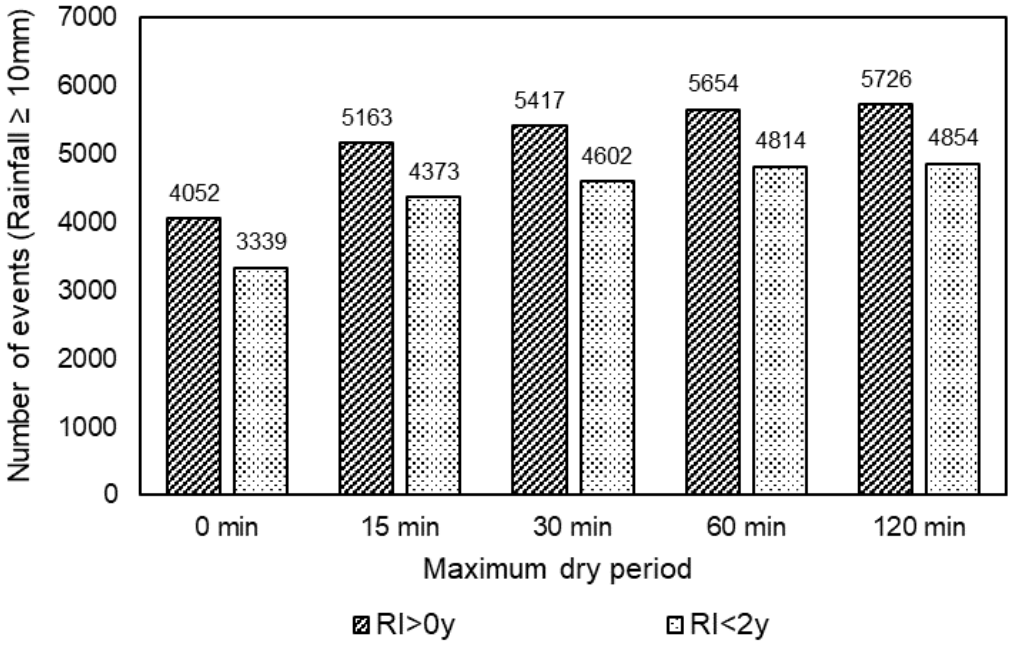

Figure 3.12: Total number of storm events and insignificant events identified based on different MDPs

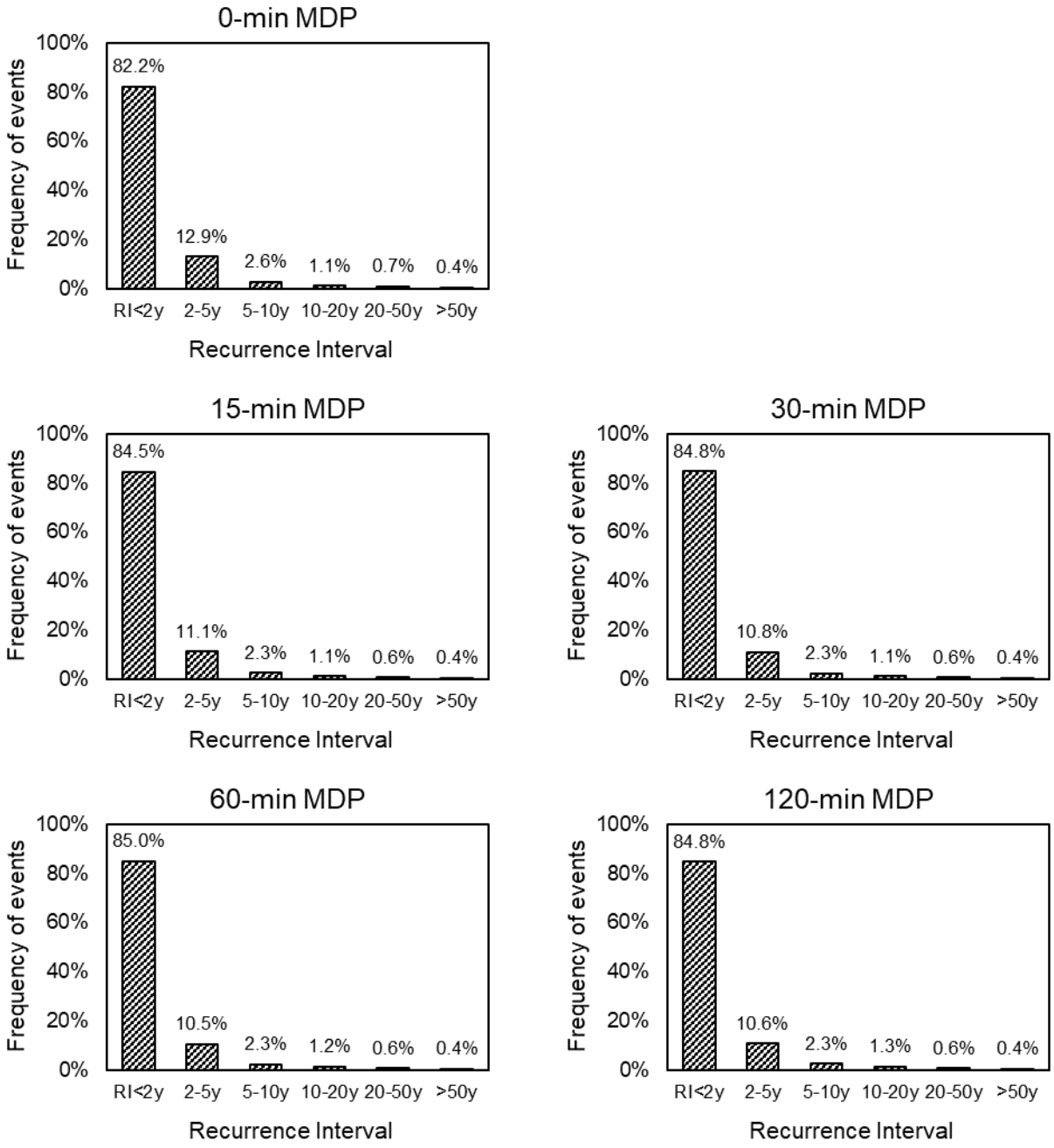

Figure 3.13: Frequency of events based on different MDPs

3.6 CHAPTER SUMMARY

This chapter has provided details about the data source, the collation of the rainfall data, and an overview of the data processing. The missing data analysis was based on the total number of missing periods during rainy months. These months, consisting of January to April and October to December, were identified by considering the average monthly rainfall of the O.R Tambo, Irene and Johannesburg Botanical Gardens stations.

The missing data as well as the data period of each station were used to classify the data quality of each rainfall station. A station was classified as either, good, average or poor, depending on the selected classification criteria. The stations with poor data sets were omitted from the study, whereas the good and average stations are used in Chapter 4 in subsequent investigations. The criteria used for the identification of individual events were also described. These criteria consisted of an MDP ranging from 0 to 120-min, an MRD of 10 mm, and an MRI of 1:2 years. In Chapter 4 a single MDP will be selected and subsequent analyses in the chapter, such as the advancement coefficient and dimensionless time to peak, are based on this MDP.

CHAPTER 4: METHODOLOGY AND DATA ANALYSIS

This chapter consists of seven sections that describe several aspects relating to the generation of synthetic design storms which provides the foundation for Chapter 5. The first section of this chapter describes the extraction of parameters relating to the CDS method, and the dimensionless time to peak relating to the Triangular (TRI) method. The significant storm events identified in the previous chapter were used to determine these storm parameters. The second section describes the design rainfall estimation of stations with good and average data sets as defined in the previous chapter, using Probability Distribution (PD) analysis. The third section describes the methodology that was developed to determine the regression coefficients associated with the CDS method. The fourth section describes the methodology that was adopted and adapted for the distribution of the design rainfall to create a 24-hour synthetic design storm. It also describes the process of extracting storm events from a 24-hour DC which is necessary for comparing the shape of synthetic design storms and significant storm events in the next chapter. The fifth section describes the comparison of the design rainfall ratios with the ratios of the SCS-SA curves and the recommendation with regards to the implementation of intermediate curve types. Due to this comprehensive comparison, the sixth section describes the comparison of the SCS curves with the SCS-SA curves and the conclusion with regards to the use of the SCS curves. In section seven standardised mass curves are developed using the significant storm events identified in the previous chapter.

4.1 STORM PARAMETERS

In this section, an appropriate MPD, as defined in Chapter 3.5, is investigated and selected. Based on this finding, the storm parameters that were then considered include the storm advancement coefficient associated with the CDS method, and the time to the peak intensity associated with the TRI method. The adaptations of the procedures to determine these parameters and the results are described below.

4.1.1 Selection of an appropriate MDP

As noted in Chapter 2 (literature review), Ramlall (2020) based the decision to use an MDP of 1-hour instead of 6-hour, on the improved correlation between total rainfall depth and total storm duration. A similar investigation was initially conducted whereby the correlation was determined using six different MDP criteria, namely, 0-min, 15-min, 30-min, 60-min, 120-min, and 360-min. This investigation was based on the significant storm events of five stations that were pooled together, namely: O.R Tambo, Irene, Vereeniging, Jhb Bot Gardens and Unisa. The results are summarised in Figure 4.1. This indicates that the correlation improves consistently as the MDP increases, but decreases dramatically with an MDP of 360-min.

This finding is consistent with the finding of Ramlall (2020), who found an increase in correlation by decreasing the MDP from 6-hour to 1-hour. However, an optimum correlation should exist with an MDP between 2-hour and 6-hour.

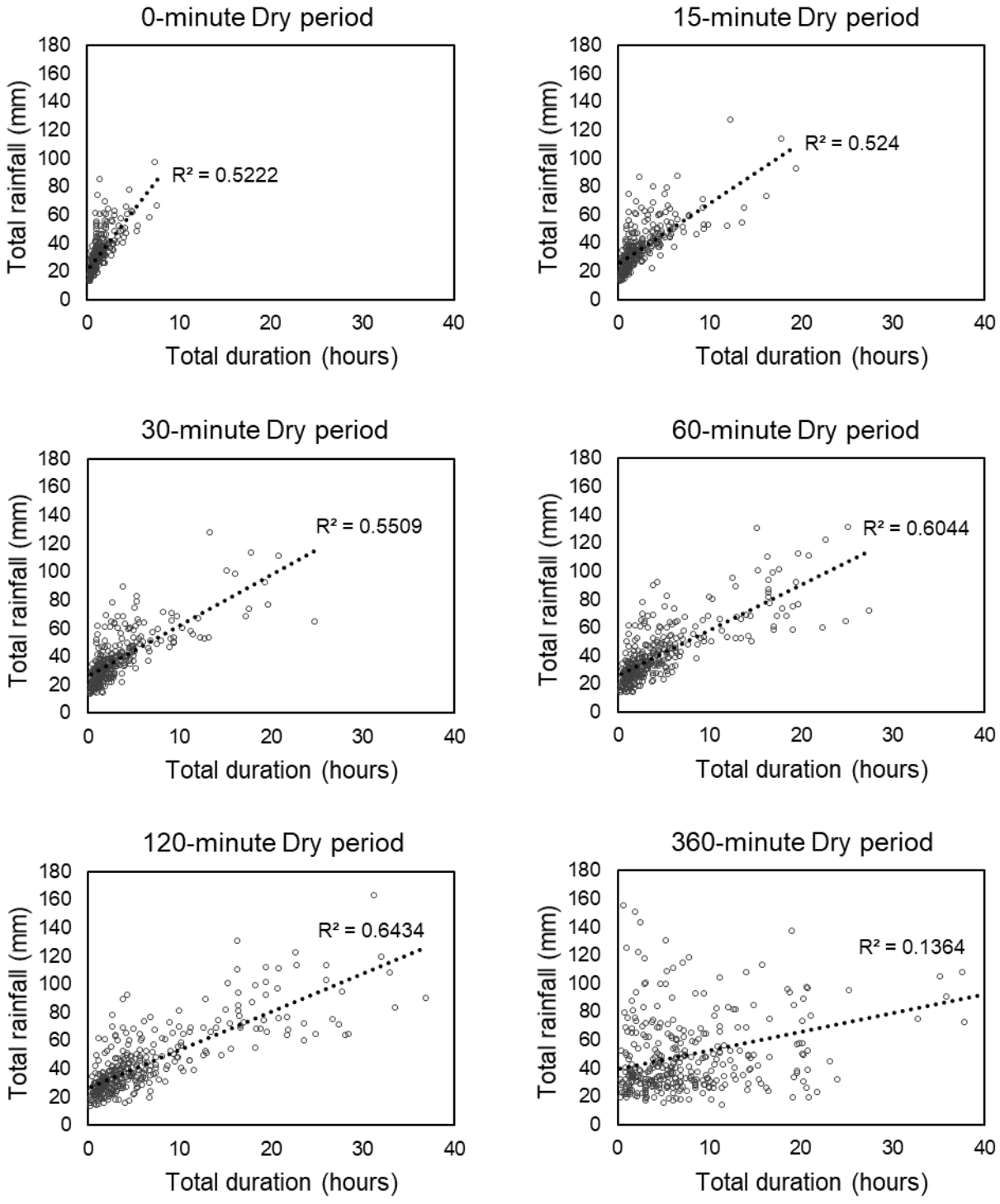

Figure 4.1 Correlation between total rainfall and duration for different MDP criterion

Subsequent to the above initial approach, an alternative approach was taken with this study which based the selection of the MDP on the response time of the catchment. It is argued that if the MDP is longer than the reaction time of a catchment, then any rainfall after a dry period would not impact the peak discharge from the first spell. The second spell is then rather seen as the start of the next event. The Antecedent Moisture Content (AMC) during the second spell is significantly impacted by the first event. The focus of this study is, however, not on the AMC but rather the shape assessment of synthetic design storms. Therefore, the alternative approach is warranted. The typical reaction time of small urban catchments are approximately 15-min, and therefore, the 15-min MDP was selected for this study.

4.1.2 Storm advancement coefficient – CDS method

As detailed in Section 2.3, the storm advancement coefficient was determined in this study using Keifer and Chu's (1957) second approach. Firstly, according to Keifer and Chu's (1957) first approach, the antecedent rainfall was determined by first identifying the maximum rainfall within a 15, 30, 60 and 120-min period within each significant storm event. Each significant storm event was then assumed to be 180 min in total, and the 180 min design rainfall for the 1:5 year storm event was divided on either side of the maximum intensity using the storm advancement coefficient. Since the significant storm events identified for this study were shown to vary significantly in terms of recurrence interval, a single design rainfall would therefore be inappropriate. Secondly, there was an insignificant difference between the coefficients determined by Keifer and Chu (1957), which were 0.387 and 0.375 for the first and second approaches, respectively. Therefore, the first approach was not considered for this study. The procedural steps that were followed to determine the advancement coefficient in this investigation, adopted from Keifer and Chu's (1957) second approach, are summarised as follows:

(a) The maximum rainfall within a 15, 30, 60 and 120-min duration within each significant storm event, was identified.

(b) For each of these durations, the ordinal position of the 5-min interval with the maximum rainfall was identified.

(c) The location of the peak intensity for each period was determined in accordance with Equation 4.1 This concept is illustrated in Figure 4.2, which depicts a typical storm event for which the location of the peak intensity for a 30-min period was calculated.

(d) The weighted average for each significant event was determined, using the location of peak intensity and weighted proportionally to 15, 30, 60 and 120-min in accordance with Equation 4.2.

(e) The average for all significant events for each of the five best stations was determined in accordance with Equation 4.3.

$$r_d = (p_o - 0.5)\frac{t_i}{d_t} \qquad [\ 4.1\ ]$$

where:

r_d = location of peak intensity,
p_o = ordinal position of interval with maximum rainfall,
t_i = duration of interval (5) (min), and
d_t = total duration (15, 30, 60 and 120) (min).

$$r_s = \frac{\sum_{t=1}^{N_d} r_d \cdot d_t}{\sum_{t=1}^{N_d} d_t} \qquad [\ 4.2\ ]$$

where:

r_s = advancement coefficient of significant storm event s, and
N_d = Number of storm durations (4).

$$r_i = \frac{1}{N_s}\sum_{s=1}^{N_s} r_s \qquad [\ 4.3\ ]$$

where:

r_i = advancement coefficient of station s, and
N_s = Number of significant storm events of station s.

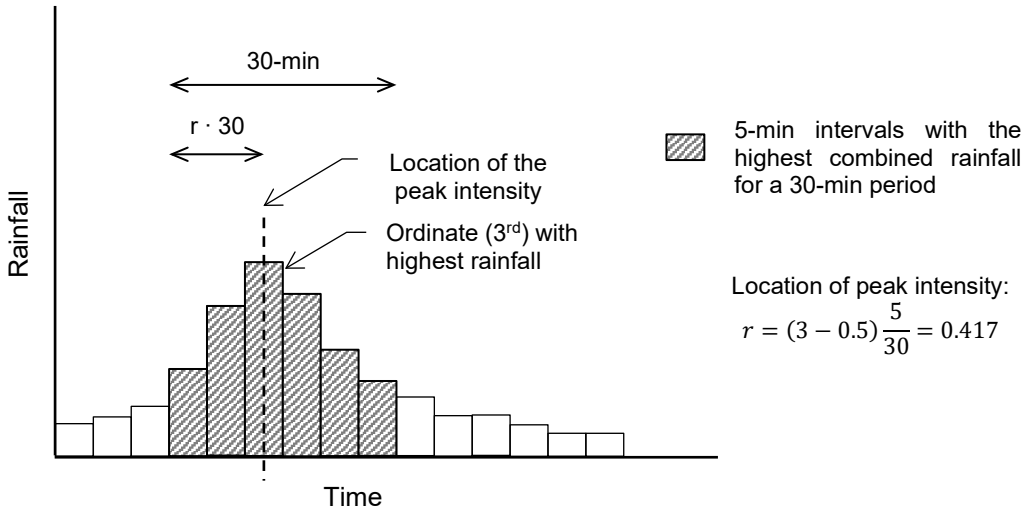

Figure 4.2: Typical location of the peak intensity within a 30-min duration

The storm advancement coefficient was calculated from the significant storm events identified from the five stations with good data sets in Gauteng, namely, O.R Tambo, Irene, Vereeniging, Jhb Bot Gardens and Unisa. The results, depicted in Figure 4.3, indicates an advancement coefficient that is very similar to the coefficient proposed by Keifer and Chu (1957) of 0.375. Therefore, an average value of 0.380 was used in this study. It is, however, recommended that the impact of the advancement coefficient has on the peak discharge, be investigated in a future study by conducting a sensitivity analysis.

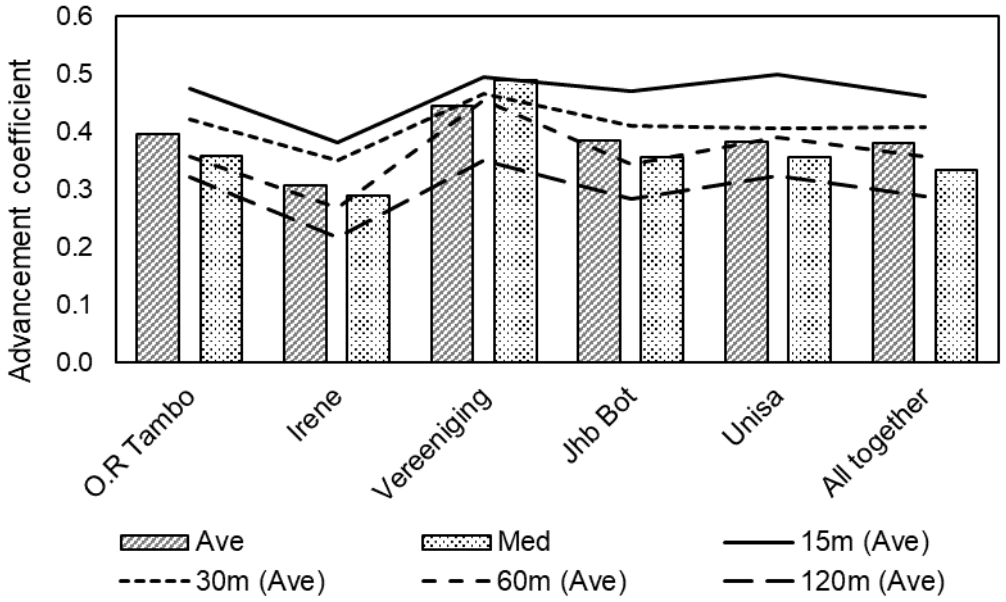

Figure 4.3 Storm advancement coefficients, based on Keifer and Chu's (1957) second approach

4.1.3 Dimensionless time to peak – TRI method

The hyetograph's first-moment arm for each significant storm event was calculated and related to a triangular representation of the hyetograph with an equal total rainfall volume and total storm duration, as described by Yen and Chow (1980). However, for some events the first-moment arm was small which resulted in an obtuse type of triangle, meaning that one angle is larger than 90 degrees. This is, however, not possible, and therefore, in such instances, a right angle was assumed. An example of such an event was observed at O.R Tambo on 4 January 1997, is depicted in Figure 4.4. The first-moment arm was calculated using Equation 2.11, which resulted in 43.2 minutes, and using Equation 2.13 to calculate the time to peak intensity, yielded negative 40.3 minutes. The negative time to peak was adjusted to zero minutes as depicted in Figure 4.4. Approximately 20% of the significant single event-based events required this adjustment. The effect of different total storm durations, total rainfall volumes and different seasons were not considered for this study, as proposed by Yen and Chow (1980).

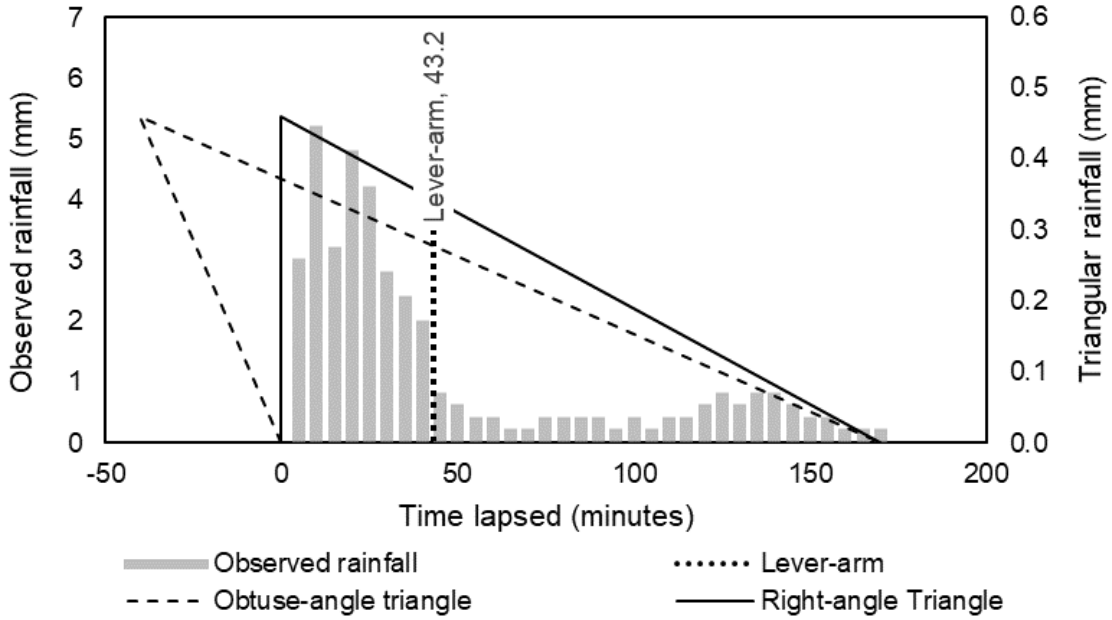

Figure 4.4: Correction of an obtuse triangle such as for the storm event at O.R. Tambo on 4 January 1997 at 00:50

Yen and Chow (1980) has determined the statistical mean values for the storm events sorted into various duration groups. The first group contained all events, the second group the 2-hour events, the third group the 3-hour events, etc. However, an insignificant difference was reported between the groups. Therefore, all events were grouped together for this study, for which the average time to peak ratio was computed at each of the five best stations, as shown in Figure 4.5. From the results the average time to peak intensity for the five stations were 0.20.

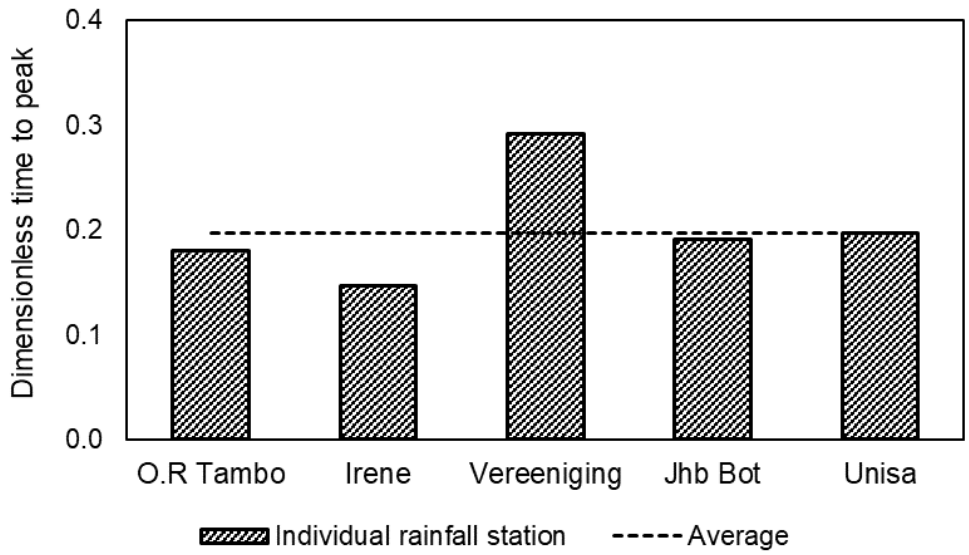

Figure 4.5 Time to peak intensity using method proposed by Yen and Chow (1980)

4.2 DEPTH-DURATION-FREQUENCY (DDF) CURVES

The development of short duration DDF curves for the rainfall stations in Gauteng is described in this section. The DDF curves were then subsequently used for further investigations in this study, namely:

(a) comparison with the DRESA design rainfall,

(b) generating rainfall distribution curves, and

(c) determining of the D-hour to 24-hour design rainfall ratios, which were then compared with the ratios of the SCS-SA curves.

Municipal stormwater infrastructure associated with minor stormwater drainage networks is generally designed to accommodate storm events with a return period of 1:5 up to 1:20 years. The DDF curves were, therefore, developed for stations that have a minimum data period of approximately 10 years. With a data period of at least 10 years the estimation of design events with a return period of up to 1:20 years is allowed, as estimation of return periods greater than twice the record length are generally not recommended (Smithers and Schulze, 2000). In terms of missing data, Smithers and Schulze (2000) found that there was no significant effect on design rainfall estimates if up to 20% of the years in the Annual Maximum Series (AMS) do not contain their true value. Even though this finding does not explicitly correlate with the missing data in the context of this study, 22 stations were identified to comply with this criterion which is located as depicted in Figure 4.6.

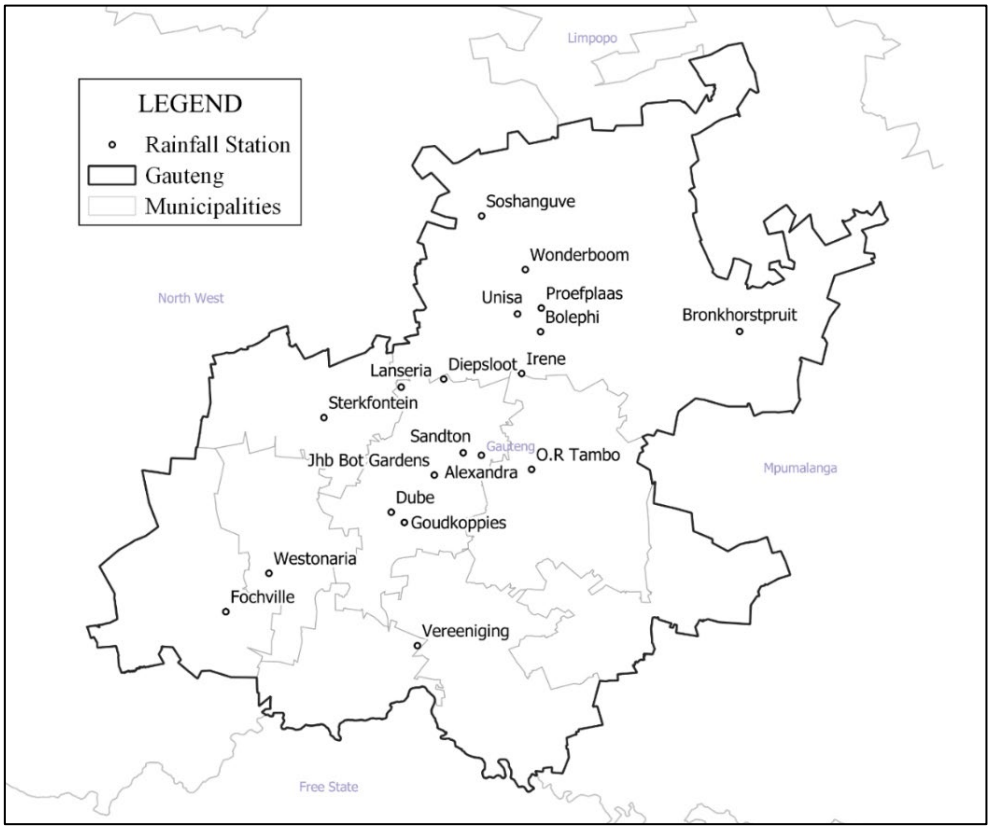

Figure 4.6: Rainfall stations in Gauteng that were used to develop IDF curves

The AMS was extracted for 16 time steps ranging from 5-min to 24-hours (standard time steps), and a PD analysis was conducted using the General Extreme Value (GEV) distribution. Based on Goodness-of-fit (GOF) tests and L-moments to fit the distributions to the data, Smithers (1996) recommended the GEV and the 3 parameter Log-Normal (LN3) distributions for short duration rainfall PD analysis in South Africa. In a further study, Smithers and Schulze (2000) concluded that if a single PD was to be adopted for all regions in South Africa, the GEV would be the most appropriate PD to use. Therefore the GEV distribution was used to estimate design rainfall in this study.

Following the PD analysis of the 22 stations, the Relative Error (RE) in the design rainfall obtained from the DRESA was computed for the 1:5, 1:10 and 1:20 year return periods, respectively. The RE was determined following Equation 4.4, and the average for all stations (ARE_t) was determined using Equation 4.5. The result of this analysis is depicted in Figure 4.7. This indicates that the ARE_t of the 1:20 year, 5-min to 15-min time steps, for example, range between negative 9% and negative 18%. These differences could be attributed to: (i) the inaccuracies in the 5-min rainfall data used in this study, (ii) the data period of the rainfall records used in this study, (iii) the GOF of the GEV distribution for short duration design rainfall, and (iv) the use of a regional approach in the DRESA study compared to the at-site approach used in this study. However, the exact cause of the errors are yet to be determined. The ARE_t for the 1:5 year, 30-min to 1.5-hour time steps, for example, range between 10% and 16%. However, the ARE_t of all standard time steps are still within the RE associated with the 90% upper and lower bounds given by the DRESA software as depicted in Figure 4.7. Therefore, the estimation of the at-site design rainfall following this PD analysis was deemed to be acceptable.

$$\mathrm{RE} = \frac{\mathrm{P_{PD}} - \mathrm{P_{SS}}}{\mathrm{P_{SS}}} \cdot 100 \qquad [\ 4.4\ ]$$

where:

RE = RE of time step t, and return period, T (%),
P_{PD} = design rainfall obtained from the PD analysis (mm), and
P_{SS} = mean design rainfall obtained from the design rainfall software (mm).

$$\mathrm{ARE\_t} = \frac{1}{\mathrm{N_t} \cdot \mathrm{N_S}} \cdot \sum_{\mathrm{t=1}}^{\mathrm{N}_t} \sum_{\mathrm{T=1}}^{\mathrm{N_S}} \mathrm{RE_{t,T}} \qquad [\ 4.5\ ]$$

where:

ARE_t = RE of time step t, and return period, T (%), and
N_S = number of stations (22), and
N_t = number of time steps (16).

$$\text{ARE\_S} = \frac{1}{\text{N}_\text{t}} \cdot \sum_{\text{t}=1}^{\text{N}_t} \text{RE}_\text{t} \qquad [\ 4.6\ ]$$

where:

ARE_S = average RE of station, S, and return period, T (%), and

N_t = number of time steps (16).

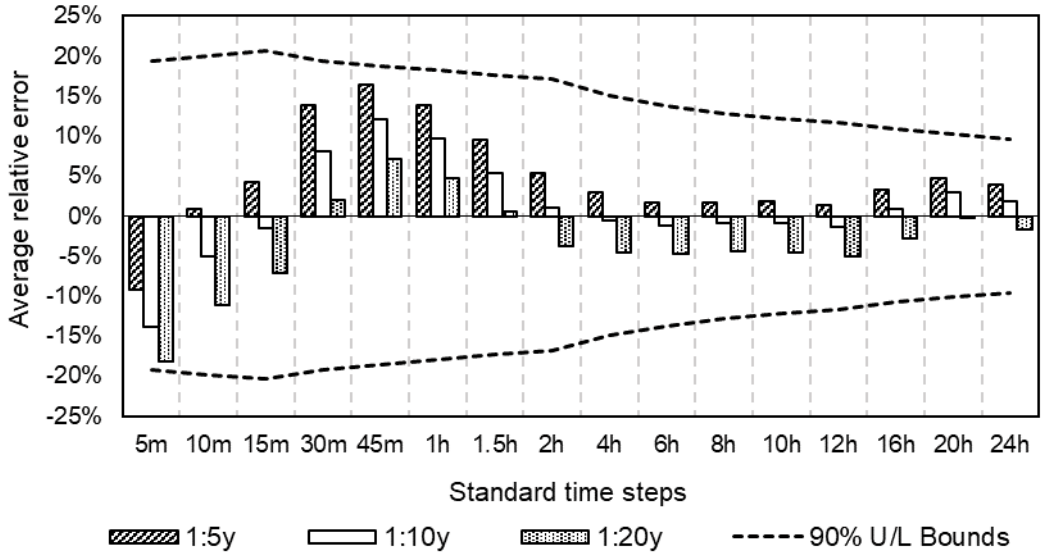

Figure 4.7: Average RE for each standard time step (ARE_t)

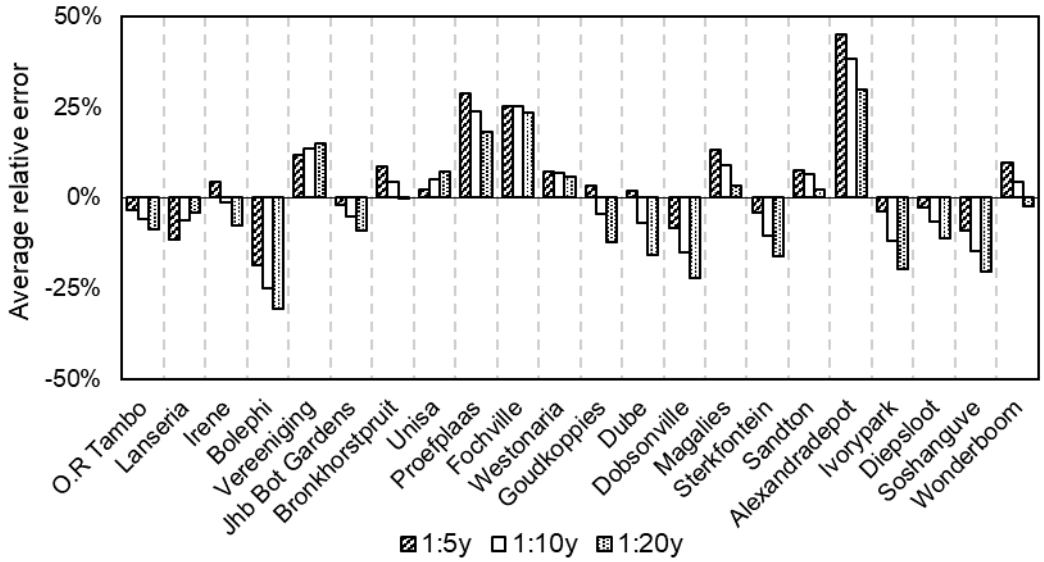

Figure 4.8: Average RE for each rainfall station (ARE_S)

4.3 INTENSITY-DURATION-FREQUENCY (IDF) REGRESSION COEFFICIENTS

A methodology of using a nonlinear algorithm to determine IDF regression coefficients as well as the RE as a measure of their accuracy are presented in this section. IDF regression coefficients (a, b, and c) are needed to generate a synthetic storm event using the CDS method. These coefficients are associated with Equation 2.2, which is reproduced here as Equation 4.7 for convenience, as follows:

$$i_a = \frac{a}{(b + t)^c} \qquad [\ 4.7\ ]$$

where:

i_a = Average rainfall intensity for a particular storm duration (mm/hour),
a,b,c = Site specific regression constants, and
t = Storm duration (min).

The design rainfall depths obtained from the DRESA were used to develop the regression coefficients. These were determined using an optimisation algorithm that adjusts the coefficients until the simulated intensity distribution is approximately equal to the actual intensities. In this case, the actual intensities are the design rainfall obtained from the DRESA software, divided by their respective durations and the simulated intensities are the intensities that were simulated using Equation 4.7. The coefficients that yielded the best design intensities were found using the Generalised Reduced Gradient (GRG) nonlinear algorithm (Lasdon et al., 1976). The GOF was determined using the Root Mean Square Error (RMSE) between the actual and simulated design intensities using Equation 4.8. The coefficients were adjusted until the RMSE was optimised by reaching a minimum. The built-in solver function of MS Excel, using the GRG nonlinear algorithm as the solving method and the calculated RMSE value as the objective value was used for this procedure.

$$\mathrm{RMSE} = \sqrt{\frac{\sum_{j=1}^{N_t}\left(\mathrm{IDF}_{A_j} - \mathrm{IDF}_{S_j}\right)^2}{N_t}} \qquad [\ 4.8\ ]$$

where:

RMSE = root mean square error,
IDF_A = actual design rainfall intensities (mm/hour),
IDF_S = simulated design rainfall intensities (mm/hour), and
N_t = number of time steps (16).

Table 4.1: Regression coefficients determined from the design rainfall obtained from the DRESA software

ID	Name	a			b	c
		1:5	1:10	1:20		
1	Jhb OR Tambo	732	885	1047	4.269	0.726
2	Lanseria	974	1158	1347	5.869	0.763
3	Irene	745	901	1067	4.528	0.735
4	Bolepi House	988	1195	1414	5.621	0.756
5	Vereeniging	781	913	1040	5.086	0.752
6	Zuurbekom	740	896	1060	4.430	0.730
8	Jhb Bot Tuine	723	874	1035	4.101	0.720
10	Bronkhorstspruit	991	1198	1418	5.693	0.757
11	Waterkloof AFB	965	1166	1380	5.956	0.767
12	Pretoria Unisa	992	1200	1420	5.710	0.757
13	Pretoria Proefplaas	979	1183	1400	5.757	0.760
18	Fochville Police	742	867	988	4.434	0.731
19	Westonaria Kloof	738	862	982	4.339	0.729
20	Goudkoppies	741	895	1059	4.423	0.730
21	Dube	741	896	1060	4.430	0.731
22	Dobsonville	719	868	1028	4.006	0.718
23	Magaliesburg Police	981	1168	1358	5.776	0.760
24	Sterkfontein	715	850	988	3.926	0.715
25	Jhb Sandton	724	875	1035	4.119	0.721
26	Alexandra Depot	740	896	1060	4.437	0.731
27	Ivory Park	760	919	1087	4.780	0.742
28	Diepsloot	968	1170	1386	5.954	0.766
29	Pta presidency	979	1183	1400	5.757	0.760
32	Baviaanspoort	977	1182	1398	5.817	0.762
34	Shoshanguve	988	1195	1414	5.686	0.757

The RE of the simulated intensities, using the optimal regression coefficients presented in Table 4.1, was calculated in accordance with Equation 4.9 as follows:

$$\mathrm{RE} = \frac{\mathrm{IDF_S} - \mathrm{IDF_A}}{\mathrm{IDF_A}} \cdot 100 \qquad [\,4.9\,]$$

where:

RE = relative error (%),

IDF_A = actual design rainfall intensities (mm/hour) estimated from the DRESA software, and

IDF_S = simulated design rainfall intensities (mm/hour) from Equation 4.7.

For example, the optimal coefficients from Table 4.1 for the 1:5-year design intensities for O.R. Tambo were 732, 4.269 and 0.726, respectively. Applying these coefficients, the simulated intensities were calculated for all standard time steps, and the RE concerning the actual intensities were determined. The same applies to the 1:10 and 1:20 year regression coefficients and the results are depicted in Figure 4.9.

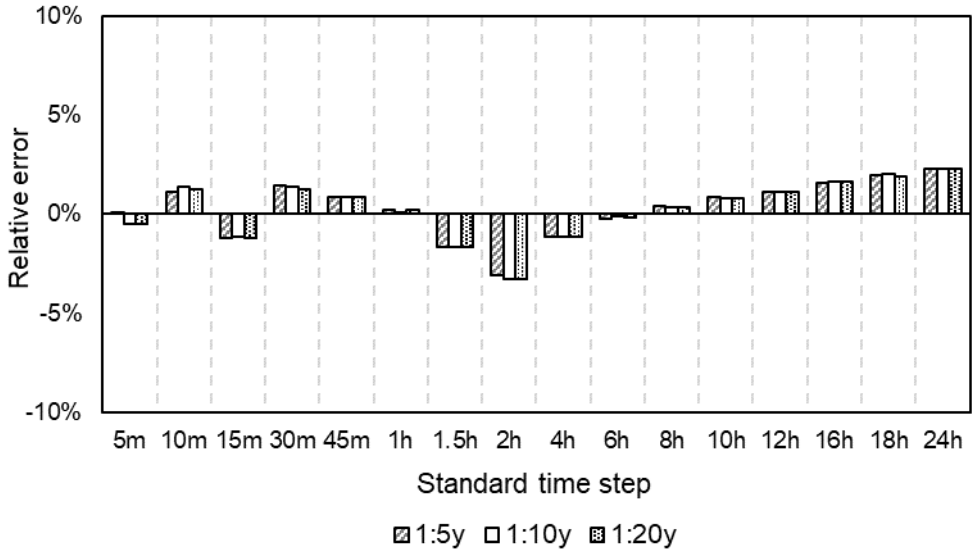

Figure 4.9: RE between actual and simulated design rainfall intensities for O.R. Tambo using the design rainfall from the DRESA software

The Average Relative Error (ARE_t) of each standard time step for the 1:5, 1:10 and 1:20 year return periods, respectively, of all stations, were determined following Equation 4.10 and the results are depicted in Figure 4.10. This indicates that the results are similar for all recurrence intervals, and the example results of O.R Tambo depicted in Figure 4.9.

$$\mathrm{ARE\_t} = \frac{1}{\mathrm{N_S}} \cdot \sum_{\mathrm{j=1}}^{\mathrm{N_S}} \mathrm{RE_{t,T}} \qquad [\,4.10\,]$$

where:

ARE_t = relative error of time step t, and return period, T (%), and
N_S = number of stations (22).

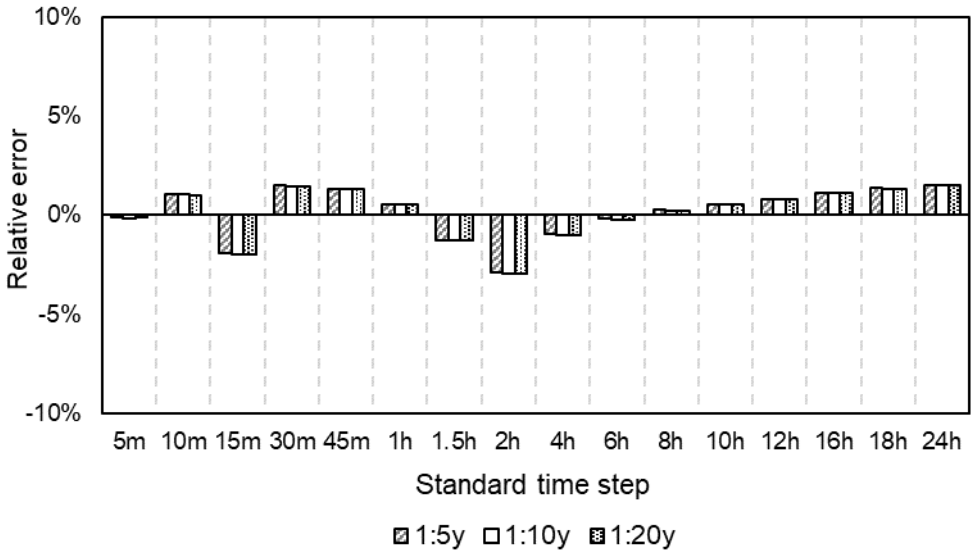

Figure 4.10: Average relative error for each standard time step (ARE_t)

4.4 RAINFALL DISTRIBUTION CURVE (DC)

The methodology of developing a DC is described in this section which is divided into two parts. The first part describes the development of a 24-hour DC using the DDF curves described in Section 4.2. Each DC was then subsequently used for the comparison between single event-based and continuous simulation modelling. The second part describes the methodology of developing a DC for a duration < 24-hours. This methodology was used for the comparison between observed and simulated storm events.

4.4.1 Development of a 24-hour DC

The development of a 24-hour DC entails the embedment of the entire short duration DDF curve in a single synthetic design storm. The peak intensity is located at the centre of the 24 hours and the design rainfall of shorter durations are then divided equally on either side of the peak intensity. This process entails the interpolation of intermediate design rainfall for durations between the standard time steps (5-, 10-, 15-, 30-, 45-min, etc.). For example, the design rainfall for durations in 5-min intervals between 15-min and 30-min is interpolated using a power regression function fitted through the incremental intensities of the standard time steps. This concept was adopted, and adapted, from the National Engineering Handbook (NRCS, 2019). This process is demonstrated in Table 4.2 and the procedural steps that were followed to complete Table 4.2 are summarised as follows:

(a) Populate Column 1 and 2 with the standard time steps and design rainfall, respectively.

(b) Calculated the rainfall ratios in Column 3 by dividing each rainfall value by the 24-hour rainfall value.

(c) Calculate the non-dimensionalised incremental intensity in Column 4 by dividing the difference in ratio by the difference in duration. For example, the 0.5-hour non-dimensionalised incremental intensity is (0.386 - 0.445) / (0.50 - 0.25) = 0.351.

(d) Calculate the logarithmic value of the duration and non-dimensionalised incremental intensity in Columns 5 and 6.

(e) Determine the power regression coefficients, defined in Equation 4.11, in Columns 7 and 8 for each duration and the next duration. For example, the coefficients 0.175 and negative 0.965 for duration = 0.083 hours, is applicable for all durations from 0.083 to 0.167 hours. The LINEST function in MS Excel is suitable for this task, which uses the least square statistical procedure to calculate the regression coefficients that best fits the data.

$$I_{increment} = a \cdot (D_{intermediate})^{b} \qquad [4.11]$$

where:

$I_{increment}$ = Dimensionless incremental intensity,
a, b = Power regression coefficients, and
$D_{intermediate}$ = Intermediate storm duration. (Hour).

Table 4.2: Example regression coefficients for incremental intensities

1	*2*	*3*	*4*	*5*	*6*	*7*	*8*
Duration (hour)	**Design Rainfall**	**Rainfall Ratio**	**Inc.Int.**	**log (hour)**	**log (Inc.Int.)**	**a**	**b**
0.083	12.1	0.161	1.928	-1.079	0.285	0.175	-0.965
0.167	18.3	0.243	0.988	-0.778	-0.005	0.177	-0.961
0.25	22.5	0.299	0.669	-0.602	-0.174	0.184	-0.933
0.5	29.1	0.386	0.351	-0.301	-0.455	0.175	-1.000
0.75	33.5	0.445	0.234	-0.125	-0.631	0.175	-1.000
1	36.8	0.489	0.175	0.000	-0.756	0.175	-0.890
1.5	41.4	0.550	0.122	0.176	-0.913	0.187	-1.051
2	44.8	0.595	0.090	0.301	-1.044	0.171	-0.918
4	52	0.691	0.048	0.602	-1.320	0.191	-1.000
6	56.8	0.754	0.032	0.778	-1.497	0.191	-1.000
8	60.4	0.802	0.024	0.903	-1.622	0.131	-0.817
10	63.4	0.842	0.020	1.000	-1.701	0.199	-1.000
12	65.9	0.875	0.017	1.079	-1.780	0.178	-0.954
16	69.7	0.926	0.013	1.204	-1.899	0.238	-1.059
20	72.7	0.965	0.010	1.301	-2.002	0.105	-0.785
24	75.3	1.000	0.009	1.380	-2.064		

Inc.Int. = Non-dimensionalised Incremental Intensity

Following the determination of the power regression coefficients, the design rainfall ratios are determined in 5-min intervals, for all durations from 5-min to 24-hour. The construction of the DC is initiated by positioning the peak ratio, namely the 5-min ratio, at the 12-hour mark. The difference between the 15-min and 5-min ratios is then divided equally before and after the peak ratio so that the total is equal to the 15-min ratio. The difference between the 25-min and 15-min ratios is again divided equally on either side of the 15-min ratios so that the total is equal to the 25-min ratio, and so on until the 24-hour ratio is distributed. The distribution of the first 55 minutes design rainfall ratios is demonstrated in Figure 4.11. Finally, the DC is created by accumulating each 5-min ratio from the start to the end of the 24-hour period. The distribution described in this section was subsequently applied to the construction of the DC5, DC10, and DC20 curves, as well as constructing the SCS-SA curves in 5-min intervals.

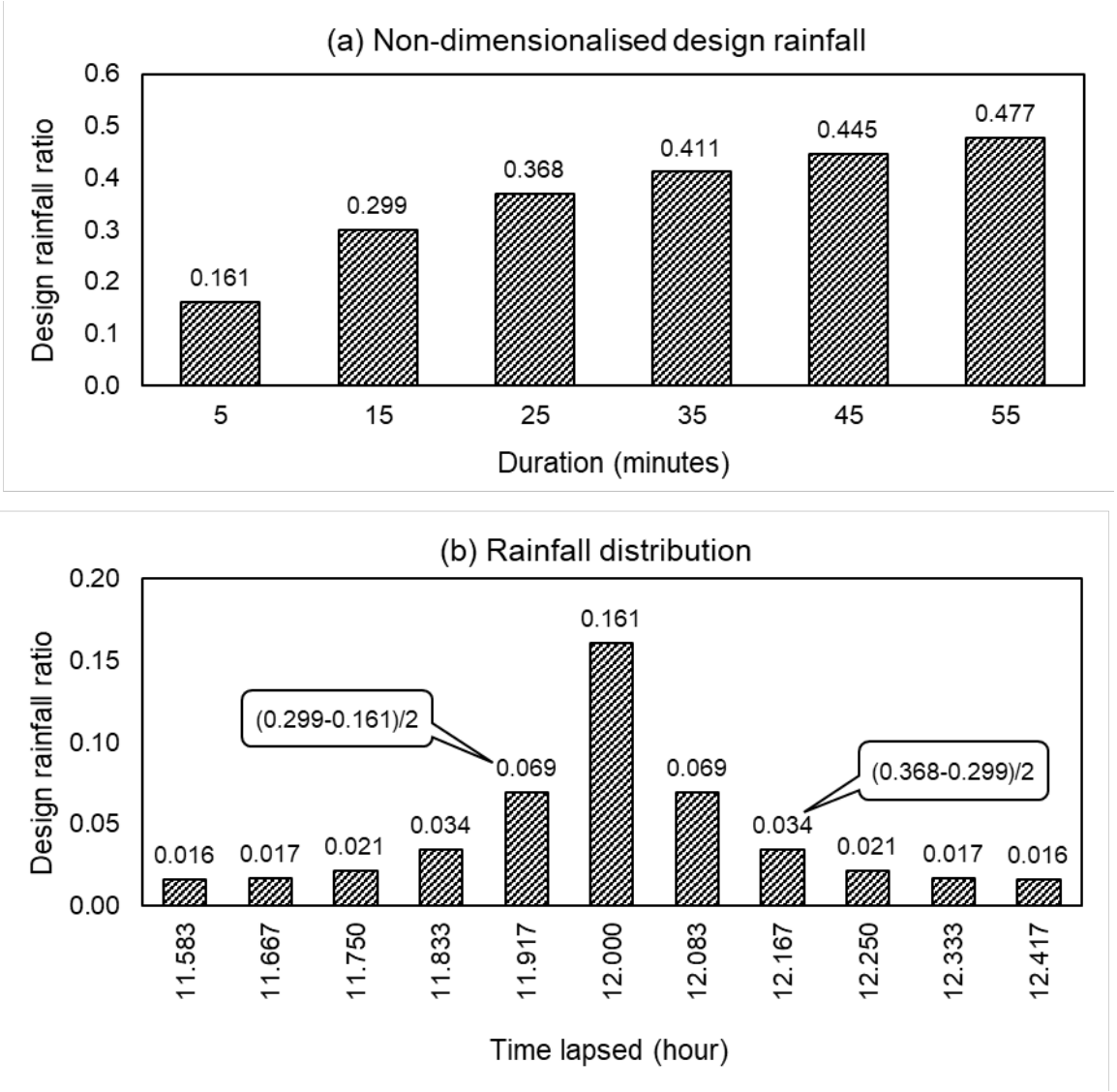

Figure 4.11: The general rainfall distribution process

4.4.2 Development of a DC for durations < 24-hours

The procedure used to develop a DC for a synthetic design storm with duration < 24-hours was adopted from the National Engineering Handbook (NRCS, 2019). As an example, the extraction of a 6-hour rainfall distribution using the SCS-SA Type 2 curve is described below. Although a DC at 5-min intervals are more appropriate, this example uses intervals at 30-min to shorten the example and still demonstrate the concept (NRCS, 2019). The calculations to extract a 6-hour event from the 24-hour SCS-SA Type 2 curve is shown schematically in Figure 4.12, summarised in Table 4.3, and the procedural steps are summarised as follows:

(a) Because a 24-hour DC is centred around 12-hour, a 6-hour DC will, therefore, start at 9-hour and end at 15-hour.

(b) The new cumulative rainfall ratio at 9-hour is zero. The unadjusted ratio at 9.5-hour is equal to the difference between 9.5-hour and 9-hour, which is 0.0169.

(c) The unadjusted ratio at 10-hour is equal to the sum of the unadjusted 9.5-hour ratio, and the difference between 10-hour and 9.5-hour, which is 0.0360.

(d) The remainder of intervals, up to 15-hour is calculated in the same way, which has an unadjusted ratio of 0.6980.

(e) Lastly, the adjusted ratios are calculated by dividing each unadjusted ratio with the unadjusted ratio of 15-hour of 0.6980, which results in the 6-hour DC, as depicted in Figure 4.12.

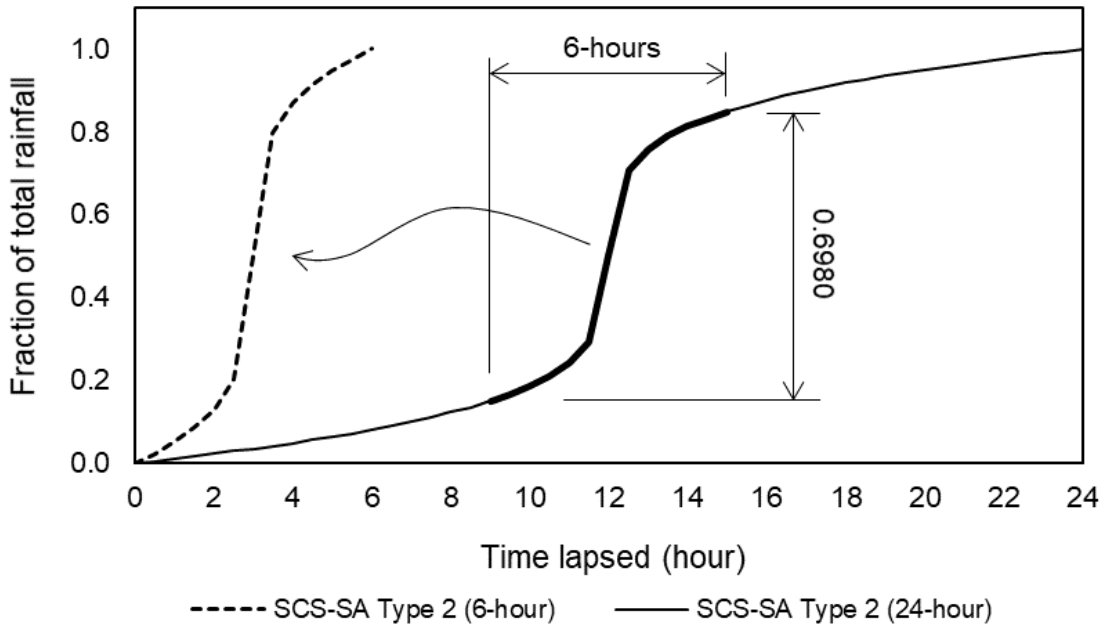

Figure 4.12: Typical adjusted six-hour DC extracted from a 24-hour DC

Table 4.3: Six-hour rainfall distribution extracted from a 24-hour rainfall distribution

Time lapsed (Hour)	SCS-SA Type 2	Unadjusted cumulative 6-hour rainfall ratio	6-Hour distribution time (hour)	6-Hour distribution cumulative rainfall ratio
0	0.0000			
0.5	0.0054			
1	0.0110			
1.5	0.0168			
2	0.0230			
2.5	0.0295			
3	0.0360			
3.5	0.0424			
4	0.0490			
4.5	0.0562			
5	0.0640			
5.5	0.0722			
6	0.0810			
6.5	0.0907			
7	0.1010			
7.5	0.1115			
8	0.1230			
8.5	0.1361			
9	0.1510	0.0000	0	0.0000
9.5	0.1679	0.0169	0.5	0.0242
10	0.1870	0.0360	1	0.0516
10.5	0.2100	0.0590	1.5	0.0845
11	0.2420	0.0910	2	0.1304
11.5	0.2920	0.1410	2.5	0.2020
12	0.5000	0.3490	3	0.5000
12.5	0.7080	0.5570	3.5	0.7980
13	0.7580	0.6070	4	0.8696
13.5	0.7900	0.6390	4.5	0.9155
14	0.8130	0.6620	5	0.9484
14.5	0.8321	0.6811	5.5	0.9758
15	0.8490	0.6980	6	1.0000
15.5	0.8639			
16	0.8770			
16.5	0.8884			
17	0.8990			
17.5	0.9094			
18	0.9190			
18.5	0.9272			
19	0.9350			
19.5	0.9432			
20	0.9510			
20.5	0.9577			
21	0.9640			
21.5	0.9705			
22	0.9770			
22.5	0.9832			
23	0.9890			
23.5	0.9946			
24	1.0000			

4.5 SCS-SA DESIGN RAINFAL RATIO COMPARISONS

In this section, the D-hour to 24-hour ratios of the design rainfall at each site were calculated and compared with the ratios of the four SCS-SA curves. This was done to confirm the use of the Type 3 curve for the Gauteng province depicted in Figure 2.9 as recommended by Weddepohl (1988). The methodology that was used to achieve this was by comparing the D-hour to 24-hour ratios of the design rainfall with the SCS-SA curves. Two sources of design rainfall were used for this analysis. The first being the design rainfall obtained from the DRESA software and the second is the design rainfall obtained from the at-site PD analysis, as describe in Section 4.2. The ratios for the SCS-SA curves were calculated using Equation 2.10 and the coefficients listed in Table 2.1. These ratios are summarised in Table 4.4 and form the baseline ratios against which the two sources of design rainfall were compared with.

Table 4.4: Sub-daily and sub-hourly ratios for the four SCS-SA curves

Duration	Type 1	Type 2	Type 3	Type 4
5m	0.084	0.135	0.174	0.209
10m	0.126	0.204	0.281	0.347
15m	0.155	0.249	0.355	0.444
30m	0.215	0.332	0.487	0.618
45m	0.256	0.384	0.561	0.710
1h	0.289	0.422	0.609	0.768
1.5h	0.341	0.478	0.672	0.835
2h	0.383	0.520	0.713	0.874
4h	0.502	0.629	0.802	0.938
6h	0.588	0.701	0.849	0.962
8h	0.657	0.755	0.881	0.974
10h	0.715	0.800	0.905	0.982
12h	0.767	0.838	0.925	0.987
16h	0.857	0.902	0.956	0.993
20h	0.933	0.955	0.980	0.997
24h	1.000	1.000	1.000	1.000

4.5.1 Comparison with DRESA design rainfall

The ratios for the design rainfall obtained from the DRESA software were calculated by dividing the rainfall for each duration with the 24-hour rainfall according to Equation 4.12:

$$RD_{t,T} = \frac{P_{t,T}}{P_{24,T}} \qquad [4.12]$$

where:

$RD_{t,T}$ = D-hour design rainfall ratio for duration, t and recurrence interval, T,

$P_{t,T}$ = Design rainfall (at-site and DRESA) for duration, t and RI, T (mm), and
$P_{24,T}$ = 24-hour Design rainfall for recurrence interval, T (mm).

The position of the design rainfall ratios relative to the ratios of the four curves were linearly interpolated and were subsequently called Intermediate Curve (IC) types. Following the calculation of the D-hour design rainfall ratios, the IC for each duration and recurrence interval was determined according to Equation 4.13. The result of this analysis is summarised in Figure 4.13 to Figure 4.15. Thereafter, the average for each standard time step (AIC_t) was determined according to Equation 4.14 and the results are depicted in Figure 4.16. This indicates that the average intermediate curve type range between 1.96 and 2.18 with an average (AIC_G) of 2.03 using Equation 4.15. The AIC_G value, therefore, represents the average of all standard time steps of the 22 stations in Gauteng. This concludes that the average curve type applicable to the Gauteng province, using the design rainfall from the DRESA software, is approximately equal to the Type 2 curve. However, the variation in the IC values with regards to the standard time steps, summarised in Figure 4.13 to Figure 4.15, is notable.

$$IC_{t,T} = \frac{RD_{t,T} - RC_{i,t}}{RC_{i+1,t} - RC_{i,t}} + C_i \qquad [4.13]$$

where:
$IC_{t,T}$ = Intermediate curve type for duration t and recurrence interval T,
C_i = SCS-SA curve type i (1, 2, 3 or 4),
$RC_{i,t}$ = SCS-SA ratio for curve type i and duration t,
$RC_{i+1,t}$ = SCS-SA ratio for curve type i+1 and duration t,
$RD_{t,T}$ = D-hour design rainfall ratio for duration t and recurrence interval T,

$$AIC\_t = \frac{1}{N_S} \cdot \frac{1}{N_T} \cdot \sum_{T=1}^{N_S} \sum_{S=1}^{N_T} IC_{T,S} \qquad [4.14]$$

where:
AIC_t = Average intermediate curve type for duration t,
IC_T = Intermediate curve type for recurrence interval T and station S,
N_S = Number of stations (22),
N_T = Number of recurrence intervals (3),

$$AIC\_G = \frac{1}{N_t} \cdot \sum_{i=1}^{N_t} AIC\_t_i \qquad [4.15]$$

where:
AIC_G = Average intermediate curve type for Gauteng,
ICT_T = Intermediate curve type for recurrence interval T and station S,
N_t = Number of standard time steps (16),

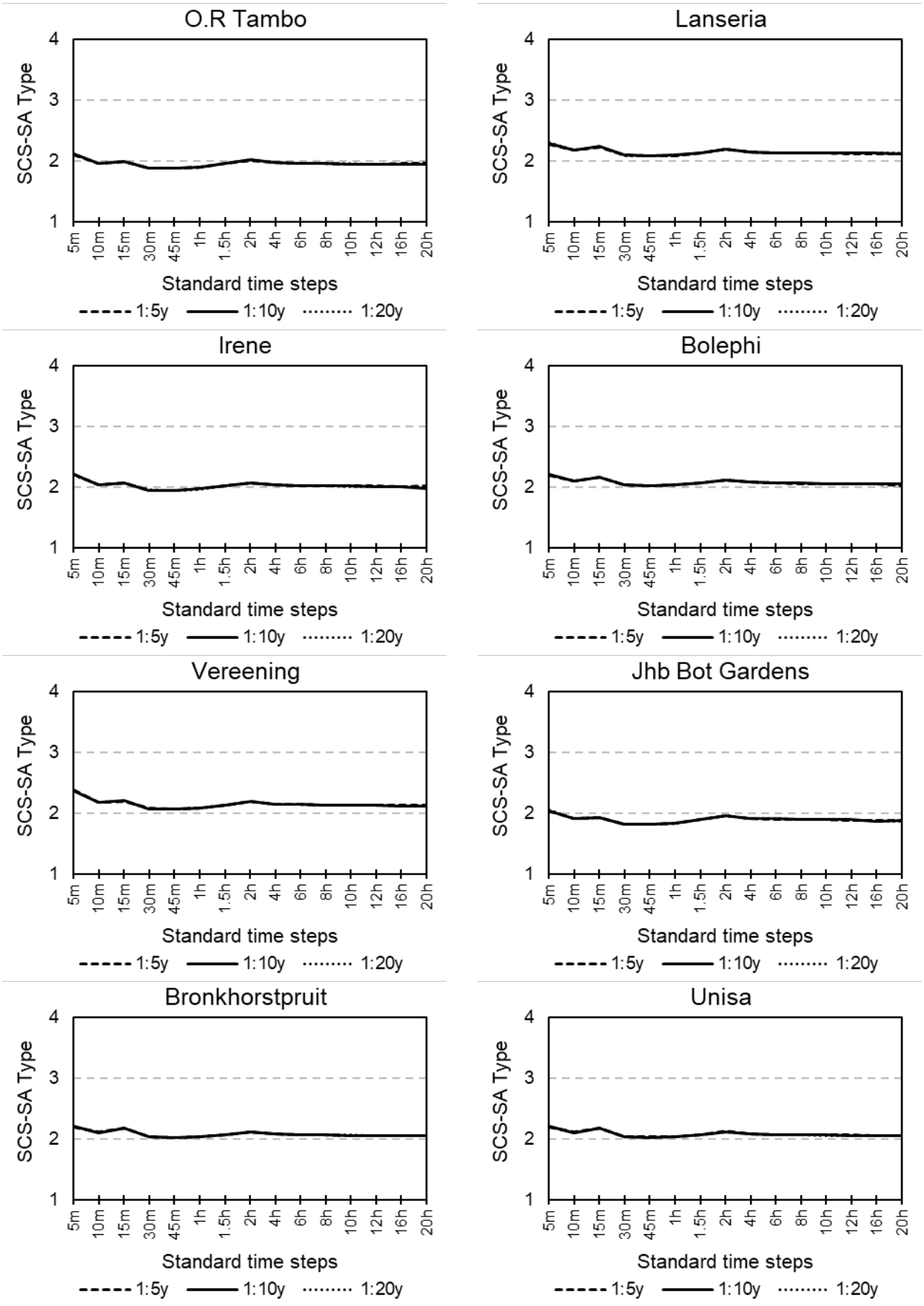

Figure 4.13: D-hour to 24-hour ratio comparison with SCS-SA curves and DRESA software design rainfall (1 of 3)

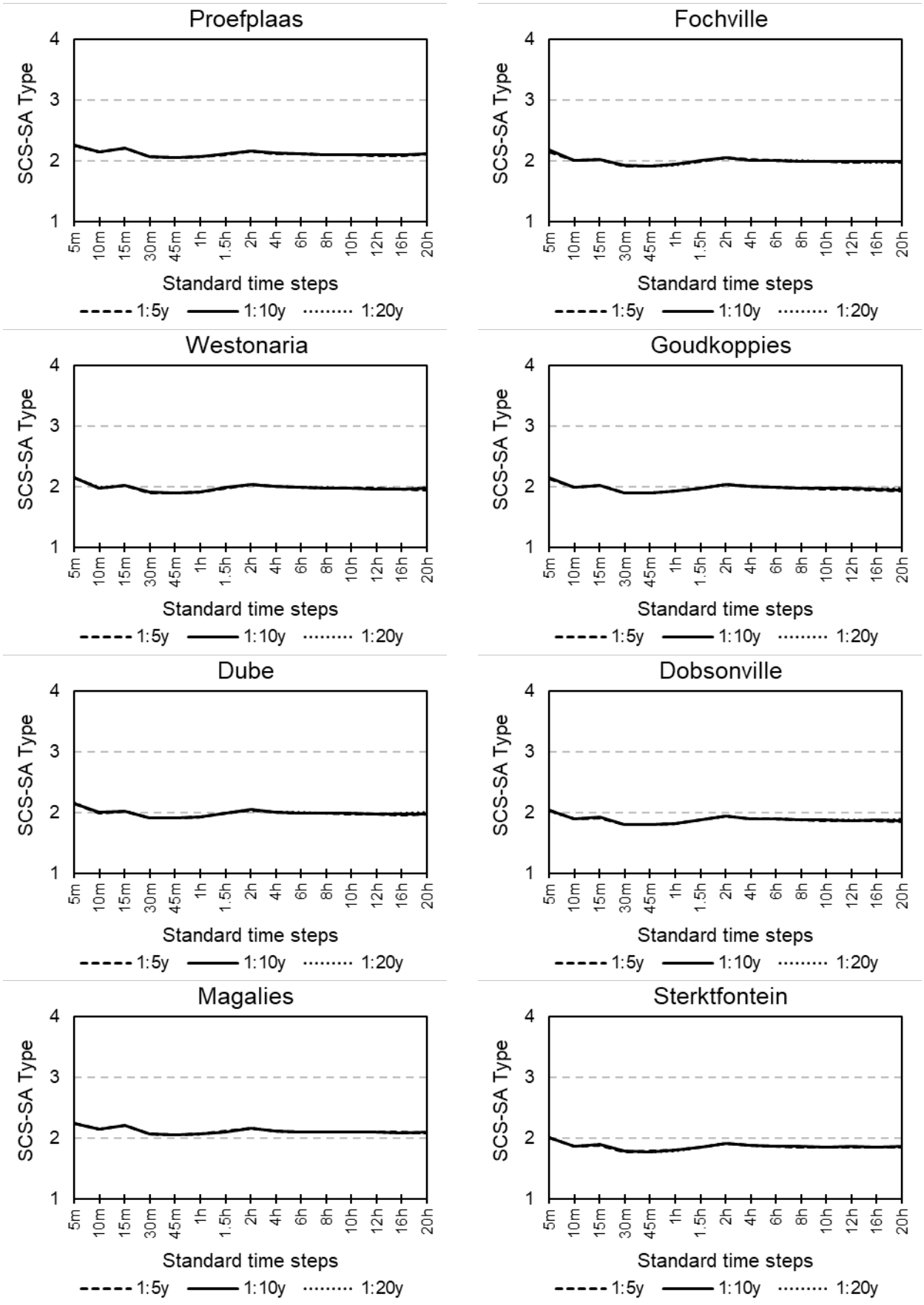

Figure 4.14: D-hour to 24-hour ratio comparison with SCS-SA curves and DRESA software design rainfall (2 of 3)

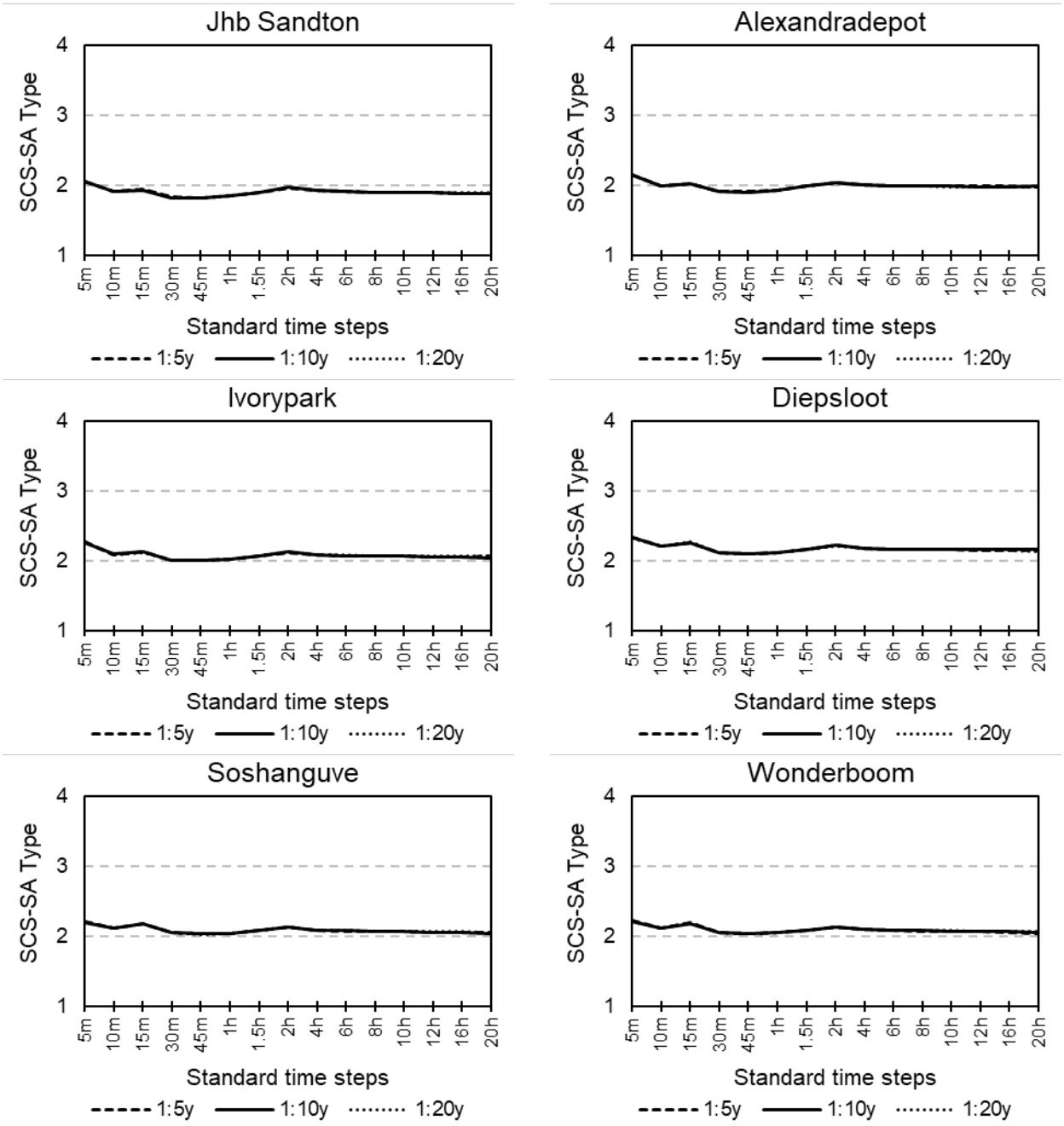

Figure 4.15: D-hour to 24-hour ratio comparison with SCS-SA curves and DRESA software design rainfall (3 of 3)

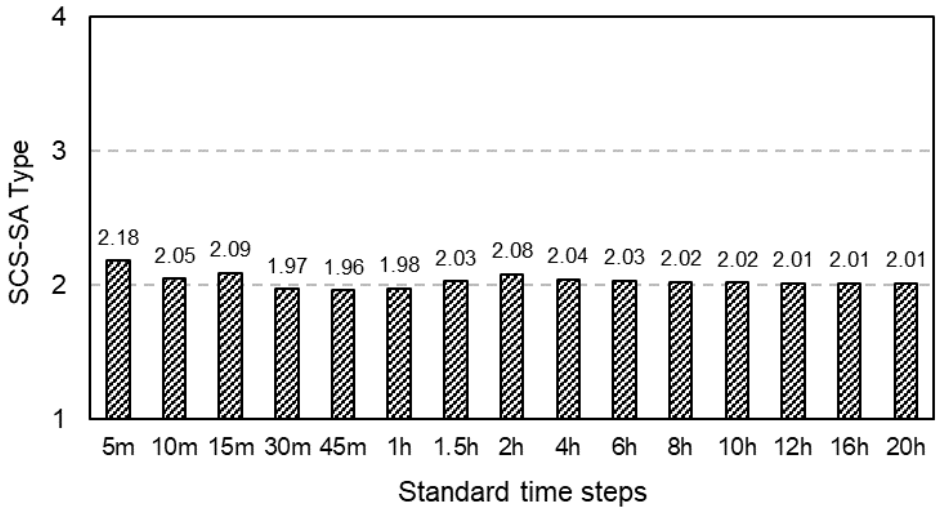

Figure 4.16: Average intermediate curve type for 22 stations computed using DRESA design rainfall

4.5.2 Comparison with at-site design rainfall

The same comparison was done using the design rainfall obtained from the PD analysis described in Section 4.2. The average for each standard time step (AIC_t) was again determined according to Equation 4.14 and the results are depicted in Figure 4.17 to Figure 4.19. This shows that the intermediate curve type (IC) varies between a minimum of 1.67 and a maximum of 2.21, with an average (AIC_T) of 1.97 using Equation 4.15. Therefore, it can be concluded that the average curve type applicable to the Gauteng province, using the at-site design rainfall, is approximately equal to the Type 2 curve. However, the variation in the IC values with regards to the standard time steps, summarised in Figure 4.17 to Figure 4.19, is much more noticeable compared to the results using the DRESA design rainfall. Therefore, a recommended solution is presented in the following section.

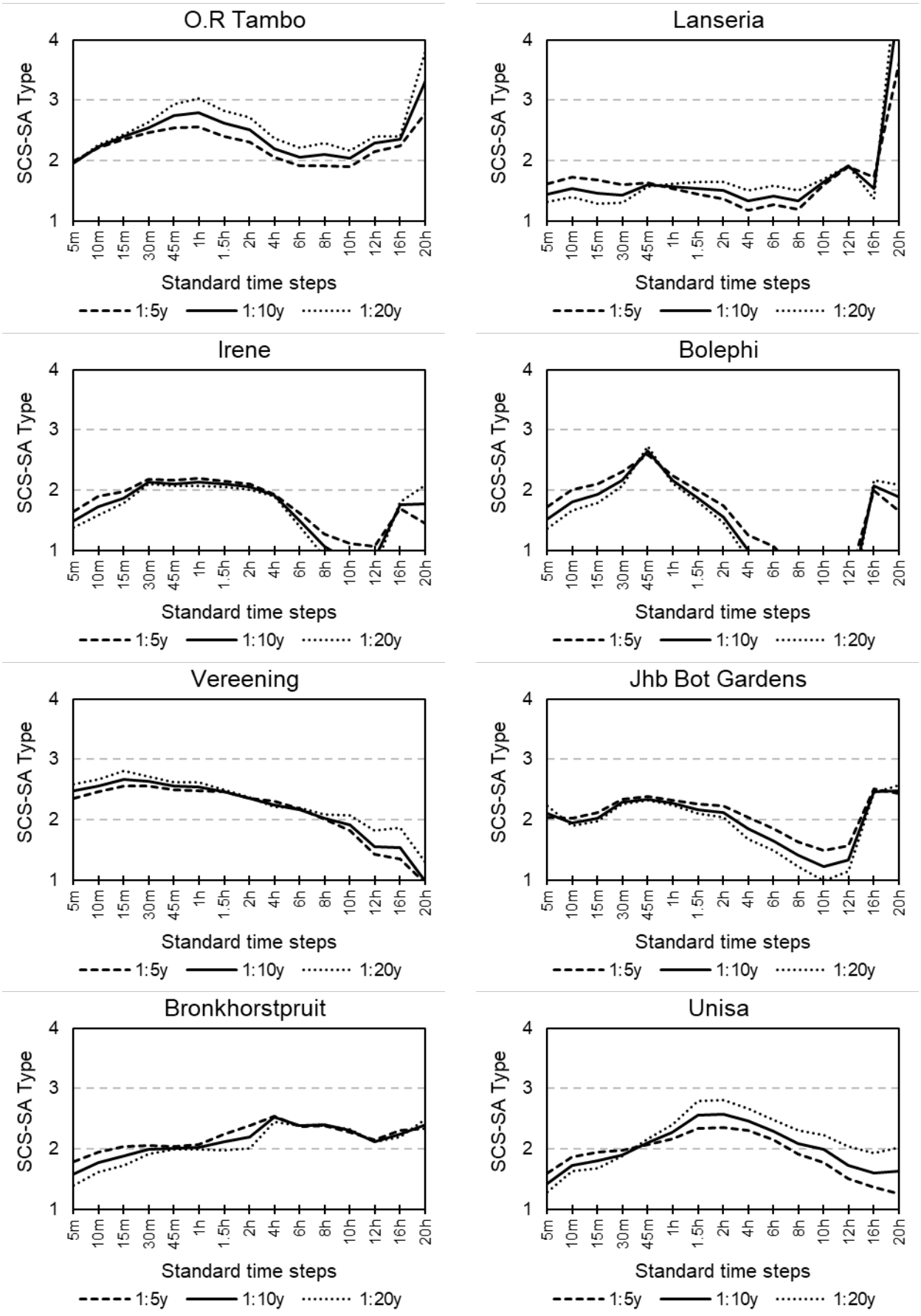

Figure 4.17: D-hour to 24-hour ratio comparison for SCS-SA curves and at-site design rainfall (1 of 3)

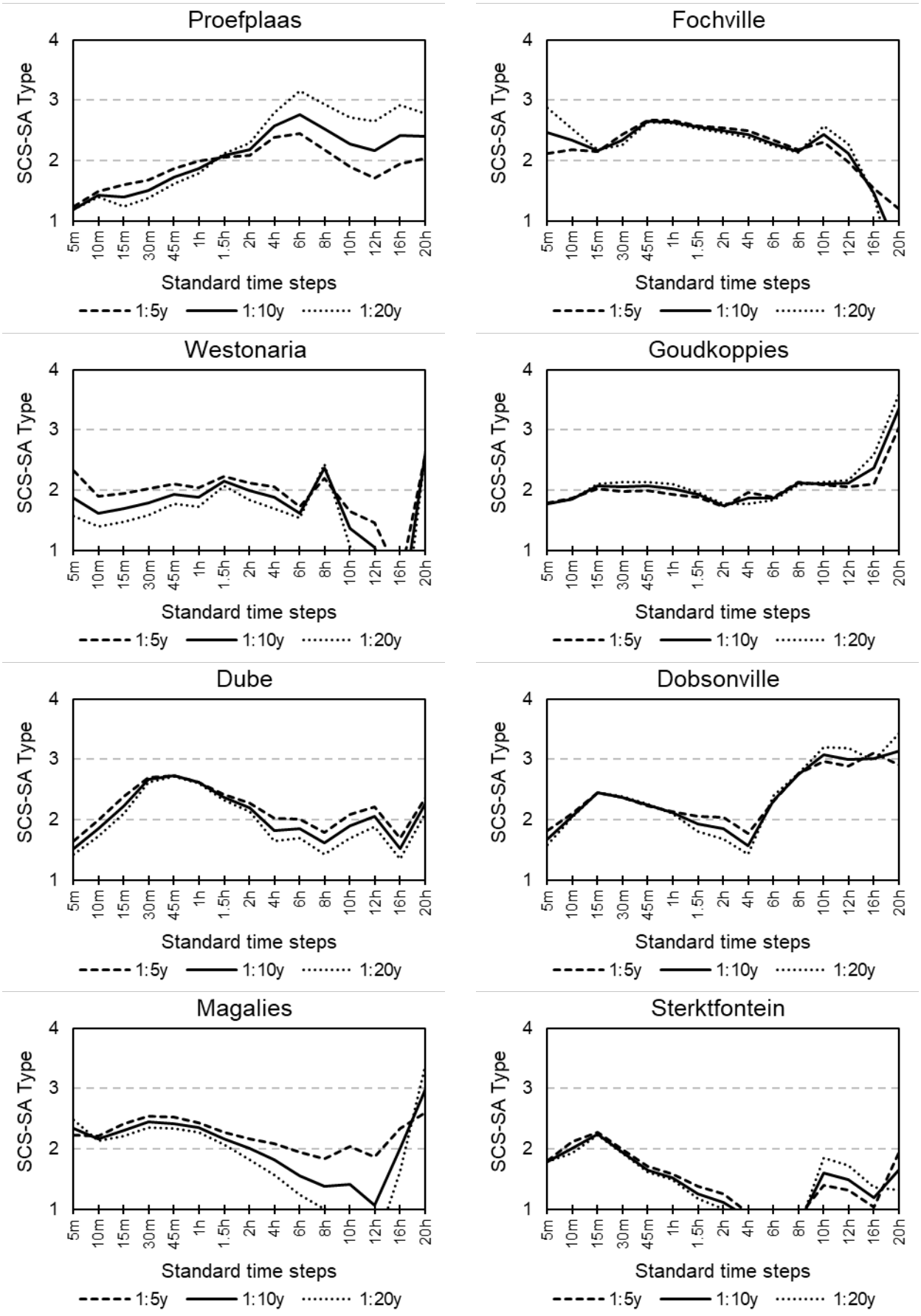

Figure 4.18: D-hour to 24-hour ratio comparison for SCS-SA curves and at-site design rainfall (2 of 3)

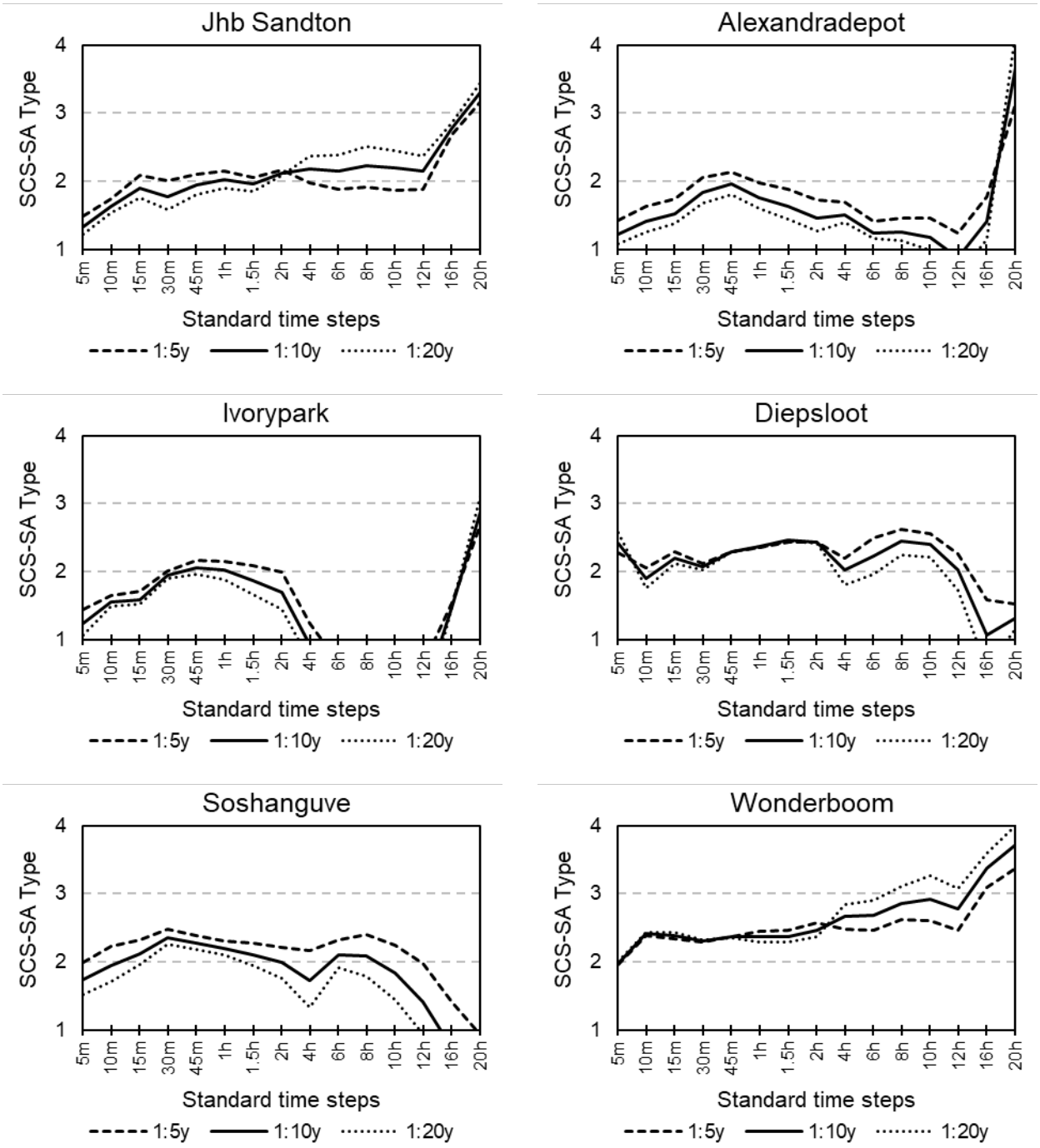

Figure 4.19: D-hour to 24-hour ratio comparison for SCS-SA curves and at-site design rainfall (3 of 3)

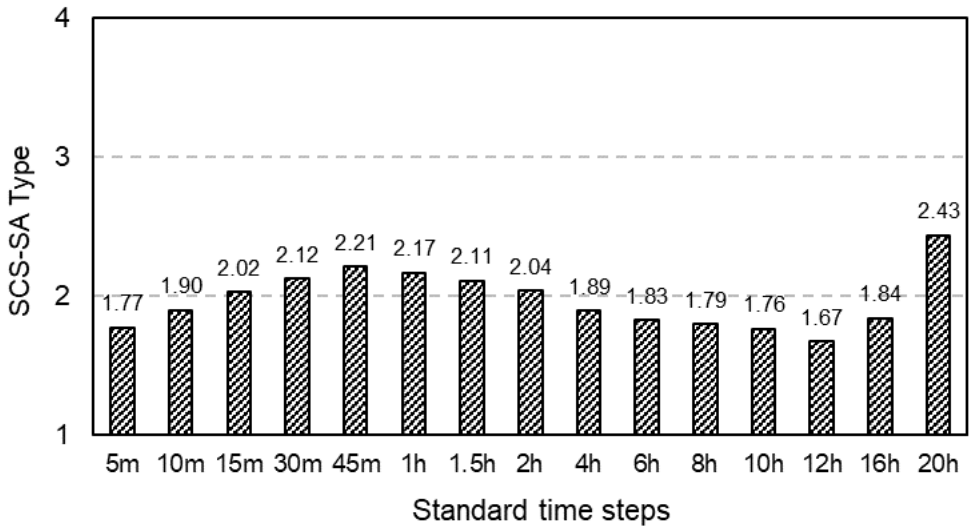

Figure 4.20: Average intermediate curve type for 22 stations using at-site design rainfall

4.5.3 Recommended intermediate curve types for Gauteng

The variation in intermediate curve types with duration and between sites in Gauteng is significant as it can lead to an underestimation or overestimation of the peak discharge. For example, if a stormwater network near O.R Tambo, with a reaction time of approximately 30-min, is simulated in a dynamic rainfall-runoff simulation model, using the SCS-SA Type 2 curve to generate a 1:20 year synthetic design storm, then the peak discharge will be underestimated. This is because the intermediate curve type for the 30-min time step at O.R Tambo is 2.64, as depicted in Figure 4.17. Therefore, the Type 3 curve would be more appropriate of the fours SCS-SA distributions, or a linear interpolated curve between the Type 2 and 3 curves that represents the intermediate curve of 2.64. This means that an intermediate DC could be determined by either following the rainfall distribution process described in Section 4.4 or by linear interpolation between the cumulative rainfall ratios, using Equation 4.16 below. An example of the final IC type 2.64 is depicted in Figure 4.21.

$$\mathrm{ICT_t} = \frac{\mathrm{IC} - \mathrm{C_i}}{\mathrm{C_{i+1}} - \mathrm{C_i}} \cdot \mathrm{RC_{i,t}} \qquad [4.16]$$

where:

$\mathrm{ICT_t}$ = Intermediate cumulative rainfall ratio for time step t,
$\mathrm{C_i}$ = SCS-SA curve type i (1, 2, 3 or 4),
$\mathrm{C_{i+1}}$ = SCS-SA curve type plus 1 (1, 2, 3 or 4), and
$\mathrm{RC_i}$ = Cumulative rainfall ratio of SCS-SA curve i and time step t.

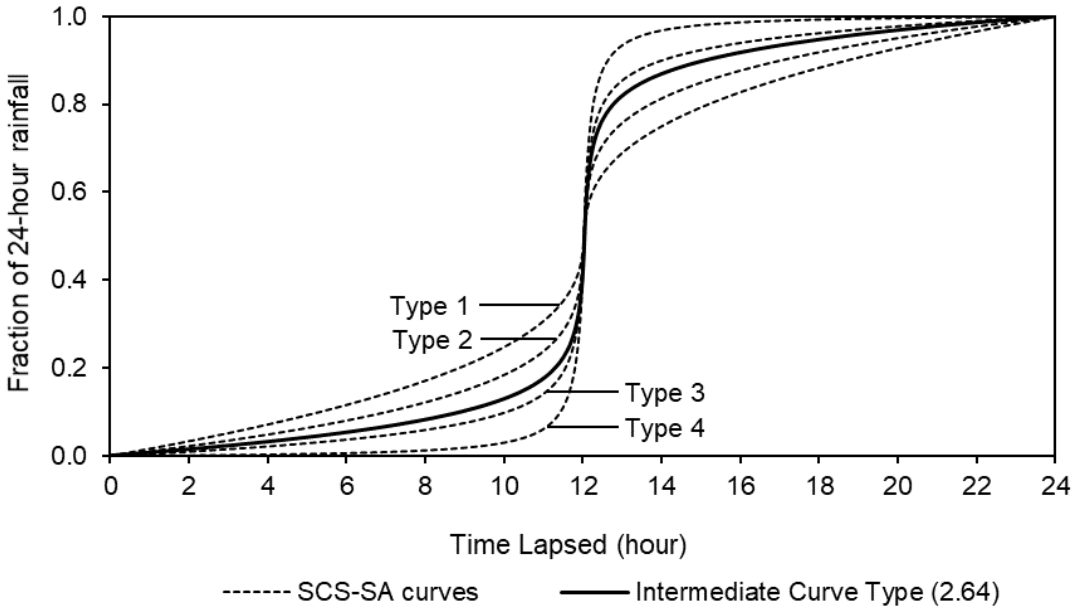

Figure 4.21: Example of an intermediate SCS-SA curve

To simplify the variation of the at-site intermediate curve types across Gauteng, the maximum of the 5-min to 30-min, 1:5 to 1:20 year recurrence intervals at each site were determined, as depicted in Figure 4.22. This means that, for example, the intermediate curve type of 2.64 for O.R. Tambo would then be applicable for all duration from 5-min to 30-min and recurrence intervals from 1:5 to 1:20 year. Although the use of the maximum value will result in an overestimation for certain durations and return period, e.g. for the 1:20 year, 5-min intermediate curve type of 1.96, the use of the maximum value will result in a conservative (i.e. most intense) rainfall distribution. However, interpolating the 2.64 intermediate curve type is an improvement from using the recommended Type 3 curve for Gauteng.

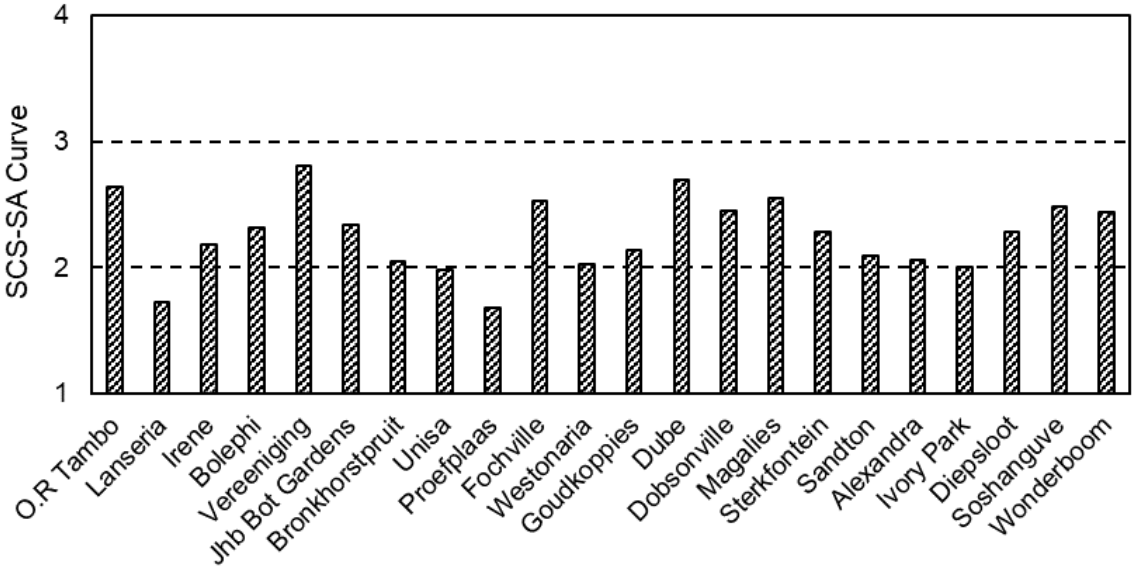

Figure 4.22: Maximum intermediate curve type for the 5 to 30-min duration range

To envisage the variation of intermediate curve types, the maximums from Figure 4.22 was interpolated with the Inverse Distance Weighting (IDW) method. Moeletsi et al. (2016) evaluated the IDW method for patching daily rainfall over the Free State Province, South Africa, and found the optimal power parameter as both 2.0 and 2.5. Although the application of the IDW in this study is somewhat different, a power parameter of 2.5 was used, and the IC types across Gauteng interpolated as depicted in Figure 4.23. The appropriate power parameter for this application needs to be determined in a future study. Smaller duration ranges for different recurrence intervals could also be considered. However, any future refinements of the intermediate curve types must be preceded by the recommendations made in Section 4.2.

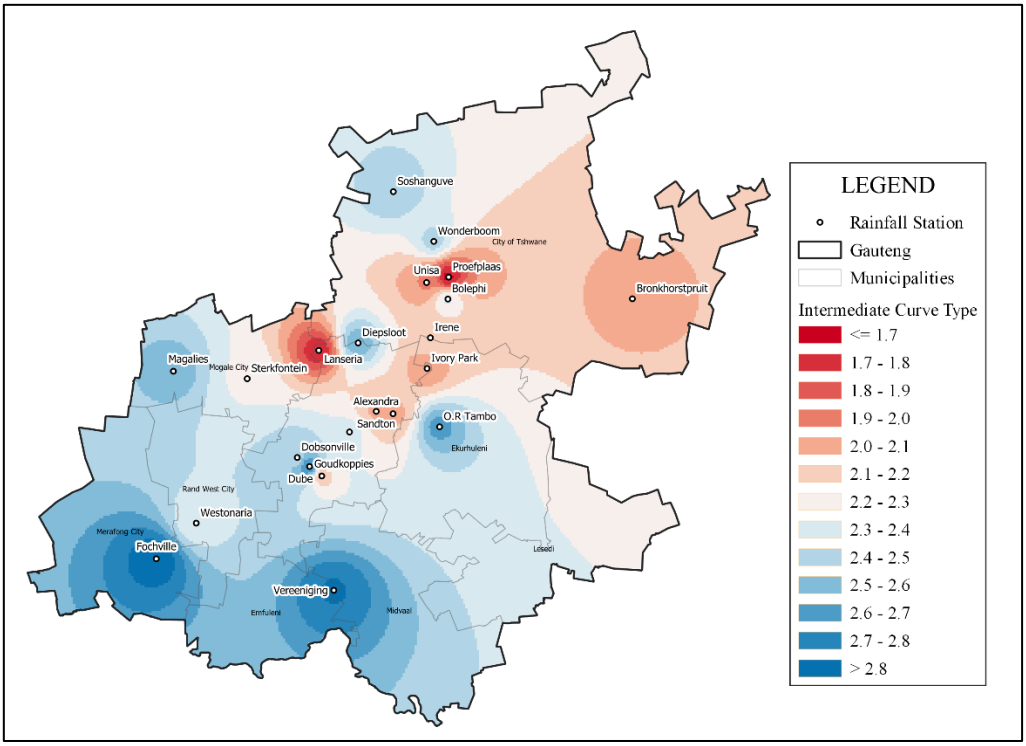

Figure 4.23 Maximum interpolated intermediate curve type for the 5-min to 30-min duration range using the IDW method

4.6 SCS CURVE COMPARISON

The use of the SCS curves (Brooker, 2021, personal communication, 22 February) is still preferred by some engineers. Hence, the SCS curves were also investigated. A comprehensive comparison between the D-hour to 24-hour ratios of the design rainfall and the ratios of the four SCS-SA curves were conducted in Section 4.5. Therefore, the SCS curves were compared to the SCS-SA curves rather than the at-site or DRESA estimated design rainfall.

The development of the SCS curves is, however, not the same as the SCS-SA curves. The approach used in the development of the SCS-SA curves follows the rainfall distribution procedure described in Section 4.4, whereas the SCS curves were based on the peak 30-min design rainfall for specific regions in the USA, as described in Section 2.5.1. The SCS curves for 6-min intervals were downloaded from NRCS's website (USDA, 2020) and the maximum ratios were extracted from the data by using a moving window period. For standard time steps which are not multiples of six minutes, the ratios were determined using the incremental intensity concept as described in Section 4.4. The final ratios for the standard time steps of the four SCS curves are summarised in Table 4.5. These ratios were then compared with the ratios of the SCS-SA curves depicted in Figure 4.24. This indicates that, for example, the SCS Type II is approximately equal to the SCS-SA Type 2. However, the 30-min IC type is 2.31 as depicted in Figure 4.25, which is the maximum ratio that could be achieved with the SCS curves. The ratio of the Type II curve decreases towards the 5-min as well as towards the 20-hour ratio. The intermediate SCS-SA curve types that are associated with the SCS Type III are all less than 2.00 for all durations less than 6-hours. Therefore, Type III as well as the Type 1 and Type 1A, are not recommended. The use of the Type II curve is, however, very limited and it must be used with caution.

Table 4.5: D-hour to 24-hour ratios for the four SCS curves

Duration	Type I	Type Ia	Type II	Type III
5m	0.061	0.020	0.112	0.070
10m	0.113	0.040	0.207	0.140
15m	0.150	0.060	0.274	0.197
30m	0.213	0.115	0.380	0.287
45m	0.252	0.147	0.423	0.359
1h	0.281	0.171	0.454	0.404
1.5h	0.330	0.215	0.501	0.458
2h	0.370	0.252	0.538	0.500
4h	0.492	0.371	0.639	0.622
6h	0.578	0.468	0.707	0.709
8h	0.647	0.548	0.760	0.772
10h	0.707	0.621	0.803	0.819
12h	0.761	0.687	0.841	0.856
16h	0.857	0.811	0.904	0.914
20h	0.935	0.917	0.955	0.961
24h	1.000	1.000	1.000	1.000

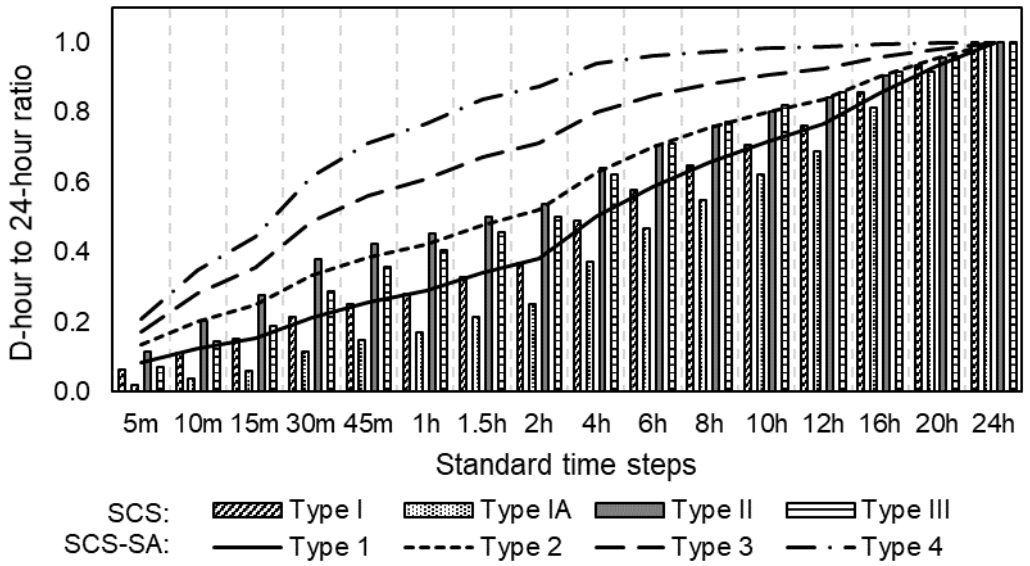

Figure 4.24: D-hour to 24-hour ratios of SCS curves compared to SCS-SA curves

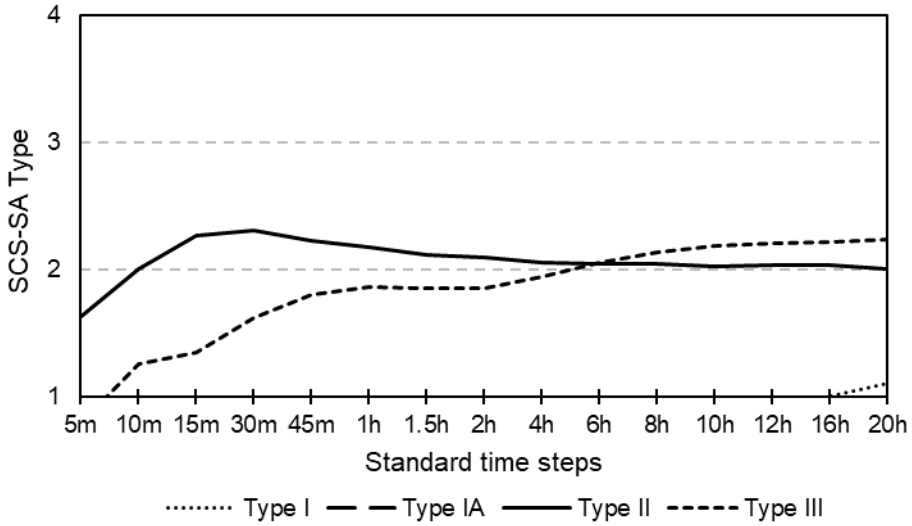

Figure 4.25: IC types associated with the SCS curves

4.7 STANDARDISED MASS CURVES

Standardised mass curves, or more commonly known as Huff curves, were developed by non-dimensionalising all significant storm events with respect to the total duration and total rainfall depth. The curves that were developed for O.R. Tambo, using the significant independent storm events that were identified in Section 3.5, are depicted as examples in Figure 4.26. The 10, 50 and 90% percentiles were determined at 0.05 dimensionless time intervals along the horizontal axis. Tenth-degree polynomials were fitted through the ordinates and coefficients in the form of Equation 4.17 were determined for each curve.

$$P = a \cdot T^{10} + b \cdot T^{9} + c \cdot T^{8} + d \cdot T^{7} + e \cdot T^{6} + f \cdot T^{5} + g \cdot T^{4} + h \cdot T^{3} + i \cdot T^{2} + j \cdot T \quad [4.17]$$

where:

P = fraction of total rainfall,

$a - j$ = regression coefficients, and

T = fraction of total duration.

The D-hour to 24-hour ratios of the first quartile, 90% standardised mass curve was then compared with the ratios of the four SCS-SA curves as depicted in Figure 4.27. Only the first quartile, 90% curve was considered because of its intensities being the highest. As demonstrated in Section 4.5, the ratios for the O.R Tambo station varies between the SCS-SA Types 2 and 3. It is seen in Figure 4.27 that the ratios of all standard time steps up to 1-hour are less than 0.1 which is an underestimation of the real ratios. This is, however, concerning because the peak discharge from catchments with rapid response times will be underestimated. The effects of different synthetic design storms applied to an EPA SWMM model are demonstrated in Chapter 5.

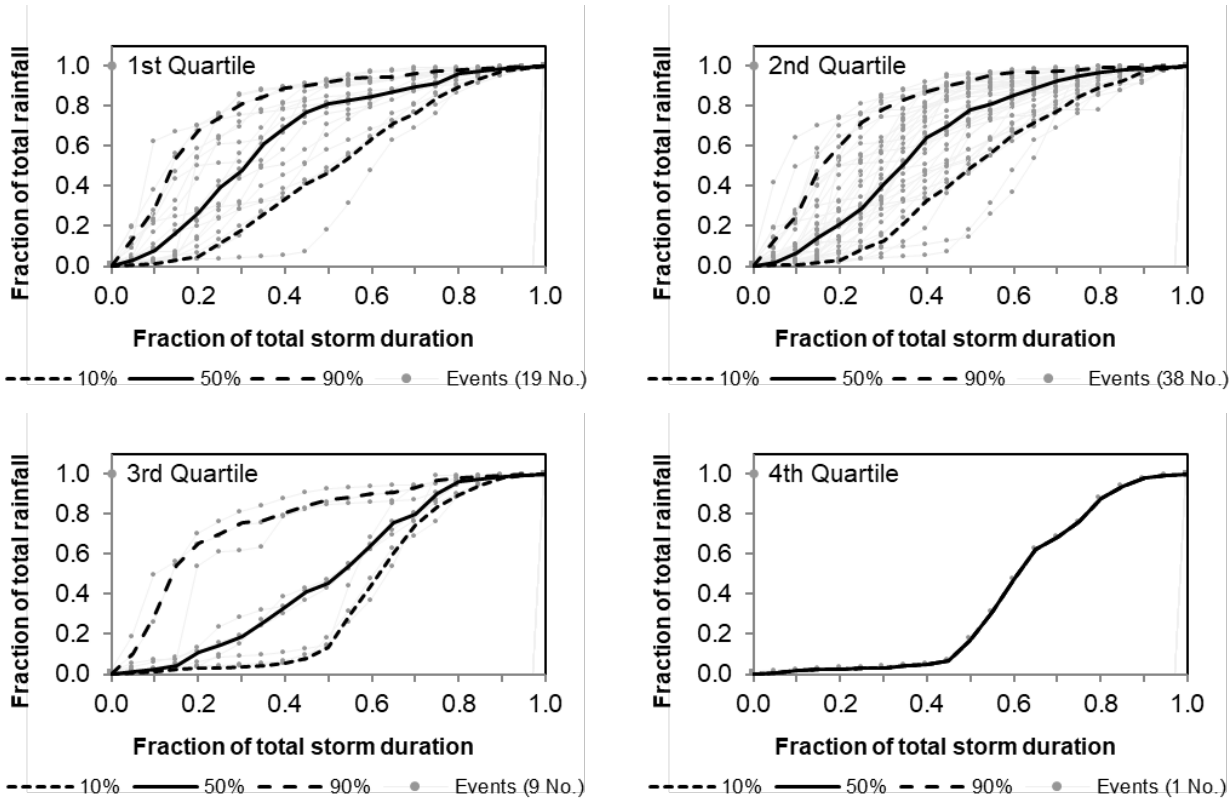

Figure 4.26: Standardised mass curves (Huff curves) for O.R. Tambo

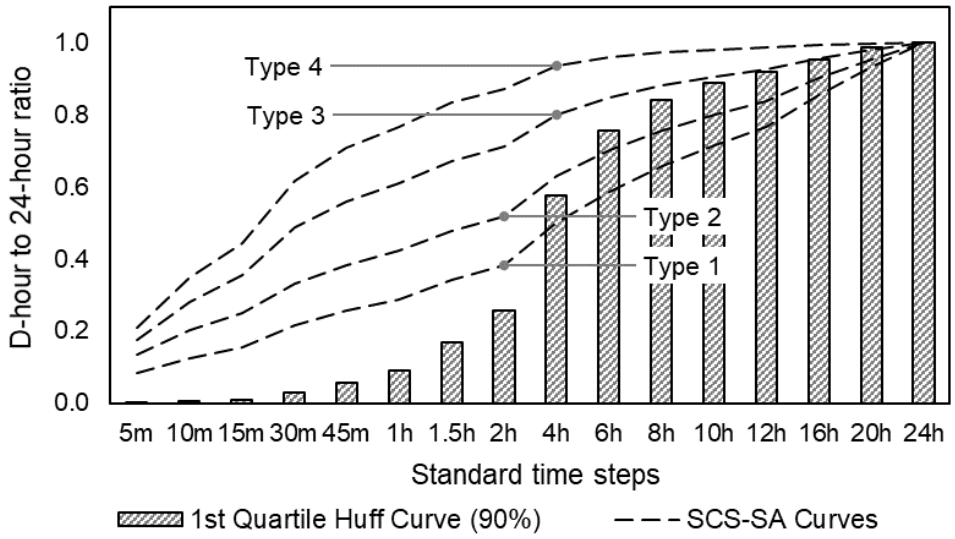

Figure 4.27: Standard time step ratios for the 1st quartile standardised mass curves (90%) for the O.R Tambo station relative to the standard SCS-SA curves

4.8 CHAPTER SUMMARY

This chapter has provided the basis to generate synthetic design storms using the methods that are considered for this study, and to assess the performance of the methods. For example, the primary storm parameters consisting of the storm advancement coefficient and the dimensionless time to peak were determined to be 0.38 and 0.20, respectively. It can be seen that the two coefficients, although similar by definition, are not similar. This is because of the difference in calculation procedure. Storm events, identified in the previous chapter, with an MDP of 15-min, were used to determine these parameters. The use of this MDP was based on the argument that if the MDP exceeds the time of concentration, any rainfall after the dry period could no longer influence the peak discharge of the previous spell.

The reaction time of the EPA SWMM model considered in the next chapter, which is representative of the catchment size targeted in this study, was found to have a reaction time of 15-min, and therefore, the 15-min MDP were selected. The storm shape and average intensity assessments in the next chapter will, therefore, also be based on the 15-min MDP. A methodology of determining regression coefficients for the CDS method, using the GRG non-linear solver was also developed. These coefficients, together with the storm advancement coefficient, will be used for the CDS method in the next chapter. The simulated design rainfall intensities, using the regression coefficients, were evaluated by determining the RE of the actual design rainfall intensities obtained from the DRESA software. From this analysis it was evident that the results obtained from the methodology, involving the GRG non-linear solver, was sufficiently accurate to determine the regression coefficients required by the CDS method.

Design rainfalls were determined using the at-site AMS for 16 standard durations for each station and then compared with the design rainfall obtained from the DRESA software. It was found that the average RE was within the 90% upper and lower bounds given by the DRESA software. Short duration design rainfall of between 5- and 30-min was identified to be substantially lower than the DRESA software and further investigation is recommended to identify the cause of the error.

The procedure to distribute design rainfall equally around the peak intensity was adapted to utilize the concept of incremental intensities for the interpolation of design rainfall for intermediate time steps. This was then subsequently utilised to generate the DC5, DC10 and the DC20 curves from the design rainfall developed from the PD analysis. The procedure to extract an event of less than 24-hour was also illustrated. This procedure will be utilised in the next chapter to extract synthetic design storms from the SCS, SCS-SA, DC5, DC10 and the DC20 curves, for durations equal to the significant events.

The D-hour to 24-hour ratios were also determined and their position relative to the four standard SCS-SA curves were determined, using the design rainfall of the DRESA software as well as the at-site design rainfall analysis. The results from both sources of design rainfall indicated that, on average, Gauteng conforms more closely to the SCS-SA Type 2 curve, rather than Type 3. However, a significant variation in the ratios for the various durations were observed because the derived ratios plotted between standard SCS-SA type curves. This led to the development of intermediate curve types whereby a curve is linearly interpolated between two standard type curves. The method of interpolating between standard type curves was also documented.

Standardised mass curves (Huff curves) were developed and based on the limited tests conducted on these curves, the results indicate an underestimation of the short duration design rainfall. Therefore, this method was not considered for the single event-based modelling in the next chapter because it will lead to an underestimation of the peak discharge.

In the next chapter, the flow results from a single event-based modelling, using the standard type curves and the intermediate type curves, will be demonstrated.

CHAPTER 5: EVALUATION OF SYNTHETIC DESIGN STORMS

This chapter contains details of the evaluation of synthetic design storm evaluation by comparison between mass curves and average intensities, as well as simulated peak discharge and runoff volumes. The evaluation of the synthetic design storms was conducted by considering two characteristics of an event, namely the shape of the mass curves, and the average intensities of standard time steps. This was achieved by non-dimensionalising each significant event in terms of rainfall and generating a synthetic storm event matching the total duration. Comparison between the simulated peak discharge and runoff volume generated with different synthetic design storms were also compared with results from continuous simulation using observed rainfall data as input. The methods used to generate synthetic design storms includes the following:

(a) the CDS method, using the regression coefficients from Table 4.1, and an average advancement coefficient of 0.38,
(b) standard curves, including the SCS-SA Type 2 [SA(T2)] and 3 [SA(T3)],
(c) DCs developed using the methodology described in Section 4.4, and the on-site design rainfall described in Section 4.3,
(d) the Rectangular (REC) method, and
(e) the Triangular (TRI) method using a dimensionless time to peak of 0.20.

5.1 MASS CURVE COMPARISON

The evaluation of the shape of the mass curves was conducted by considering each significant storm event with an MDP of 15-min. The GOF of the shape of the synthetic storm event compared to the observed storm event at 5-min intervals were determined using the Mean Absolute Relative Error (MARE) technique. The average of all significant events was the final score given to the method used to generate the synthetic storm event. The general MARE formula for the shape of the mass curve (MARE_S) is expressed in Equation 5.1.

$$\mathrm{MARE\_S} = \frac{1}{N_s \cdot \overline{N_d}} \sum_{j=1}^{N_s} \sum_{i=1}^{N_d} \left[\frac{\left| S_{i,j} - O_{i,j} \right|}{O_{i,j}} \right] \qquad [\ 5.1\ ]$$

where:

$S_{i,j}$ = synthetic depth for duration i and storm j (mm),
$O_{i,j}$ = observed depth for duration i and storm j (mm),
$\overline{N_d}$ = average number of 5-min data points per storm, and
N_s = number of storms.

A typical result of the GOF between an observed individual storm event and the synthetic design storms is summarised in Figure 5.1. The storm event that occurred on 29 October 1994 at O.R. Tambo is used to illustrate the assessment process followed for all significant events identified in Section 3.5. For example, this event had a total duration of 50-min and the total rainfall was 17 mm. Considering the results presented in Figure 5.1 the DC5 best represents the shape of the observed mass curve with a MARE_S of 0.311. The MARE_S of the DC10, and DC20 curves performed slightly worse with values of 0.326 and 0.350, respectively. The SA(T2) and SA(T3) also showed good performance with values of 0.366 and 0.337, respectively. The CDS method performed better than the REC and TRI, with values of 0.431, 0.535, 0.494, respectively. Therefore, considering this single event and the O.R Tambo station, the DC5 presented the best fit of all the methods, and the REC the worst.

To determine the overall performance of the methods, the average and median MARE_S values were determined for all the significant events from the five best stations in Gauteng, namely O.R Tambo, Irene, Vereeniging, Johannesburg Botanical Gardens, and Unisa. The significant events from the five stations were pooled together before the analysis was conducted. The result of this analysis is depicted in Figure 5.2. It is seen that the TRI best represents observed events with the lowest MARE_S values, followed by the REC. The results of both TRI and REC outperformed CDS, DC5, DC10, DC20, SA(T2) and SA(T3). It is important to note that this means the methods that use a single point on the IDF curve according to Figure 2.17, performed better than the methods that use the entire IDF curve. This is attributed to the position of the peak intensity relative to the total duration. For DC5, DC10, DC20, SA(T2) and SA(T3) the peak intensity is in the middle of 24-hours, whereas with CDS it is slightly earlier. Therefore, the effect of adjusting the position of the peak, was investigated. This is described in the next section.

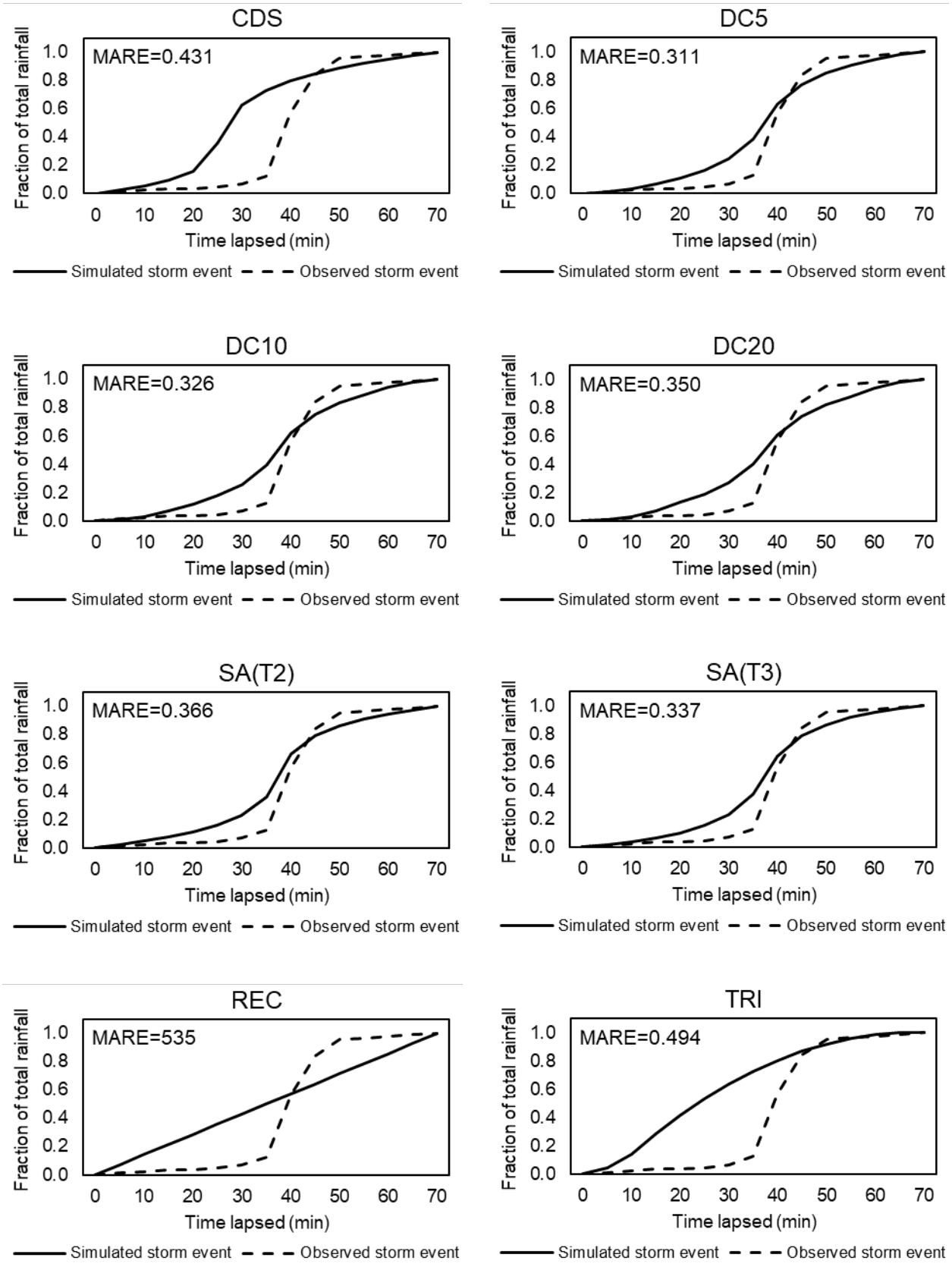

Figure 5.1: Typical GOF between the shape of an observed individual storm event at O.R Tambo on 29 October 1994, and a synthetic storm event

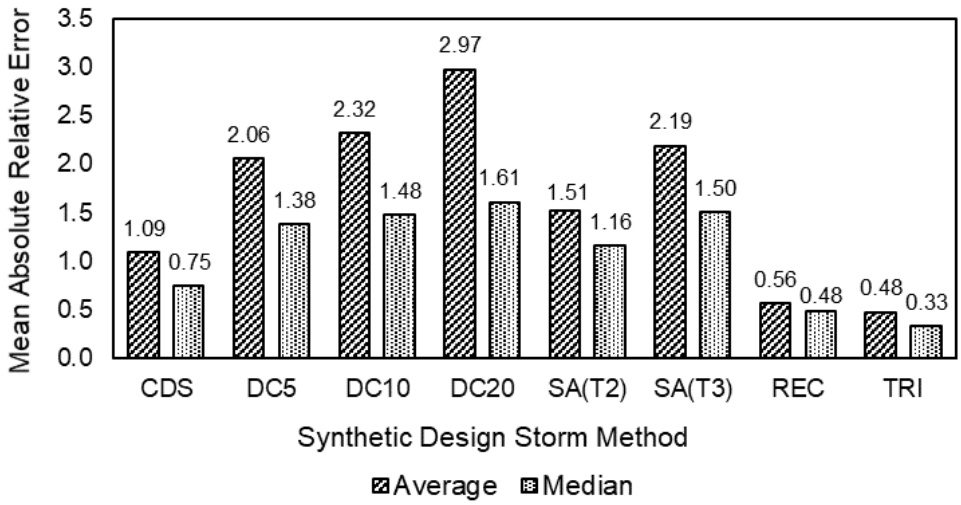

Figure 5.2: MARE_S between observed storm events and synthetic design storms at the five best stations in Gauteng

5.2 ADJUSTMENT OF THE PEAK INTENSITY'S POSITION

This chapter describes the development of a procedure to adjust the position of the SCS-SA curves. The updated results of the mass curve comparison, described in Section 5.1, using the modified curves are also presented below.

As described in Section 2.5.2 of the literature review, the SCS-SA curves were developed with the peak intensity at the centre of 24-hours and the design rainfall of increasing durations divided equally on either side of the peak intensity. Conversely, with the CDS method the peak intensity can be positioned anywhere between the start and end of the event, but with the average intensities of all durations still embedded in the event as depicted in Figure 2.3. Therefore, the same methodology used to determine regression coefficients described in Section 4.3 was used to determine the coefficients of the SCS-SA curves. This means that the SCS-SA curves were recreated using the CDS method, but with the peak earlier during the event. The optimised regression coefficients of the SCS-SA curves are summarised in Table 5.1.

Table 5.1: CDS Regression coefficients for the SCS-SA curves

Description	SCS-SA curves	
	Type 2	Type 3
a	10.079	27.517
b	6.470	11.686
c	0.755	0.891

The CDS method with IDF regression coefficients described in Section 4.3, were also re-evaluated, but with an optimized advancement coefficient. The updated results for the mass curve comparison are depicted in Figure 5.3. It is seen that the results for the CDS, SA(T2) and SA(T3) improved significantly. An advancement coefficient of 0.01 was found to give the best results with improved average GOF values. The same optimization procedure was, however, not attempted for the DC5, DC10 and DC20 curves. This will entail the smoothing of the DDF curves described in Section 4.2, which falls outside the scope of this study. Therefore, only improved results for the CDS, SA(T2) and SA(T3) are depicted in Figure 5.3.

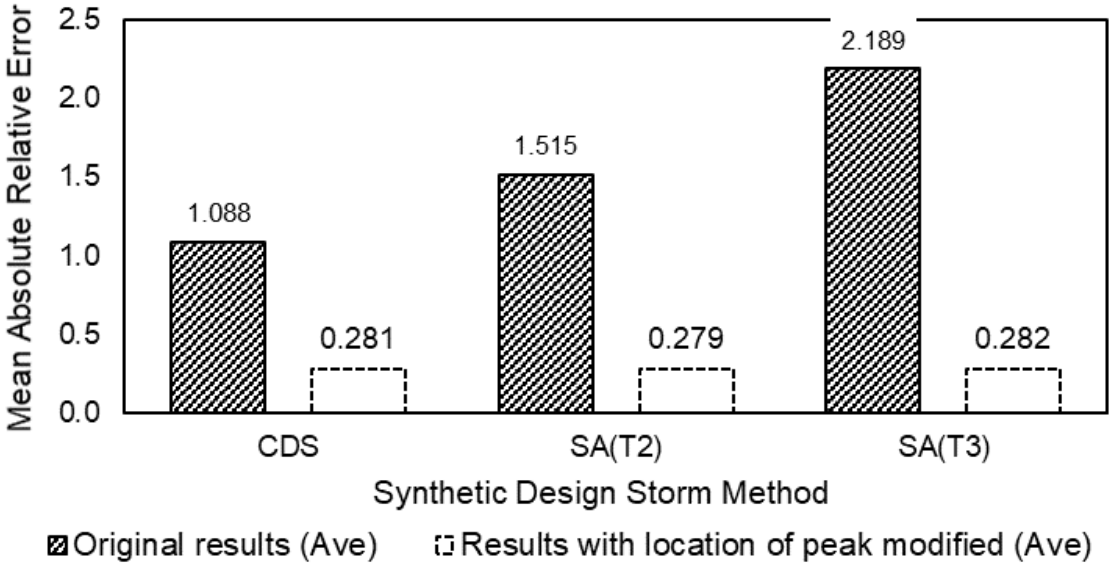

Figure 5.3: Synthetic design storms modified with peak earlier during an event

It can be concluded that the performance of the methods that use the entire IDF curve can be altered and improved by modifying the position of the peak intensity relative to the total duration of an event. However, any value of MARE_S above zero implies that the shape of a synthetic design storm does represent observed hyetographs. Another factor that contributes to an MARE_S value above zero is the variation of recurrence interval within observed storm events. Conversely, synthetic design storms assume that intensities of increasing durations, embedded in an event, have the same recurrence interval. This can lead to an overcompensation by reducing the advancement coefficient to a value beyond the true optimum point. This phenomenon is explained in detail in Section 5.3 which describes the assessment of the average intensities between observed storm events and synthetic design storms.

5.3 AVERAGE INTENSITY COMPARISON

The evaluation of the intensities was conducted by considering the ratios of average intensities of the standard durations (5, 10, 15, 30, 45-min, etc.) of each significant storm event. The GOF of the ratios of the synthetic design storms compared to the observed storm events was determined using the general MARE formula for the average intensity ratios (MARE_I), expressed in Equation 5.2.

$$\text{MARE\_I} = \frac{1}{N_s}\sum_{j=1}^{N_s}\left[\frac{\left|S_j - O_j\right|}{O_j}\right] \qquad [\ 5.2\ ]$$

where:

S_j = synthetic intensity for storm j (mm/h),

O_j = observed intensity for storm j (mm/h), and

N_s = number of storms.

Similar to the mass curve assessment, the average intensity ratio assessment was conducted considering the CDS, DC5, DC10, DC20, SA(T2), SA(T3), REC and TRI methods. The same storm event, depicted in Figure 5.1, is used to illustrate the comparison of the average intensity ratios, although all significant storm events were used for the assessment. The results for the example event are depicted in Figure 5.4. In contrast to MARE_S, the MARE_I result for REC is the worst. This is attributed to the uniform intensity assumed by the REC method. The result for TRI is slightly better than REC because of the minor increase in variation of intensities. This can be seen by considering Equation 2.14 which stipulates that the peak intensity of a triangular hyetograph is twice the total rainfall depth of the event, divided by the total duration. This means the longer the duration of an event, the lower the peak intensity becomes, which explains the poor MARE_I for the TRI method. The results for the CDS, DC5, DC10, DC20, SA(T2) and SA(T3), depicted in Figure 5.4, are all very similar with MARE_I ranging from a minimum of 0.218 for SA(T2) to a maximum of 0.307 for DC20.

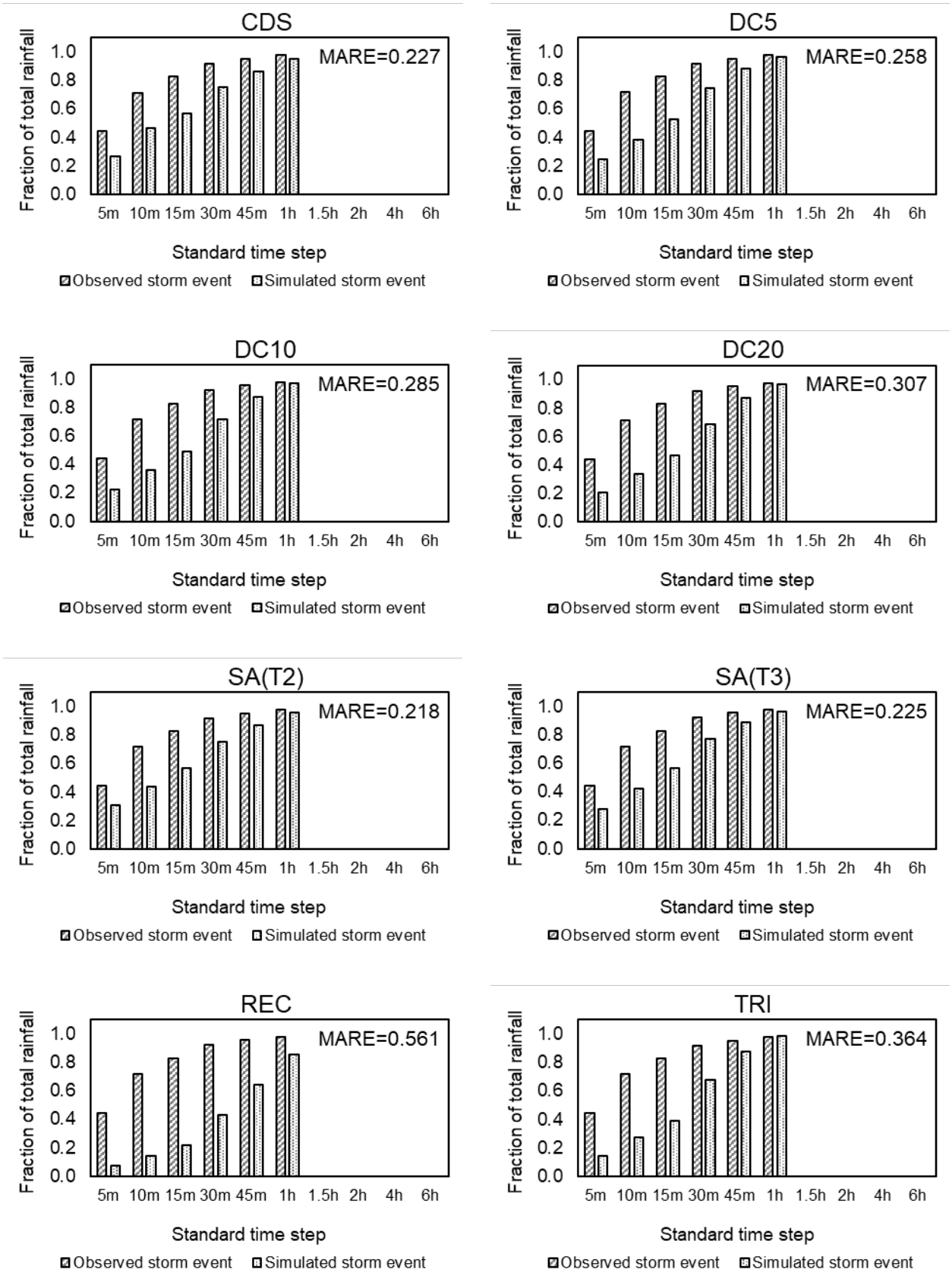

Figure 5.4: Typical GOF between the average intensities of an observed individual storm event at O.R Tambo on 29 October 1994, and a synthetic storm event

Following the analysis of individual storm events, the average and median values of the five stations with the best data sets were determined and the results for significant events at these sites are shown in Figure 5.5. The average and median values for the REC and TRI methods are approximately equal, which indicates an approximately symmetrical frequency distribution. According to this results the REC method has the worst representation of average intensities, followed by the TRI method. The median values for the CDS, DC5, DC10, DC20, SA(T2) and SA(T3) methods are similar and much lower than the REC and TRI methods. This indicates a much better representation of average intensities. However, a significant difference between the average and median values for these methods can be observed. This shows that the results are skewed, which is confirmed by considering the frequency of occurrences depicted in Figure 5.6.

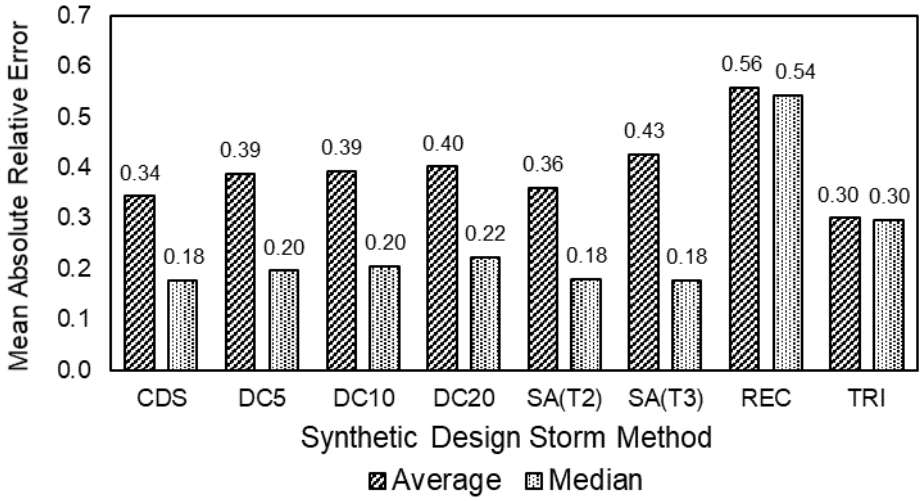

Figure 5.5: MARE_I between observed storm events and synthetic design storms at the five best stations in Gauteng

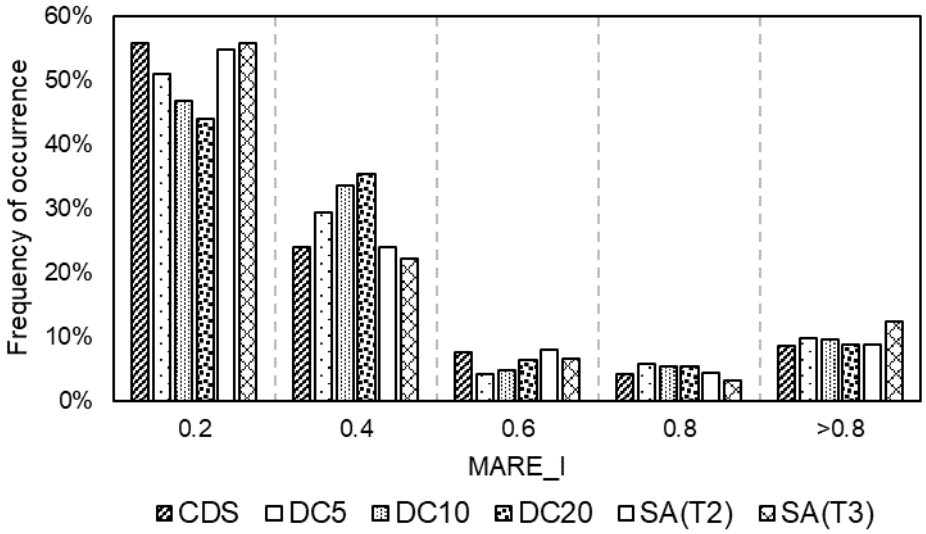

Figure 5.6: MARE_I frequency of occurrence for methods base on entire IDF curve

The results depicted in Figure 5.5 show that the CDS, SA(T2) and SA(T3) performed the best of all the methods considering the MARE_I. However, the modification to the location of the peak intensity applied in Chapter 5.2 will not improve the MARE_I value. This is because of the embedment of all intensities with increasing duration in a single event associated with the methods that utilize the entire IDF curve. This procedure, therefore, does not alter the intensities of the synthetic design storm but merely the location of the peak. The variation of the Recurrence Interval (RI) of average intensities during an observed event was therefore further investigated in Section 5.4 to see the causes of the MARE_I value.

5.4 VARIATION IN RI OF AVERAGE INTENSITIES

To determine the variation in RI of the average intensities during a storm event, the MRI criterion described in Section 3.5 was applied. This was done by determining the RI ratio (RIR) of the standard durations relative to the Maximum RI (RIM) of each storm event with the same maximum standard duration. The average RIR of the five best stations in Gauteng, depicted in Figure 5.7, which was determined using Equation 5.3.

$$\mathrm{RIR}_{t,D} = \frac{1}{N_s \cdot N_{SD}} \sum_{s=1}^{N_S} \sum_{i=1}^{N_{SD}} \frac{\mathrm{RI}_{t,i,s}}{\mathrm{RIM}_i} \qquad [\ 5.3\ ]$$

where:

RIR = recurrence interval ratio of time step t, and total duration D,
N_{SD} = number of storm events with total duration D,
N_S = number of stations (5),
$\mathrm{RI}_{t,i,s}$ = recurrence interval of time step t, storm event i, and station s (year), and
RIM_i = maximum recurrence interval of storm event i, (year).

The results depicted in Figure 5.7 show that, on average, the maximum standard durations for 6, 8, 12 and 16-hour events have the maximum RI, and the smallest duration the minimum RI. For example, storm events with a total duration of more than 12 but less than 16 hours, denoted by the 12h curve, have a 12-hour RIR of approximately 1.0, but a 5-min RIR of approximately 0.1. This finding contradicts the assumption that the RI of all standard durations have the same RI, which is associated with the methods that utilize the entire IDF curve.

For storm events with total duration less than 6-hours, the RI of the maximum time steps starts to decrease which indicates a tendency for the maximum RI to shift to the shorter time steps. Considering the 1h and 2h curves, the RIR of the 1 and 2-hour time steps are lower than the 30-min and 1-hour RIR, respectively. This effect is presented as the cause of an MARE_I above zero, as described in Section 5.3.

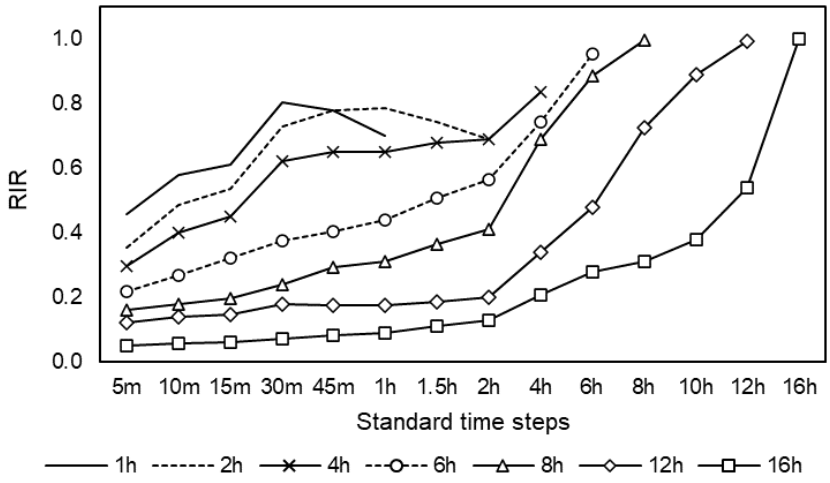

Figure 5.7: Variation in Recurrence Interval (RI) for the five best stations in Gauteng

5.5 EVENT-BASED AND CONTINUOUS SIMULATION

An assessment was conducted in terms of the peak discharge and runoff volume simulated from a SWMM model of a hypothetical catchment area. This was achieved by comparing the result of an event-based simulation with the results from a continuous simulation application of the model. The hydrological urban catchment defined by Gironas et al. (2009) as depicted in Figure 5.8 was used in this assessment. The catchment has a total area of 11.6 ha which was divided into seven sub-catchment areas. The characteristics of the sub-catchments are summarised in Table 5.2.

Figure 5.8: The catchment used for the SWMM modelling

Table 5.2: Sub-catchment SWMM characteristics

Description	Sub-catchment						
	S1	S2	S3	S4	S5	S6	S7
Area (ha)	1.829	1.906	1.505	2.740	1.930	0.793	0.935
Width (m)	480.1	500.3	438.8	706.2	506.6	208.1	273.4
Slope (%)	2.5	2.5	4.5	4.0	2.5	2.5	3.8
Imperv (%)	56.8	63.0	39.5	49.9	87.7	95.0	0.0
N-Imperv	0.015	0.015	0.015	0.015	0.015	0.015	0.015
N-Perv	0.240	0.240	0.240	0.240	0.240	0.240	0.240
Dstore-Imperv (mm)	1.5	1.5	1.5	1.5	1.5	1.5	1.5
Dstore-Perv (mm)	7.5	7.5	7.5	7.5	7.5	7.5	7.5
Zero-Imperv (%)	25	25	25	25	25	25	25
Subarea Routing	Outlet	Outlet	Outlet	Outlet	Outlet	Outlet	Outlet
Percent Routed (%)	100	100	100	100	100	100	100
Suction head (mm)	110	110	110	110	110	110	110
Conductivity (mm/h)	11	11	11	11	11	11	11
Initial deficit (m/m) Note	0.263	0.263	0.263	0.263	0.263	0.263	0.263

Note: Difference between porosity and field capacity

5.5.1 Peak discharge comparison

The catchment depicted in Figure 5.8 has a single outfall node, namely O1. This node was selected to conduct the flow comparison between the continuous simulation and the event-based model. The time step used in the simulations was 5-min. The observed rainfall data of five stations with the best available data sets were used as input data for five different continuous simulation models, namely O.R. Tambo, Irene, Vereeniging, Johannesburg Botanical Gardens and Unisa. Small continuity errors existed following the simulations which confirm the validity of the analysis results. The AMS of the flow rates, using the five different rainfall data sets, were extracted, and are summarised in Table 5.3. This was followed by a PD analysis using the GEV distribution to estimate deign peak discharges. The result of the PD analysis is summarized in Table 5.4.

Table 5.3: Annual peak discharge at node O1 using the observed rainfall data at the five best stations in Gauteng

YEAR	PEAK FLOW RATE (m^3/s)				
	O.R Tambo	Irene	Vereeniging	Jhb Bot	Unisa
1994	1.282	1.251	4.466	1.042	2.770
1995	0.935	2.365	5.208	1.129	2.292
1996	0.954	1.561	1.455	2.102	4.317
1997	1.543	1.567	2.446	1.047	2.057
1998	0.958	1.050	2.264	1.433	0.676
1999	1.126	1.945	1.988	0.960	1.303
2000	1.257	2.368	1.334	1.818	1.132
2001	2.350	1.556	1.263	0.472	0.932
2002	1.496	0.853	0.741	1.010	1.811
2003	1.348	0.626	0.749	0.814	0.977
2004	1.146	1.020	0.790	1.109	1.916
2005	1.070	1.213	0.974	2.448	1.580
2006	1.211	1.213	0.920	0.800	1.476
2007	0.495	1.053	0.677	1.593	1.169
2008	0.872	1.007	1.059	1.015	2.069
2009	1.380	0.849	1.887	1.683	2.207
2010	1.611	1.362	1.182	3.198	1.337
2011	1.946	1.294	1.180	2.184	1.414
2012	1.365	0.958	2.299	1.100	1.431
2013	1.242	1.646	1.295	1.746	1.042
2014	1.291	2.591	1.804	1.241	2.894
2015	2.601	1.506	2.483	1.214	0.933
2016	4.160	1.268	1.588	1.225	1.362
2017	1.089	1.423	1.207	1.995	1.118
2018	0.882	0.765	1.563	1.085	1.247
2019	2.241	1.266	1.434	1.510	0.840
2020	1.245	2.159	1.317	3.097	1.771

Table 5.4: Estimated peak discharge at node O1 using the GEV PD for the five best stations in Gauteng

RI (years)	FLOW RATE (m^3/s)				
	O.R Tambo	Irene	Vereeniging	Jhb Bot	Unisa
1:2	1.286	1.328	1.460	1.376	1.472
1:5	1.866	1.797	2.321	1.969	2.131
1:10	2.302	2.096	2.959	2.366	2.606
1:20	2.765	2.371	3.629	2.744	3.090
1:50	3.437	2.711	4.595	3.238	3.760

The same catchment depicted in Figure 5.8 was then simulated using a single event-based approach, using synthetic design storms as input data. Synthetic design storms for the 1:5, 1:10 and 1:20-year RIs were generated using the SA(T2), SA(T3), CDS, DC5, DC10 and the DC20 curves. A storm duration of 2-hours was considered for these methods since it will generally be adequate to exceed the longest time of concentration (Watson, 1981). Longer durations will lead to higher levels of soil moisture content, and therefore, the 24-hours was also considered to evaluate the effect on the peak discharge.

The REC and TRI methods were applied by finding the critical duration for the REC method and determining the minimum duration for the TRI method. This process is explained in detail in Section 5.5.3. Again, small continuity errors were obtained after each simulation which confirms the validity of the analysis results. The peak discharge at node O1 from the event-based simulation was obtained which was then compared to the peak discharge obtained from the continuous simulation which used the observed rainfall from of each rainfall station.

The average percentage RE between the results from the continuous simulation for each station, and the results from the REC and TRI methods, are depicted in Figure 5.9. The results using the CDS, SA(T2) and SA(T3) methods for the 2-hour and 24-hour single event-based modelling, are depicted in Figure 5.10 and Figure 5.11, respectively.

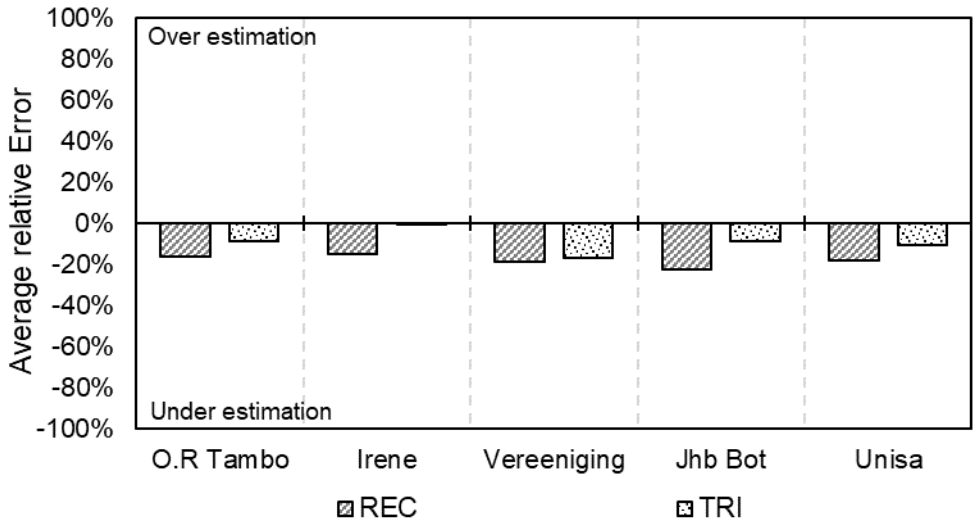

Figure 5.9: Average RE of the peak discharge at node O1 between continuous simulation and single event-based modelling using the REC and TRI methods

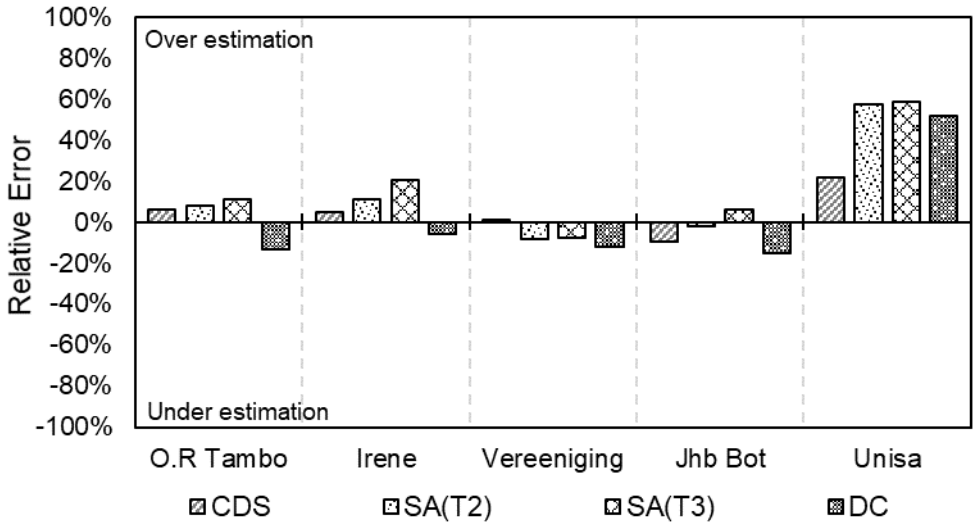

Figure 5.10: Average RE of the peak discharge at node O1 between continuous simulation and single event-based modelling using a 2-hour storm event

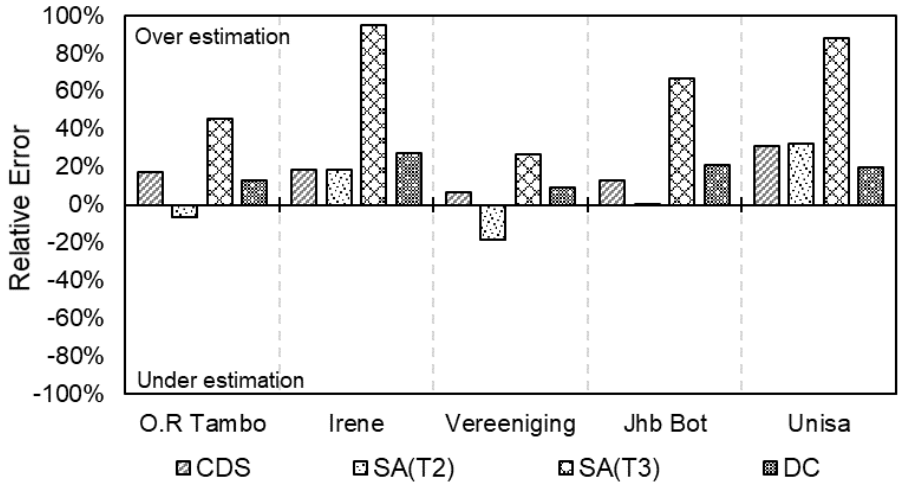

Figure 5.11: Average RE of the peak discharge at node O1 between continuous simulation and single event-based modelling using a 24-hour storm event

The average percentage RE depicted in Figure 5.9 to Figure 5.11 represents the average for the 1:5, 1:10 and 1:20 year results. This indicates that both the REC and TRI methods underestimated the peak discharge at all five stations. Since the same parameters were used in both the continuous simulation and single event-based modelling, the underestimation is attributed to the incorrect initial deficit applicable to single event-based modelling.

In terms of the results depicted in Figure 5.9 to Figure 5.11, the following are observed:

(a) The difference between SA(T2) and SA(T3) for the 24-hour event is much greater than the difference for the 2-hour event. This is attributed to the change in the ratio characteristics which is described in detail in Section 5.5.4.

(b) The RE for the CDS method is much greater for the 24-hour event compared to the error for the 2-hour event, which is expected because of the consistency provided by the CDS method in terms of average intensities. In other words, the average intensities of the 5, 10, 15-min, etc. remains constant, irrespective of the total duration of the event. This means that if the average intensities remain consistent, the soil has reached a higher level of soil moisture content during a 24-hour event compared to a 2-hour event.

(c) The results of the DC5, DC10 and the DC20 curves relative to SA(T2) and SA(T3) is consistent with the SCS-SA design rainfall ratio comparison described in Section 4.5. This consistency is described in detail in Section 5.5.5.

(d) The cause for the larger overestimation by the CDS, SA(T2), SA(T3), DC5, DC10 and DC20 at the Unisa station relative to the other stations is unknown and requires further investigation.

(e) The results of the CDS method, using a 2-hour event, is consistent with the results obtained from the continuous simulation. This can be seen with the small positive RE at O.R Tambo, Irene, and Vereeniging. The RE at Unisa was approximately 20% which is less than the overestimation of up to 60% by the SA(T2), SA(T3) and DC methods.

5.5.2 Runoff volume

An assessment of runoff volume was done by identifying the events that resulted in the annual peak discharge. The process involved the extraction of a three-day time series, one day before and one day after the date of the maximum, as depicted in Figure 5.12. The start and end of the event associated with the maximum discharge were determined graphically, and the event was then extracted for which the cumulative runoff volume was determined as depicted in Figure 5.13. This process was repeated for each annual maximum peak discharge and the associated runoff volume was calculated. The process is illustrated using the rainfall event of 9 February 2020 for O.R. Tambo in Figure 5.14. It is seen that the magnitude of the annual maximum discharge and associated runoff volumes is approximately related. However, the relationship is not directly related which can be seen, for example, by comparing the results for the years 1994 and 1995. In 1995 the maximum discharge is lower than the previous year, whereas the runoff volume was higher. Similar occurrences of this inconsistency are observed in 1997/98, 1998/99, 2003/04, 2009/10.

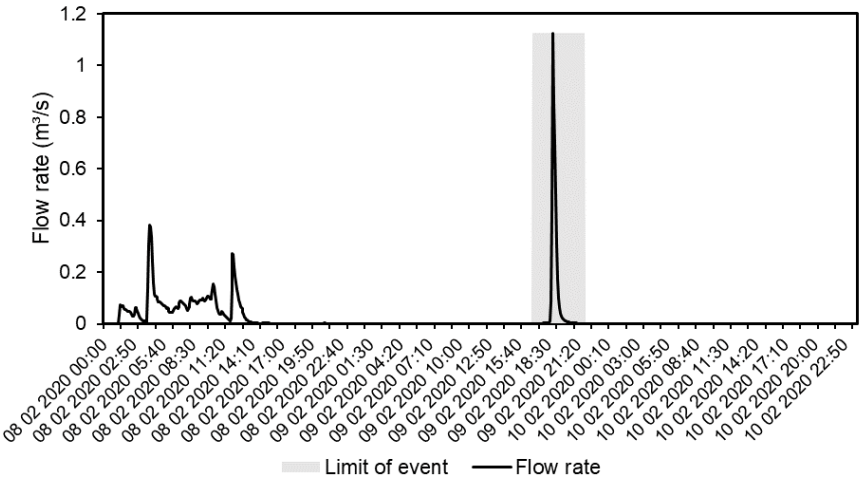

Figure 5.12: Three-day time series containing the event that resulted in the peak discharge at O.R. Tambo in the year 2020

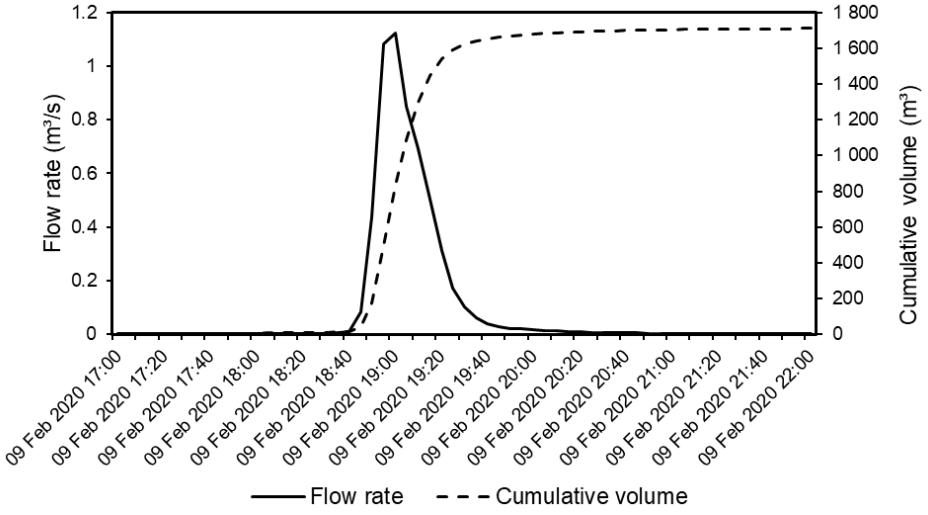

Figure 5.13: Extracted event that resulted in the peak discharge at O.R. Tambo in the year 2020

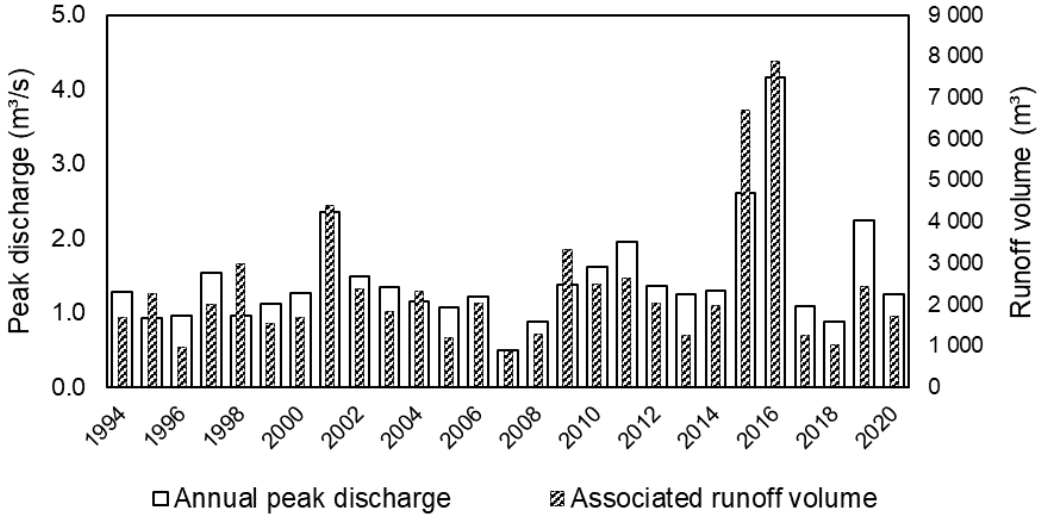

Figure 5.14: Annual peak discharge and associated runoff volume obtained from a continuous simulation for O.R. Tambo

The inconsistency in the runoff volume and peak discharge is observed by ranking the events in descending order according to the peak discharge as depicted in Figure 5.15. For example, the runoff volume in the years 2009, 1998 and 1995 should be ranked much higher. The smoothing of the runoff volume was therefore necessary to improve the consistancy, to prevent some runoff volumes with lower RIs to be more than others with higher RIs. Therefore, the same recurrence interval of the peak discharge was assigned to the runoff volume, and a logarithmic regression line for the runoff volume with the RI as the dependent variable, was determined as depicted in Figure 5.16. The R^2 of 0.795 indicates a reasonable fit to the data. The same process was followed for Irene and Johannesburg Botanical Gardens and R^2 of 0.524 and 0.072 were obtained. Only these three stations was used in this analysis, and future analyses could include additional sites.

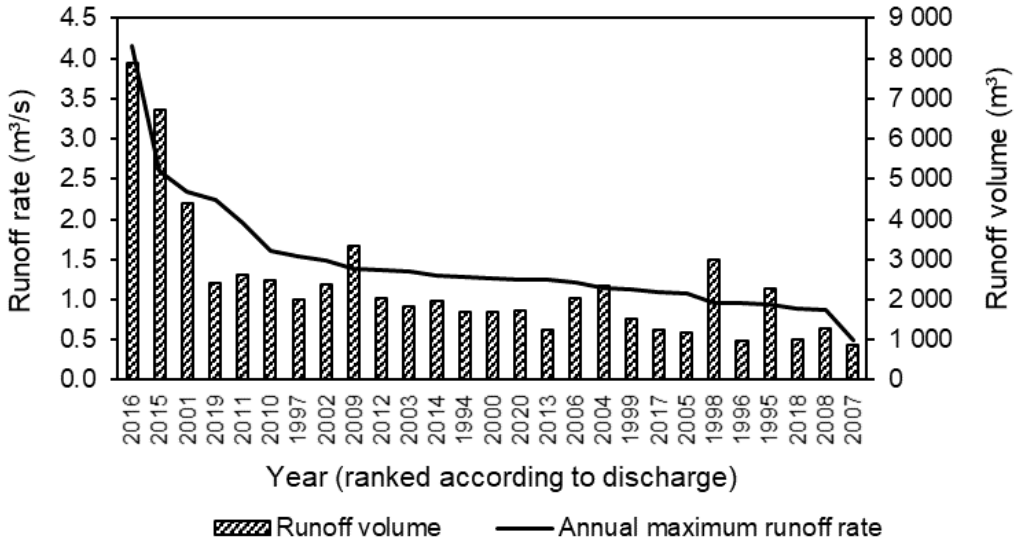

Figure 5.15: Annual peak discharge and corresponding runoff volume for O.R Tambo

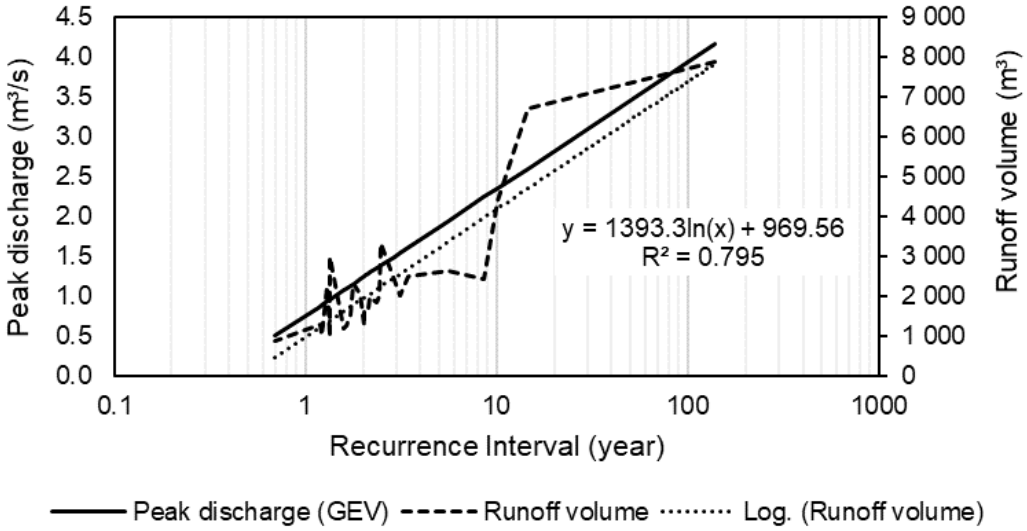

Figure 5.16: Interpolation of runoff volume for O.R Tambo

The runoff volume for the 1:5, 1:10 and 1:20 year recurrence intervals for O.R Tambo was calculated according to the logarithmic relationship depicted in Figure 5.16. These volumes were then used for comparison with the runoff volume obtained from the event-based simulations. The runoff volume was determined at the outfall node O1 depicted in Figure 5.8, using all the synthetic design storms as input data. The 2-hour rather than the 24-hour event was used for the SA(T2), SA(T3), CDS and DC methods because the total discharge from a 24-hour event would be much higher. The percentage RE between the runoff volumes of the single event-based simulations is depicted in Figure 5.17. It is seen that the peak discharge was underestimated by between 35% and 55% using the REC and TRI as input data. The peak discharge obtained from the SA(T2), SA(T3), CDS and DC methods are overestimated by up to 45%. The poor performance could be attributed to the poor R^2 between the RI and runoff volume.

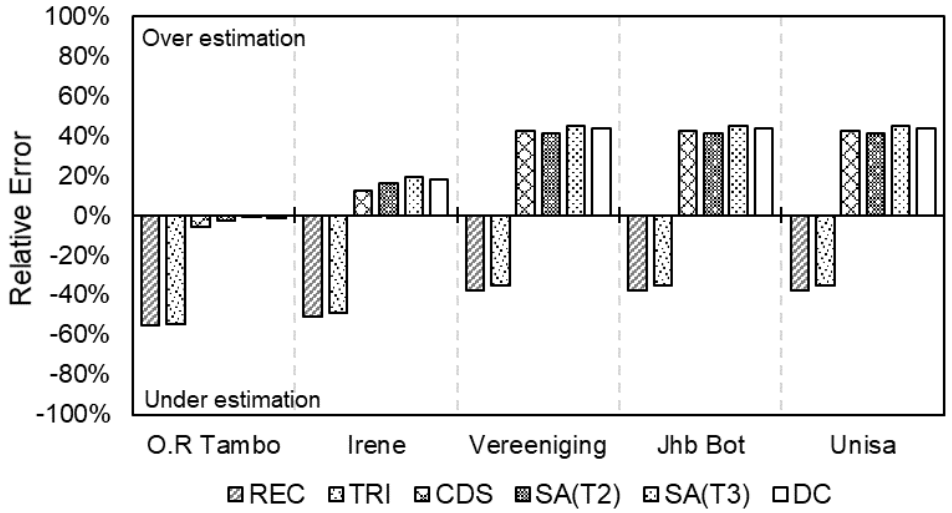

Figure 5.17: Percentage RE of the runoff volume between continuous simulation and single event-based modelling

5.5.3 Critical and minimum durations

The critical and minimum durations required to apply the REC and TRI methods, respectively, to a dynamic rainfall-runoff simulation model are described in this section. The critical duration refers to the duration which allows sufficient time for discharge to reach the outlet point. However, the duration must be as short as possible so that the discharge is not underestimated. This involves the simulation of multiple synthetic design storms, starting at 5-min and gradually increasing the duration until the discharge has reached a maximum. If the duration of the synthetic design storm is less than the critical duration, then the discharge from the remote parts of the catchment has not yet reached the point of discharge. This is according to Mulvaney (1851), as cited by Dooge (1974), who states that the peak discharge from the catchment will occur when the discharge from every portion of the catchment arrives simultaneously at the point of discharge. Conversely, if the duration exceeds the critical duration, then the intensity of the synthetic design storm will be lower which will result in a lower peak discharge.

The results of applying this concept to the catchment shown schematically in Figure 5.8, and using the design rainfall estimation for O.R Tambo described in Section 4.2 as input data, the critical storm duration was found to be 15-min, as shown in Figure 5.18.

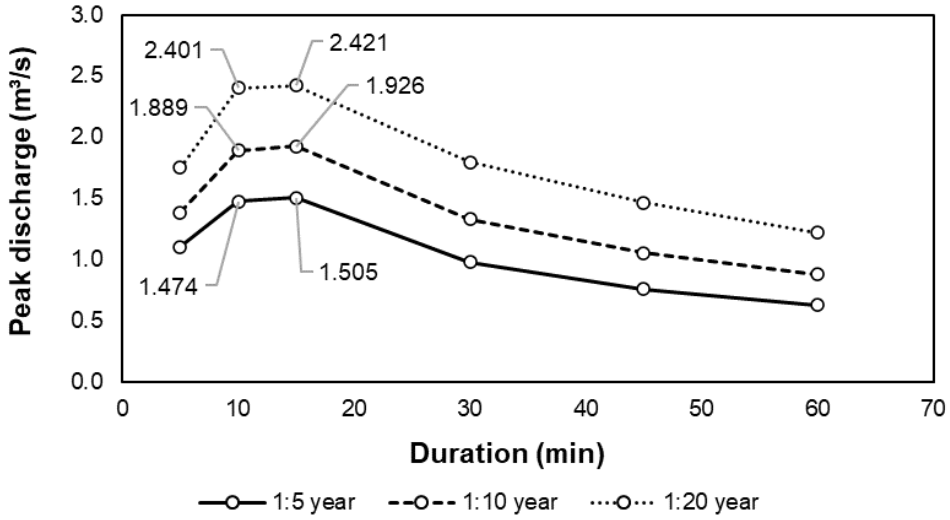

Figure 5.18: Critical storm duration for O.R Tambo according to the REC method

The minimum duration applicable to the TRI method was determined by limiting the maximum intensity of the triangular hyetograph expressed in Equation 2.14 to the maximum intensity following the PD analysis described in Section 4.2. An example of this limitation is depicted in Figure 5.19. From the IDF graph, the intensity of the 5-min duration is equal to 125 mm/h. However, the maximum intensity for a 5-min triangular hyetograph computed using Equation 2.14, is 250 mm/h. Therefore, generating a 5-min triangular hyetograph is incorrect. Limiting the triangular hyetograph to 30-min as shown in Figure 5.19, will therefore ensure that the peak intensity is not exceeded. The results for the five best stations, following this methodology, are depicted in Figure 5.20

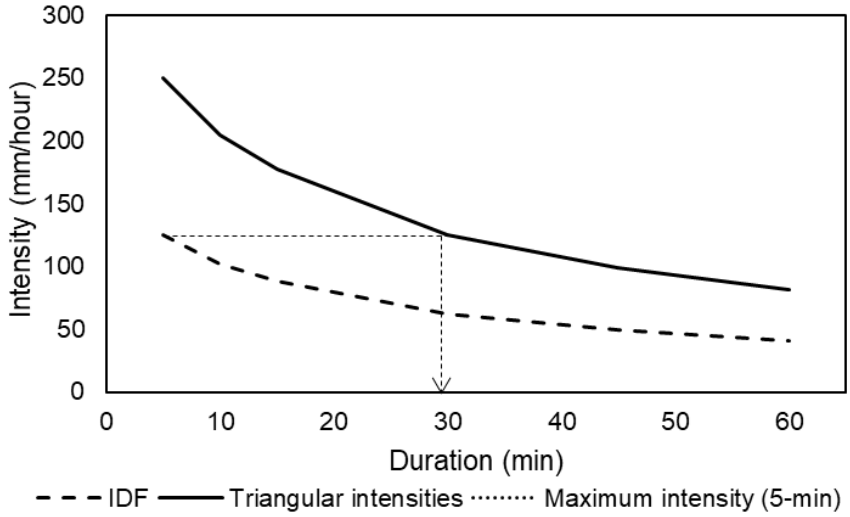

Figure 5.19: Example of determining the minimum storm duration for the TRI method

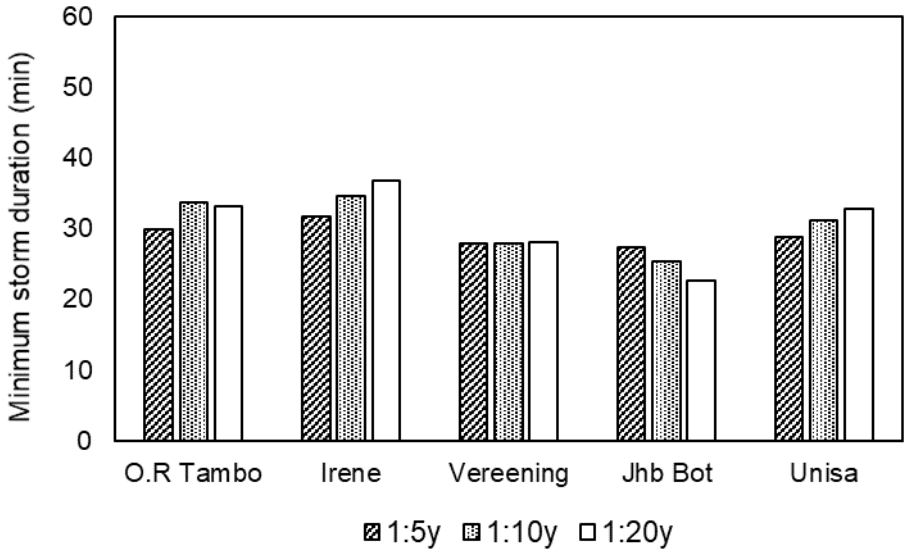

Figure 5.20: Result of the minimum storm durations for the five best stations in Gauteng

5.5.4 SCS-SA ratios for 2-hour events

To create 2-hour events from the standard SCS-SA curves, the development of a DC for a duration < 24-hours, as described in Chapter 4.4, was applied. This involved determining the D-hour to 2-hour ratios as depicted in Figure 5.21. Considering the critical storm duration of 15-min depicted in Figure 5.18, the ratios for the 2-hour, Types 2, 3 and 4 curves at 15-min duration, as depicted in Figure 5.21, are approximately equal. The 15-min ratios for the 24-hour storm event are, however, very different. This explains the difference between the peak discharge comparison for the SA(T2) and SA(T3) considering a 24-hour event compared to a 2-hour event, as described in Section 5.5.

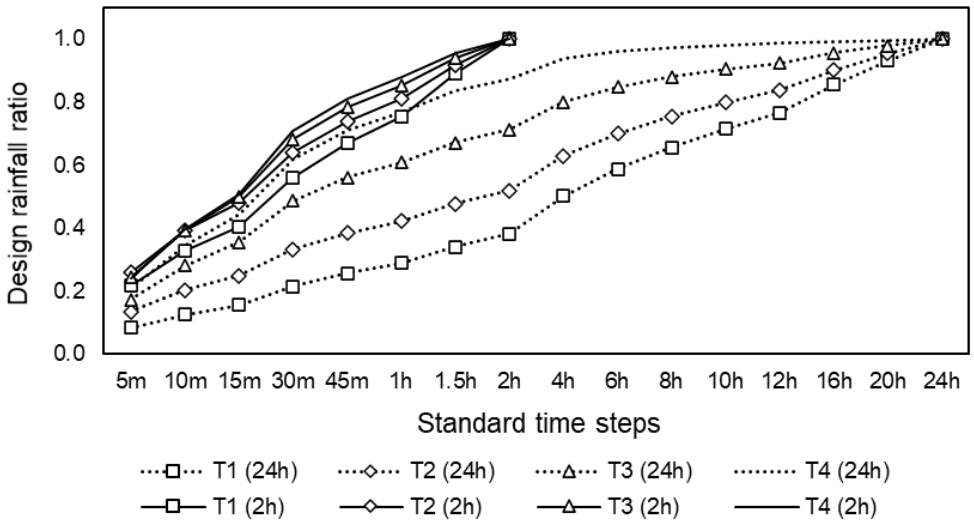

Figure 5.21: Design rainfall ratios in relation to 2-hour rainfall

5.5.5 Consistency of DC

This section contains a comparison between the D-hour to 24-hour ratios, with the results of the peak discharge comparison, as described in Section 5.5. Using the rainfall distribution process to determine DCs as described in Section 4.4, includes the embedment of the entire IDF curve in a single event. These ratios were found to vary between the standard SCS-SA curves as described in Section 4.5. By considering the critical storm duration of 15-min depicted in Figure 5.18, the intermediate curve types for the five best stations were determined as shown in Figure 5.22. The same method of determining intermediate curve types as described in Section 4.5.3 was followed to determine the intermediate curve types for the results of the DC method. As depicted in Figure 5.22, the comparison between the intermediate curve types following the two methodologies is consistent. This confirms the validity of the 15-min critical duration for the model depicted in Figure 5.8.

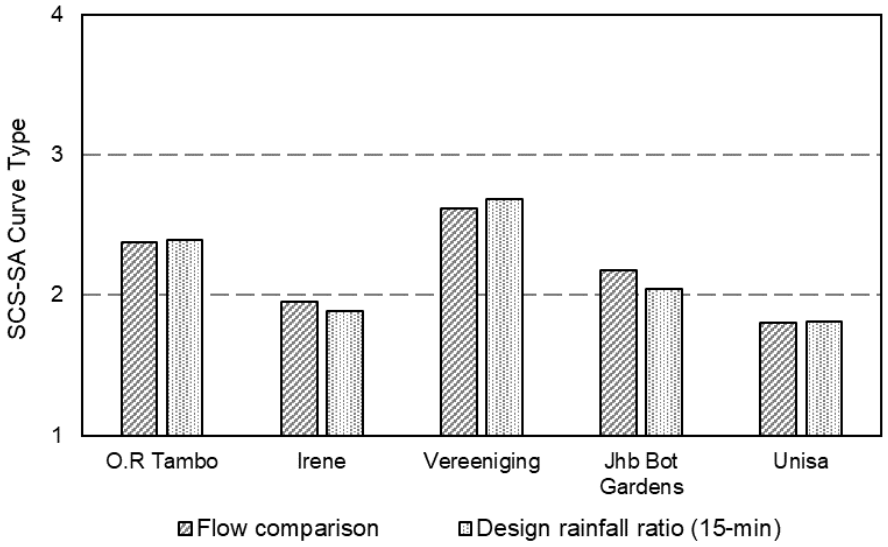

Figure 5.22: Intermediate curve type determined from flow results

5.6 CHAPTER SUMMARY

This chapter has provided details of the synthetic design storm evaluations. The shape and average intensities of synthetic design storms were compared with observed storm events. It was concluded that the shape and average intensities of the REC method least represents observed events. It was, however, further demonstrated that the REC method can be used to determine the response time of a catchment. This was based on the concept of the critical duration which allows sufficient time for discharge from the entire catchment to reach the point of discharge.

The methods that consider an entire IDF curve, which includes the CDS, SA(T2), SA(T3) and DC methods, were also shown to be a poor representation of observed events. By manipulating the position of the peak intensity, it was demonstrated that the GOF has improved considerably. However, the variation of the RI relative to the average intensities of the standard time steps, also contributes to the poor GOF. It was also demonstrated that the maximum RI of 6-hour and longer events is likely to be associated with the maximum standard duration. It was, however, concluded that the shape of synthetic design storms are not similar to observed events.

Following the shape and average intensity assessments, the synthetic design storms were used in a dynamic rainfall-runoff simulation model. A stormwater network in a catchment was simulated in EPA SWMM. The rainfall data from the five best stations in Gauteng was used as input data for the model. The AMS of the flows and volumes were determined following a continuous simulation and a PD analysis was conducted. The results from the analysis were used as baseline for the comparison with the results of single event-based simulations. The REC, TRI, CDS, SA(T2), SA(T3), DC5, DC10 and DC20 methods were used to generate synthetic design storms. The results of the SA(T2) and SA(T3) was successfully related to the intermediate curve types, and it was demonstrated that the characteristics of 2-hour events were very different to 24-hour events.

The peak discharge initial deficit associated with the infiltration parameters of the Green-Ampt model method is questioned, and further research is recommended. The effect of the location of peak intensity and the total duration of the storm event should also be further investigated as it was shown that these two parameters can have a significant effect on the peak discharge.

The next chapter contains a general discussion and conclusions drawn from the findings of this study and includes areas recommended for future research.

CHAPTER 6: DISCUSSION, CONCLUSIONS AND RECOMMENDATIONS

This chapter presents a discussion of the results from the study and conclusions that emanated from this study. The proposed way forward is also described.

6.1 OBJECTIVE

The aim of this study was to test the performance of the existing synthetic design storm generation methods, and to identify the method most suited for conditions in small catchments in Gauteng, using the 5-min interval rainfall records obtained from the SAWS. The specific objectives of the study to meet this aim were to: 1) identify and assess the performance of currently available methods to estimate synthetic design storms used as input for single-event modelling in the selected pilot study area; 2) to propose an improved procedure to generate a synthetic design storm applicable to small catchment areas in the study area; and 3) to disseminate the information to managers, designers and technicians involved in urban stormwater planning and design.

6.2 DISCUSSION

The literature review found that existing synthetic design storms have a strong scientific basis, with synthetic design storms being classified into three categories: a) methods that are derived from the Intensity Duration Frequency (IDF) curves; b) standardised mass curves generated directly from rainfall records, which includes the Huff and NOAA Atlas 14 curves; and c) the simulation from a stochastic rainfall model, which includes the daily rainfall disaggregation model for South Africa.

Although the existing synthetic design storms were developed using the best data, technology, and engineering judgement available at the time, they do present some degree of insufficiency. For example, the total precipitation volume is systematically underestimated by the rectangular hyetograph (Arnell, 1982), and it was also realised that it gives a wrong picture of a hyetograph (Niemczynowicz, 1982). In terms of the triangular hyetograph method, Veneziano and Villani (1999) have noticed that, although it is quite simple and intuitive, it does not have a strong conceptual basis and may produce biased flow estimates. The CDS method, on the other hand, utilises point rainfall data that applies to a particular site and therefore the variability and unique character of the rainfall patterns will automatically be embedded in the CDS method. Methods that utilise the entire IDF curve to generate a synthetic design storm hold much potential since the design rainfall has been regionalised by Smithers and Schulze (2000). Some of the variability and unique character of the rainfall pattern will therefore automatically be embedded in these methods.

The first aim of this study was to identify and assess the performance of currently available methods to estimate synthetic design storms used as input for single-event modelling in the selected pilot study area. In order to achieve this aim, short-duration observed rainfall data recorded at 35 automatic rainfall stations situated in the Gauteng province, were collected, and assessed in terms of completeness. The missing data as well as the data period of each station were used to classify the data quality of each rainfall station. A station was classified as either, good, average or poor, depending on the selected classification criteria. The stations with poor data sets were omitted from the study, whereas the good and average stations are used in subsequent investigations. Five stations have good data sets with each having a data period of 26 years and less than 5% of missing data during the rainy months. A further 17 stations were identified with average quality data sets. The criteria used for the identification of individual events were also described. These criteria consisted of an MDP ranging from 0 to 120-min, an MRD of 10 mm, and an MRI of 1:2 years. The correlation between the total storm duration and total rainfall depth related to different MDPs was consistent with the findings from Ramlall (2020). However, this study is based on an MDP associated with the reaction time of a small urban catchment. Appropriate storm parameters were determined which were 0.38 for the advancement coefficient and 0.20 for the dimensionless time to peak. The determination of regression coefficients for any DDF curve, and by re-generating the SCS-SA curves, using the GRG nonlinear algorithm to determine appropriate coefficients, was demonstrated. Design rainfalls were determined using the at-site AMS for 16 standard durations for each station and then compared with the design rainfall obtained from the DRESA software. It was found that the average RE was within the 90% upper and lower bounds given by the DRESA software. Short duration design rainfall of between 5- and 30-min was identified to be substantially lower than the DRESA software and further investigation is recommended to identify the cause of the error. The procedure to distribute design rainfall equally around the peak intensity was adapted to utilize the concept of incremental intensities for the interpolation of design rainfall for intermediate time steps. This was then subsequently utilised to generate the DC5, DC10 and the DC20 curves from the design rainfall developed from the PD analysis. The procedure to extract an event of less than 24-hour was also illustrated. The D-hour to 24-hour ratios were also determined and their position relative to the four standard SCS-SA curves were determined, using the design rainfall of the DRESA software as well as the at-site design rainfall analysis. The results from both sources of design rainfall indicated that, on average, Gauteng conforms more closely to the SCS-SA Type 2 curve, rather than Type 3. However, a significant variation in the ratios for the various durations were observed because the derived ratios plotted between standard SCS-SA type curves. This led to the development of intermediate curve types whereby a curve is linearly interpolated between two standard type curves. The method of interpolating between standard type curves was also documented. The design rainfall ratios of the SCS curves were compared with the SCS-SA curves and concluded that the application of the SCS curves is very limited and that it must be applied with caution. A methodology of determining regression coefficients for the CDS method, using the GRG non-linear solver was also developed. The simulated design rainfall intensities, using the

regression coefficients, were evaluated by determining the RE of the actual design rainfall intensities obtained from the DRESA software. From this analysis it was evident that the results obtained from the methodology, involving the GRG non-linear solver, was sufficiently accurate to determine the regression coefficients required by the CDS method. Standardised mass curves (Huff curves) were developed and based on the limited tests conducted on these curves, the results indicate an underestimation of the short duration design rainfall. Therefore, this method was not considered for the single event-based modelling in the next chapter because it will lead to an underestimation of the peak discharge.

The synthetic design storm evaluation was conducted by comparing the synthetic design storms with the observed rainfall events. Two aspects were evaluated, namely the shape of the mass curves, as well as the average intensities embedded in each synthetic design storm. It was concluded that the shape and average intensities of the REC method least represents observed events. It was, however, further demonstrated that the REC method can be used to determine the response time of a catchment. This was based on the concept of the critical duration which allows sufficient time for discharge from the entire catchment to reach the point of discharge. The methods that consider an entire IDF curve, which includes the CDS, SA(T2), SA(T3) and DC methods, were also shown to be a poor representation of observed events. By manipulating the position of the peak intensity, it was demonstrated that the GOF has improved considerably. However, the variation of the RI relative to the average intensities of the standard time steps, also contributes to the poor GOF. It was also demonstrated that the maximum RI of 6-hour and longer events is likely to be associated with the maximum standard duration. It was, however, concluded that the shapes of synthetic design storms are not similar to observed events. This analysis provided sound evidence that synthetic design storms do not exist in nature.

Following the shape and average intensity assessments, the synthetic design storms were used in a dynamic rainfall-runoff simulation model. A stormwater network in a catchment was simulated in EPA SWMM. The rainfall data from the five best stations in Gauteng was used as input data for the model. The AMS of the flows and volumes were determined following a continuous simulation and a PD analysis was conducted. The results from the analysis were used as baseline for the comparison with the results of single event-based simulations. The REC, TRI, CDS, SA(T2), SA(T3), DC5, DC10 and DC20 methods were used to generate synthetic design storms. The results of the SA(T2) and SA(T3) was successfully related to the intermediate curve types, and it was demonstrated that the characteristics of 2-hour events were very different to 24-hour events. Various observations were made from these results of which the most important was that the suggested values for the initial deficit associated with the Green-Ampt infiltration parameters did not result in good simulations. The effect of the location of peak intensity and the total duration of the storm event should also be further investigated as it was shown that these two parameters can have a significant effect on the peak discharge.

The CDS method was also shown to provide consistent results compared to continuous simulation. However, a sensitivity analysis must be conducted to determine the effect of the advancement coefficient and total storm duration on the peak discharge. This method has the following advantage:

(a) The IDF coefficients can be accurately determined from the rainfall obtained from the DRESA software, which can them be used to generate a synthetic design storm.

(b) The location of the peak intensity concerning the total duration of the event can be adjusted to be anywhere between the start and end of the event.

6.3 CONCLUSIONS

It is, in general, concluded that synthetic design storms, applied to a single event-based model, provides the engineer with the ability to assess the complex hydrological and hydraulic characteristics of an urban stormwater network. Despite its unrealistic assumptions, shortcomings, and the criticism the synthetic design storm concept has received, applying it to a single event-based model has resulted in good peak discharge and runoff volume estimates. Three methods, to generate synthetic design storms, were identified that could be applied to a single event-based model. They are the REC, SCS-SA and CDS methods.

The REC method also provides a means of evaluating the response time of an urban catchment, but the initial deficit defined as the difference between the porosity and field capacity, associated with the Green-Ampt infiltration method, did not result in good simulations. The design rainfall ratio comparisons from both the at-site and DRESA design rainfall, provided the bases to conclude the inappropriateness of the SCS-SA Type 3 curve for Gauteng. However, it was also concluded that an interpolation between the standard type curves is needed for better single event-based simulation results. The methodology that was used to determine the CDS regression coefficients from the DRESA design rainfall was sufficient and resulted in good results when applied to a single event-based simulation.

It can, therefore, be concluded that all three project aims were achieved, namely:

(a) The performance of currently available methods to estimate synthetic design storms was assessed and used as input for single-event modelling in the selected pilot study area.

(b) An improved procedure to generate a synthetic design storm for the study area was proposed. An improved procedure to generate a synthetic design storm applicable to small catchment areas in the study area was proposed through the development of intermediate SCS-SA curve types. The intermediate curves could be used in combination with the interpolated map of Gauteng with lower values to the north of the province and higher values to the south.

(c) The results of this project were disseminated to managers, designers and technicians involved in urban stormwater planning and design through a WRC workshop presented in conjunction with the annual National Flood Studies Programme's workshop, as well as at the 2022 UP Flood Hydrology course.

6.4 RECOMMENDATIONS

Recommendations that emanated from this study are summarised as follows:

(a) The impact the advancement coefficient and total storm duration have on the peak discharge must be investigated by conducting a sensitivity analysis. The parameters that could be considered for the analysis includes the size of catchment, slope, roughness, and soil types.

(b) The impact that missing data has on the design rainfall estimation and by implication the design rainfall ratios, in the context of this study, should be investigated.

(c) The current DRESA software, be further developed to provide the user with an opportunity to determine a synthetic design storm for a specific location.

(d) The discrepancy between the dates of the daily and 5-min data, and the annual maximum daily rainfalls from the daily and the 5-min data.

(e) The appropriateness of the GEV PD for short duration rainfall should be re-confirmed.

(f) An appropriate power coefficient for the IDW interpolation technique should be investigated.

(g) The suggested values for the initial deficit associated with the Green-Ampt infiltration parameters should be investigated.

(h) The relevance of the CDS, SCS-SA and REC methods for generating synthetic design storms applicable to single-event based modelling of small urban catchments must be expanded on a national scale, with the possibility of following a regional approach and ensemble modelling investigated.

.

CHAPTER 7: REFERENCES

Adamson, P. T. 1981. *Southern African storm rainfall.* Technical Report No TR 102, Department of Environment Affairs, Pretoria, RSA. pp 19.

Arnell, V. 1982. Estimating runoff volumes from urban areas*. Journal of the American Water Resource Association,* Vol 18, No 3, June, pp 383-387.

Asquith, W. H. Bumgarner, J. R. and Fahlquist, L. S. 2007. A triangular model of dimensionless runoff producing rainfall hyetographs in Texas. *Journal of the American Water Resources Association,* Vol 39, No 4, June, pp 911-921.

Bonnin, M. Martin, D. Lin, B. Parzybok, T. Yekta, M. and Riley, D. 2011. NOAA Atlas 14 Volume 1 Version 5, *Precipitation-Frequency Atlas for the United States.* NOAA, National Weather Service, Silver Spring, MD, USA.

Bonta, J. V. 1997. Proposed use of Huff Curves for hyetograph characterization. pp 111-124. In: C.W. Richardson *et al. (ed.)* Proceedings of the Workshop on Climate and Weather Research. Denver, Colorado. July 17-19, 1995. USDA-Agricultural Research Services, 1996-03, pp 223.

Bonta, J. V. 2004. Development and utility of Huff curves for disaggregating precipitation amounts*. Applied Engineering in Agriculture*, Vol 20, No 5, pp 641-653.

Bonta, J. V. and Shahalam, A. 2003. Cumulative storm rainfall distributions: comparison of Huff curves.*Journal of Hydrology*, Vol 42, No 1, June, pp 65-74.

Boughton, W. 2000. *A model for disaggregating daily to hourly rainfall for design flood estimation.* Cooperative Research Centre for Catchment Hydrology, Monash University, Clayton, Victoria, Australia. Report 00/15, 36 pp.

Boussinesq, J. and Flamant, A. 1886. Notice sur la vie et les travaux de Barré de Saint-Venant. *Annales des ponts et chaussées*, Vol 12, pp 557-595.

Brooker, C. 2021. Personal communication, 22 February 2021, Mr Chris Brooker, CBA Specialist Engineering, Gauteng, South Africa, 2055.

Cordery, I. and Pilgrim, D. 1993. *Handbook of hydrology.* McGraw-Hill, New York, USA.

Ellouze, E. Azri, C. and Abida, H. 2009. Spatial variability of monthly and annual rainfall data over Southern Tunisia. *Atmospheric Research,* Vol 93, No 4, pp 832-839.

El-Sayed, E. A. H. 2017. Development of synthetic rainfall distribution curves for Sinai area*. Ain Shams Engineering Journal*, Vol 9, No 4, December, pp 1949-1957.

Gomez, M. and Sanchez, X. 2014. *Rational method application (Lecture notes).*5 December 2020, https://ocw.camins.upc.edu/ocw/home.htm?execution=e1s6.

Green, W. H. and Ampt, G.A. 1911. Studies on Soil Physics. *The Journal of Agricultural Science,* Vol 4, No 1, pp 1-24.

Horton, R. E. 1933. The role of infiltration in the hydrologic cycle. *Transactions American Geophysical Union,* Vol 14, No 1, June, pp 446-460.

Huff, F. A. 1967. Time distribution of rainfall in heavy storms. *Water Resources Research*, Vol 3, No 4, December, pp 1007-1019.

Huff, F. A. 1990. *Time distributions of heavy rainstorms in Illinois.* Department of energy and natural resources, Champaign.

Izzard, C. F. 1946. Hydraulics of runoff from developed surfaces. *Proceedings, highway research board,* Vol 26, pp 129-146.

Keifer, C. J. and Chu, H. H. 1957. Synthetic storm pattern for drainage design. *ASCE Journal of the hydraulics division,* Vol 83, No 4, pp 1332.1-1332.25.

Knoesen, D.M. 2005. *The development and assessment of techniques for daily rainfall disaggregation in South Africa.* University of KwaZulu-Natal, School of Bioresources Engineering and Environmental Hydrology, Pietermaritzburg.

Males, R. Braune, M. van Bladeren, D. and Mahlangu, D.J. 2004. Regional hydrological modelling of City of Tshwane municipality using Visual SWMM. *Journal of Water Managment Modelling,* Vol 12, No R220-30, pp 627-649.

Malik, U. and James, W. 2007. Reliability of design storms used to size urban stormwater system elements. *Journal of water management modelling*, pp 309-326.

Munro, G. 2021. Personal communication, 23 August 2021, Mr Gerhard Munro, Oracle Java Certified SE Programmer, Gauteng, South Africa, South Africa, 1709.

Niemczynowicz, J. 1982. *Areal intensity duration frequency curves for short term rainfall events in Lund.* Hydrology Research, Sweden.

NRCS. 2019. National Engineering Handbook. Part 630 Hydrology. *Chapter 4: Storm rainfall depth and distribution.* Department of Agriculture, Washington.

NRCS, 2020. United States Department of Agriculture, September 2021, https://www.nrcs.usda.gov/wps/portal/nrcs/detailfull/national/water/manage/hydrology/?cid=stelprdb1044959.

Ramlall, R. 2020. *Assessing the performance of techniques for disaggregating daily rainfall for design flood estimation in South Africa.* University of KwaZulu-Natal, School of Agricultural Earth and Environmental Sciences, Pietermaritzburg.

Perica, S. Pavloci, S. St. Laurent, M. Trypaluk, C. Unruh, D. and Wilhite, O. 2018. NOAA Atlas 14 Volume 11 Version 2, *Precipitation-Frequency Atlas for the United States, Texas.* National Weather Service, Silver Spring, MD.

Restrepo, P. J. and Eagleson, P. S. 1982. Identification of independent rainstorms.*Journal of Hydrology*, Vol 55, pp 303-319.

Schmidt, E.J. and Schulze, R. E. 1987. *Design stormflow and peak discharge rates for small catchments in Southern Africa.* Water Research Commission. WRC Report No. TT 31/87. Pretoria. pp 65-70.

Schulze, R. E. 1984. *Hydrological models for application to small rural catchments in southern Africa: Refinements and development.* University of Natal, Department of Agricultural Engineering, Pietermaritzburg.

Schulze, R. E. and Arnold, H. 1979. *Estimation of volume and rate of runoff in small catchments in South Africa, based on the SCS technique.* University of Natal, Department of Agricultural Engineering, Pietermaritzburg.

SCS. 1973. *A method for estimating volume and rate of runoff in small watersheds.* US Department of Agriculture, Soil Conservation Service, Washington, D.C.

Sherman, C. 1931. Frequency and intensity of excessive rainfall at Boston, Massachusetts. *American Society of Civil Engineers,* Vol 95, pp 951-960.

Silveira, A. L. L. 2016. Cumulative equations for continuous time Chicago hyetograph method*. Brazilian Journal of Water Resources,* Vol 21, No 3, pp 646-651.

Smith, A. A. 2004. MIDUSS Version 2, Reference Manual. Alan A. Smith Inc., Dundas, Ontario, Canada.

Smithers, J. C. 2012. *Methods for design flood estimation in South Africa.* Water Research Commission, Vol 38, No 4, July, pp 633-646.

Smithers, J. C. and Schulze, R. E. 2000. *Development and evaluation of techniques for estimating short duration design rainfall in South Africa.* Water Research Commission.WRC Report No. 681/1/00. Pretoria.

Smithers, J.C. and Schulze, R.E. 2002. *The estimation of design rainfall for Tshwane – Report to SRK Consulting*. School of Bioresources Engineering and Environmental Hydrology. Pietermaritzburg. ACRUcons Report 38.

Smithers, J. C. and Schulze, R. E. 2003. *Design rainfall and flood estimation in South Africa.* Water Research Commission.WRC Report No 1060/01/03. Pretoria.

Veneziano, D. and Villani, P. 1999. Best linear unbiased design hyetograph*. Water Resources Research*, Vol 35, No 9, September, pp 2725-2738.

Watson, M. D. 1981. *Application of ILLUDAS to stormwater drainage design in South Africa.* University of the Witwatersrand, Johannesburg.

Weddepohl, J. P. 1988. *Design rainfall distributions for southern Africa.* University of Natal, Department of Agricultural Engineering, Pietermaritzburg.

Weesakul, U. Chaowiwat, W. Rehan, M.M. and Weesakul, S. 2017. Modification of a design storm pattern for urban drainage systems considering the impact of climate change*. Engineering and Applied Science Research,* Vol 44, No 3, pp 161-169.

U.S. Weather Bureau. 1961. Generalised Estimates of Probable Maximum Precipitation and Rainfall-Frequency Data for Puerto Rico and Virgin Islands. *U.S. Department, Soil Conservation Service,* Technical paper, No 42.

Yen, B. C. and Chow, V. T. 1980. Design hyetographs for small drainage structures. *ASCA Journal of the hydraulics division,* Vol 106, No HY6, pp 1055-76.

Yu, Y. S. and McNown, J. S. 1964. Runoff from impervious surfaces. *Journal of hydraulic research,* Vol 2, No 1, pp 3-23.